Design of a Miniaturized Automated External Defibrillator

Auteur : Deflandre, Sophie
Promoteur(s) : Redouté, Jean-Michel
Faculté : Faculté des Sciences appliquées
Diplôme : Master en ingénieur civil biomédical, à finalité spécialisée
Année académique : 2020-2021
URI/URL : http://hdl.handle.net/2268.2/11393

University of Liege - Faculty of Applied Sciences
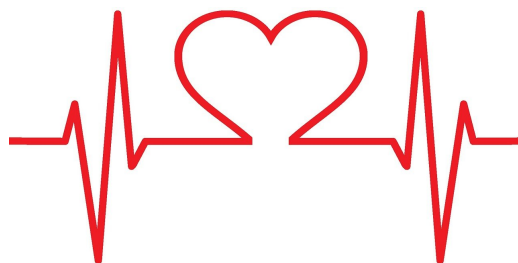
Design of a Miniaturized Automated External Defibrillator

Master thesis conducted by

Deflandre Sophie - 20160767

with the aim of obtaining the degree of Master in Biomedical Engineering

Under the supervision of Pr. Jean-Michel Redouté

Academic year 2020-2021

Contents

1 Abstract

The purpose of this project is to go through the designing steps of an automated external defibrillator of small size to allow ease of use and portability.

Since the design of the first defibrillator in 1947, a lot of improvements have been made in terms of technologies. This device has evolved through time to try to give the best treatment with the easiest use possible. These last years, defibrillators have already seen their size decrease a lot. However, a pocket-size AED is not yet on the market. Some companies have shown promising solutions, but most of them still need to be classified as medical devices. These improvements show that this topic of research is a field in which a lot of interest is placed.

The device should be fully automated, meaning that the heart rhythm should be automatically detected, and the defibrillation process should start by itself if needed. The first shock should deliver an energy pulse between 100 and 200 joules depending on the transthoracic impedance (TTI) measured and the next shocks should increase with steps of 50 joules with a maximum of 360 Joules until a normal heart rhythm is detected.

In order to reach this goal, the project has been divided into 3 main parts. At first, a low voltage acquisition board has been made. This board needs to measure the patient's TTI as well as to record the ECG signal. The second part is the high voltage defibrillation part. The working principles have been investigated and are described in this work. Finally, an arrhythmia detection algorithm has been computed, using a machine learning model. This allows to detect ventricular fibrillation and tachycardia which are the shockable rhythms, i.e. rhythms for which a shock can be delivered to restart the heart.

2 Context of the research

2.1 Why this device?

The idea of this project was proposed by doctor Bodson from the CHU of Liege. He pointed out the lack of accessibility of defibrillation devices. Indeed, when a cardiac arrest occurs, the timing is really important and the rate of survival decreases at an alarming rate when no cardiac massage is given. In this situation, a few minutes can have a huge impact, as in general after 4 minutes brain cells are already well damaged. It is a real problem, especially when being at home. If a cardiac arrest occurs, the time needed for an ambulance to arrive is often way too long and the rate of survival is very low. This problem of accessibility is even more increased by the fact that only a few percentages of the Belgian population can perform a cardiac massage. Adding to this issue the fact that with panic a lot of people will take quite a long time to react and try a cardiac massage, it will often be too late.

Sudden cardiac arrest is one of the main causes of death in Europe and it accounts for 50% of the overall cardiovascular mortality [1]. Every year 350 000 to 700 000 patients suffer from it and the survival rate is only of about 50 to 70% when the defibrillation is given within 3 to 5 minutes after the collapse [3]. Thus, it appears that less than 5% of the out-of-hospital patients will survive [2] while they are 60 to 80 % to encounter this pathology at home. The median time of emergency arrival appears to be about 5 to 8 minutes [3]. This problem is enhanced by the fact that AED are only considered cost-effective if there is at least 1 cardiac arrest every 5 years in a certain place.

A portable AED could be especially appropriate for at-risk patients. In some cases, symptoms can be detected in advance and these patients could use the device on themselves. Obviously, it isn't easy to detect all patients at high risk, but several factors can increase the risk of cardiac arrest. These patients should be aware of the symptoms to properly use the device in the right time. But in the end, if people would have easy access to a portable defibrillator device, it could save many lives. Indeed, about 30 cardiac arrests happen every day in Belgium and the rate of survival is only 8% [5]. Unfortunately, it is not feasible to give total access to AED, it wouldn't be cost-effective to have one device in each home but new sharing systems could be introduced to ease the access to these devices in every neighborhood.

To resume, the goal of this device would be to provide easier access to AED and to allow people and especially at-risk patients to possess, or at least to have at disposal, one device of this kind. Firstly, the main goal is to reduce the size of AED to have an easy-to-use handheld device of maximum 20 x 10 x 4 cm that would be easy to transport and small enough to fit in a little bag or in a large pocket. The price should also be considered so that it is affordable. It should detect ventricular fibrillation and tachycardia, which are the main causes of sudden deaths. The big challenge with this kind of device is to deliver a high voltage pulse, needed to defibrillate the heart, using a small circuit. The pulse delivered to the heart will need to adapt itself automatically to the patient transthoracic impedance (TTI). It will be off all the time and will be switched on when electrodes are pulled. Some other properties could be added as such as a call to emergency services directly after an anomaly is detected.

3   Heart biology

First of all, it is important to understand the underlying mechanisms of heart activity. In this section is reviewed the behavior of the heart in terms of electrical activity and the main pathologies leading to cardiac arrest.

3.1   Heart electrical activity [6]

At the cell level, gap junctions are present between cardiac cells (cardiomyocytes). They allow the flow of ions between cells, which manages depolarization and excitation processes. Cardiomyocytes are excited when the nervous influx is higher than a certain threshold. Indeed, an action potential induces membrane depolarization. Firstly, the depolarization is due to the entrant of sodium ions in the cell which reverses the membrane potential. Secondly, the repolarization is induced by an exit of potassium ions out of the cells. The action potential (AP) of cardiac cells is a bit different from AP of other cells, there is a plateau of depolarization due to the entry of calcium ions (Figure 1). This process allows the contraction of the heart muscle fibers.
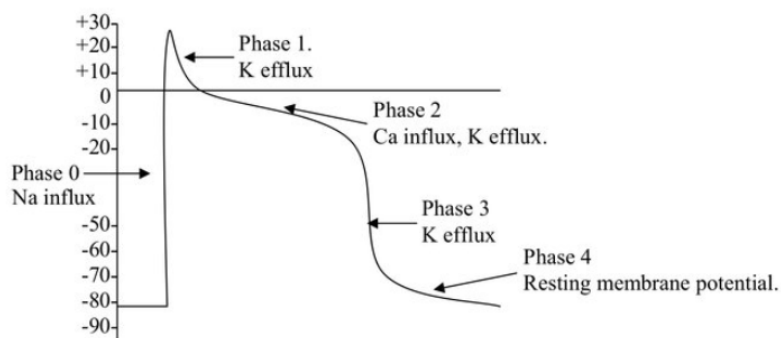
Figure 1: Cardiomyocyte Action Potential (Ioannis Androulakis, *The effect of heart rate on CAC Scoring*)

At the level of the whole heart, the electrical activity results from the sum of the activity of each cell (see Figure 2). However, the heart beats as it is made up of one unique cell, the system of conduction is present to regulate the influx and coordinates the whole.

The conduction tissue is made of rythmogene cells which can depolarize themselves spontaneously at regular intervals. This system is regulated by several nodes (Figure 2) that control the influx flow:

- **Sinusal node:** Is located between the superior vena cava and the right atrium. Its frequency determines the cardiac frequency as it has a frequency of depolarization higher than the other nodes. However, if this node encounters some malfunction, the others can take the relay to ensure a viable cardiac output.

- **Atrioventricular node:** Is situated above the tricuspid valve and has an influx delayed of about 0.1 seconds to allow the atrium contraction to finish before initiating ventricles contraction.

- **Atrioventricular bundle:** The influx can propagate in the whole heart by passing through the atrioventricular bundle that is divided into two bundles that go into both sides of the heart and conduct the influx through the ramifications called the Purkinje fibers.
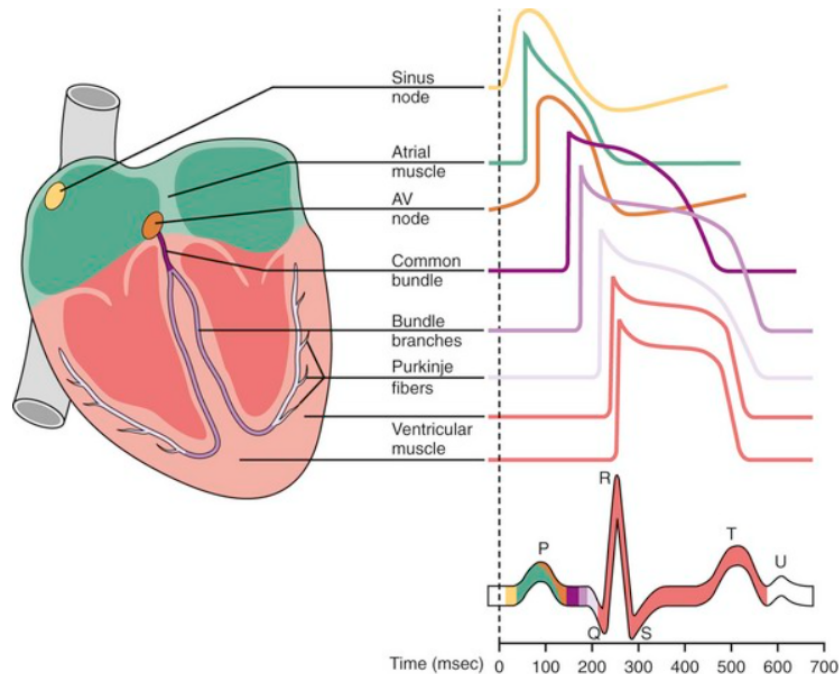
Figure 2: Electrical activity of the heart (https://thoracickey.com/cardiac-electrical-stimulation/)

3.2 Electrocardiogram [6]

The electrocardiogram usually called ECG is the recording of heart electrical activity thanks to electrodes that can be directly put at the surface of the skin. Indeed, the electrical influx is easily transmitted to liquids present in the environment and thus allows to record the signal in this way. ECG signal shows the global activity of the heart and is typically made up of 5 waves (Figure 3). The first one, the P wave, is due to the depolarization of the atrium by the sinusal node. Then, the QRS complex is formed by the ventricles' depolarization. Next, follows the T wave induced by the ventricles' repolarization. Healthy hearts have a quite constant duration and succession of these different waves. These waves are mainly located in the range of frequencies going from 0.5 to 30Hz.

One important point to consider when analyzing an ECG signal is the number of electrodes used. Indeed, with more than 3 electrodes, the signal will usually be quite good and the different waves will be detected, as a driven right leg is used to remove noise. This is why, using only 2 electrodes, it is possible to obtain a signal less clear. The signal will be noisier and the different waves will not be necessarily well detectable.
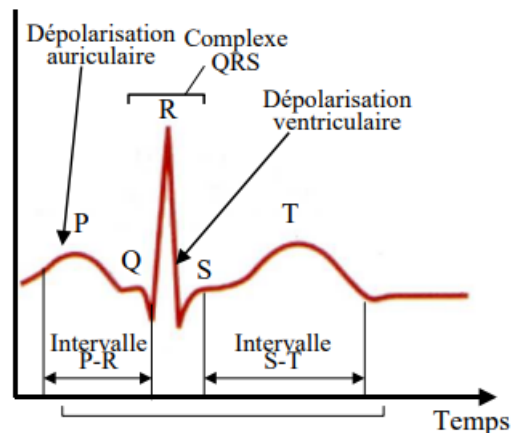
Figure 3: ECG signal [6]

The electrode's position also impacts the signal quality. When using a defibrillator, the electrodes are placed to enable the current to pass through the heart. Their position is thus limited by the need to defibrillate effectively. One electrode should be below the right clavicle and the other one placed on the left side of the chest just below the breast (as represented in Figure 4). With this placement, the ECG recording is usually good, as we measure near the heart. The distance between electrodes is small, which limits the noise picked up by wires.
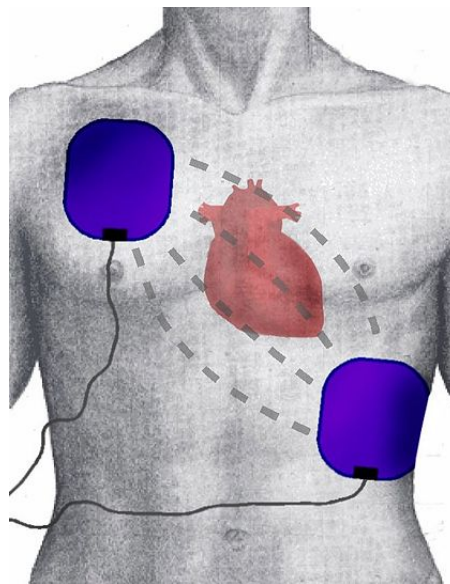
Figure 4: Defibrillation Electrode Position, *Wikimedia Commons*

In the next subsection, is shown how this signal can vary in pathological cases.

3.3 About cardiac arrest

First of all, it is important to determine who are the high-risk patients. Indeed, these identified patients should have 24/7 access to a defibrillator device to ensure their safety. Usually, a cardiac pathology is the main reason for cardiac arrest, the main one being the age increase leading to coronary artery disease [2]. However, the pathology is often unknown before this event. Moreover, genetic syndromes can lead to heart malfunction and even when screening the ECG, it can be hard to detect abnormalities, as they can be subtle and vary from day to day [2].

Several pathologies and habits of life can be factors of risk for cardiac arrest. Here is a non-exhaustive list of the main factors to focus on when classifying at-risk people with no cardiac pathologies known: [7]-[10]

- Obstructive sleep apnea

- Epilepsy

- Hypertension

- Hypercholesterolemia

- Tobacco

- Obesity

- Anxiety, depression, work overload

- Physical inactivity

- Family history

- Diabetes

These factors are vast and the risk of sudden cardiac arrest (SCA) may remain quite low even if these factors are encountered. It is thus quite hard to determine which kind of person should be targeted. However, one of the main points could be to advise the device to people that do not benefit from an internal cardiac defibrillator (ICD) but who have been found to be at risk. Indeed, certain diseases do not need the implantation of an ICD but still increases the risk of SCA. ICD is often recommended when there is a *presence of structural heart disease or genetic arrhythmia syndromes frequently impart a clinically significant risk* [2]. Moreover, people having comorbidities and who are diagnosed to live less than one year will usually not benefit from an ICD. By the way, they could benefit from the rent of a defibrillator as a safety measure. ICD is not without risk and should not be advised if not necessary, the risk due to complication being about 3% (perforation, bleeding, pneumothorax, ...) and the risk related to the intervention being less than 1% [2]. Finally, it is known that patient who survived myocardial infarction are at high risk of SCA in the following months, especially the first one [4]. Thus, this last group could also find benefit in renting an AED device.

In a second time, it could be important to detect if a patient has early symptoms of cardiac arrest. In some cases, symptoms can appear and being aware of these could save lives as preventive measures could be done to avoid cardiac arrest. Indeed, SCA can occur *unexpectedly or within 1h of an abrupt change from a stable clinical state* [4]. In the case of this portable AED, if the patient detects some symptoms, he could put the device on himself to be ready if a cardiac arrest occurs before the arrival of the emergency. Some known symptoms are listed above and could be detected in about half of the middle-aged patients [11]:

- Chest pain (less often in women)

- Dyspnea

- Shortness of breath

- Palpitation or syncope

- Influenza-like symptoms

As previously told, the device should detect ventricular fibrillation and tachycardia as these are the main causes of cardiac arrest, occurring when the electrical activity of the heart is disorganized in the ventricles. In fact, ventricular tachycardia (VT) is an abnormal cardiac rhythm that can lead to ventricular fibrillation (VF) or asystole (absence of cardiac signal) not compatible with life. VT and VF are rhythms that are shockable and need to be detected rapidly in order to increase the survival rate.

- **Ventricular Tachycardia**:

    VT is characterized by an abnormal cardiac output having a heartbeat frequency higher than 100 heartbeats per minute. VT with 160 to 180 heartbeats per minute induces a drop in cardiac output and the subject passes out. When VT is sustained, meaning lasts for longer than 30 seconds [1], it often leads to ventricular fibrillation, which induces cardiac arrest.

    Sustained VT is often a result of reentry involving a myocardial scar that is usually caused by a previous infarct [4]. Idiopathic VT is defined by the presence of VT in the absence of a structural heart disease [2], which can enhance the risk of cardiac arrest. If the pathology is not discovered in time, no treatment is given to the patient to prevent SCA. This kind of VT is often due to a genetic condition or metabolic abnormalities [4]. Finally, monomorphic and polymorphic VT can be distinguished, the first one is characterized by the same QRS configuration beat to beat and the second one by variability in QRS complex (see Figure 5 and 6). Polymorphic VT having QT prolongation, waxing and waning of QRS amplitude are called "torsades de pointes" [2] (see Figure 7) and is one of the main cause of SCA [4]. The ischemic disease appears to be one of the main cause of polymorphic VT as well as VF. Acute ischemia is characterized by a leakage of potassium ions which depolarizes myocytes in the ischemic border and leads to disorganized electrical conduction in the heart [4].

Figure 5: Monomorphic VT https://acls-algorithms.com/rhythms/other-tachycardias/

Figure 6: Polymorphic VT https://acls-algorithms.com/rhythms/other-tachycardias/
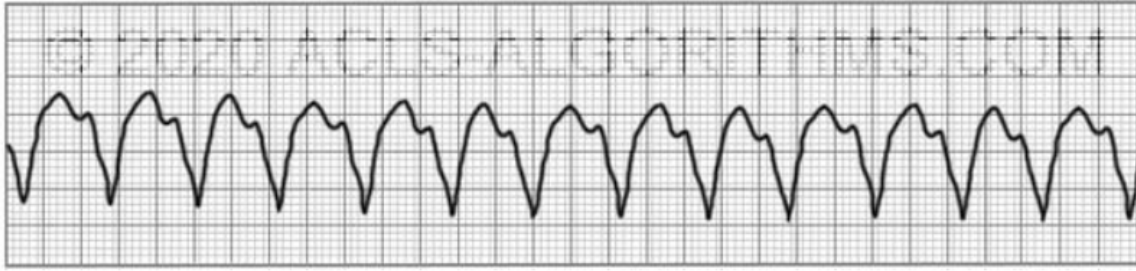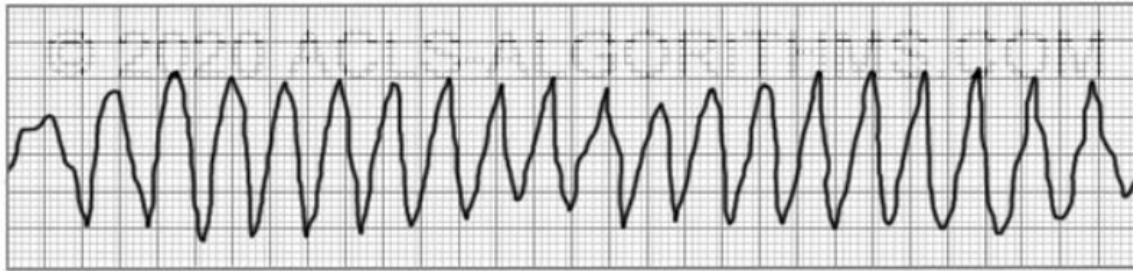
Figure 7: Torsades de pointes https://bossrn.com/torsades-de-pointes/

- **Ventricular fibrillation:**

  VF (Figure 8) often results from sustained VT, the ventricle lost its ability to contract and there is no cardiac output anymore leading to an incompatibility with life. This rhythm is still shockable. The survival rate is about 3 to 30 % out-of-hospital, when the fibrillation is installed for less than 30 seconds. The more the time spent in fibrillation increases, the more the heart is subject to develop global ischemia. Fibrillation cycle length is about 200 ms in human beings, meaning a frequency of 5Hz. Moreover, there are almost no intervening periods between each action potential. The rate of survival increases if the shock is given at the beginning of the action potential. [12]

  When emergency records ECG of a patient a certain time after the collapse, asystole is often discovered. However, when fast recording is possible VF is detected in about 76 % of the cases [3], meaning that VF is the main cause of collapse.
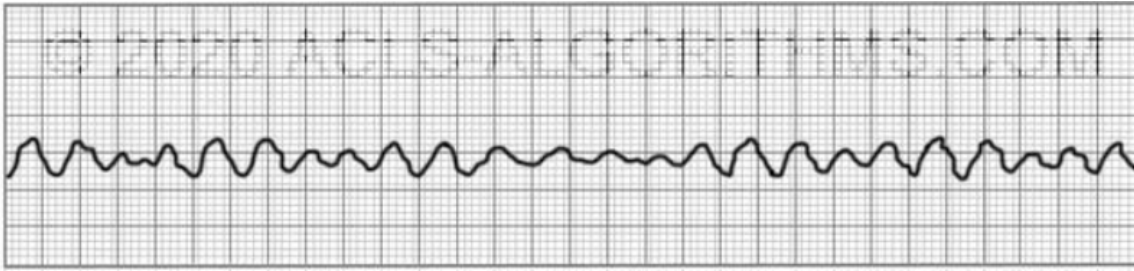
Figure 8: Ventricular Fibrillation https://acls-algorithms.com/rhythms/ventricular-fibrillation/

4 Defibrillation

4.1 Working principle

The goal of a defibrillator is to bring a subject heart activity back to normal. When an abnormal heart rhythm is detected, an electrical shock is sent to the heart to temporarily stop it. In order to do that, a huge amount of charge is stored in a capacitor and is then released to the patient. To this purpose, two electrodes are needed, to create a path passing through the heart of the patient. The bigger the electrode surface, the lower the impedance of the path, meaning that less energy is required. Defibrillators are composed of two main parts: the low voltage, acquisition part which mainly records the ECG signal and measure patient's TTI; the high voltage, defibrillation part which accumulates energy in a capacitor using high voltage and then releases it to the patient in a controlled way. In addition to these parts, a microcontroller is needed to manage the whole system. The structure of the device is shown in Figure 9.
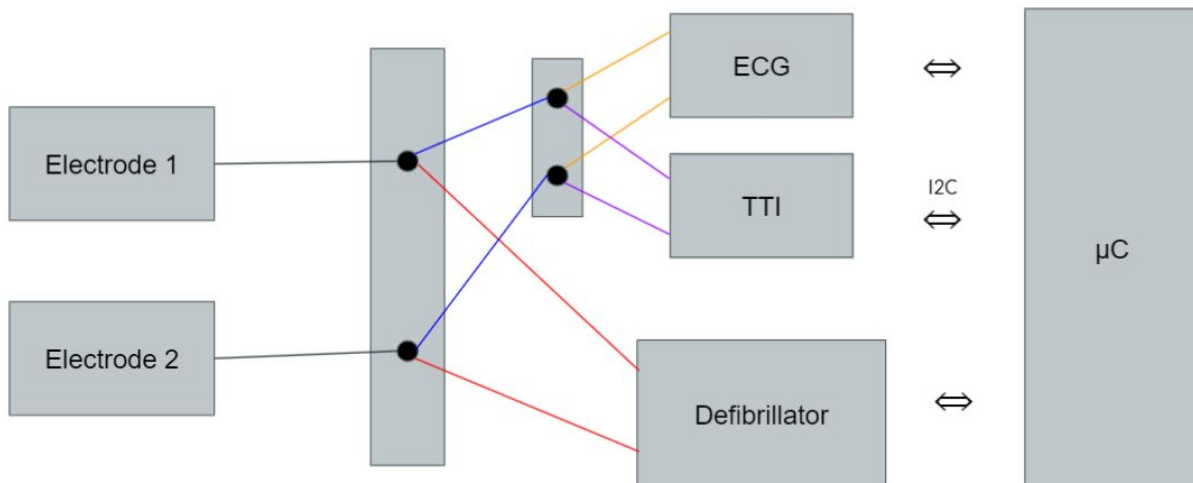
Figure 9: Whole structure

In order to connect the electrodes to the desired part of the circuit according to the current state of the system, several switches are needed. The first one being the one to disconnect the acquisition part from the electrodes when the charging process is triggered. This switch is important as the high voltage in the defibrillator part can't go through the low voltage part. For this purpose, a relay will be preferentially used.

Another important point to consider is the powering of the device, the voltage should go up to 3000V to provide enough energy to the capacitor. Indeed, the energy needed to defibrillate is considered to be between 150J and 360J. The first shock should be at 100J-150J and several shocks can be given, increasing the energy at each time. TTI should also be considered when deciding which energy is needed. If the impedance measured is quite high, the first shock should be higher than 150J. The voltage needed will increase with the energy that needs to be delivered. [13]-[28]

The size of the capacitor that needs to store this energy is limited by the size of the device as well as the time it needs to charge/discharge. The time constant of a RC circuit is given by $\tau = RC$ meaning that the higher the capacitor value is, the more time will be needed to charge/discharge and the timing is really important in the case of defibrillation process. Nevertheless, with a high power small size circuit, the challenge is often to provide enough current and/or voltage to power the circuit. Larger batteries are often needed in high consumption circuits, which makes the realization of this device challenging. To better understand the needs of the circuit, some tuning of parameters are presented in Section 4.2.

Finally, it is important to note that biphasic defibrillation pulses have been shown to be the best kind of pulse to use. At the beginning of defibrillators, damped sinusoids were used, but they are no longer of relevance. Different biphasic pulses that allow to compensate for TTI and which are commonly used are presented in Section 4.3.

4.2 RC circuit simulations and challenges

The defibrillation part is modeled by a RC circuit, C being the capacitor to be charged to store the energy and R the total impedance of the patient-electrodes path (TTI). This impedance is in the range 25 to 200Ω with usual values included between 50 and 100Ω [24]. This value depends on many factors as such as electrode paddles size, body weight, chest size, chest thickness, the effect of repeated shocks (decrease of TTI due to inflammatory response) [14]. The impedance seen by the defibrillator can be considered purely resistive, as no phase difference is detected between applied voltage and measured current [18]. However, a small capacitor is present due to cardiac cells. Indeed, cardiac cells can be represented by a RC circuit having a time constant of about 2 to 5ms. This time constant has a big importance as the defibrillation pulse duration is optimized when the membrane response is at its maximum, meaning that shorter or longer duration reduces the effectiveness [26]. The pulse duration is considered to be optimal between 2 and 20 ms [23]. It should even be lower than 10ms if possible and using biphasic pulses. Higher success rates have been demonstrated with a pulse duration less than 5ms [29]. The second phase should ideally be between 1.5 to 2.5ms according to some studies but it appears to be less important than the first phase and is mainly useful to remove the residual charge from stimulated cells [29].

In this section, is shown the challenges faced when designing a defibrillator. Indeed, there are a lot of compromises between the voltage needed, the capacitor value and the discharging/charging time of the circuit. First, the voltage needed in function of the energy that needs to be delivered is computed using the relationship from the paper [25]:

$$V = \sqrt{\frac{E * R}{\frac{(R*C)}{2} * (-e^{\frac{-2*tauP}{R*C}} + 1)}} \tag{1}$$

R and C are respectively the impedance of the patient-electrodes path and the capacitor that stores the energy; tauP is the pulse duration time desired and E the target energy.

This formula is derived from the equation of the energy provided in the paper. Indeed, knowing the voltage, the capacitor value and the resistance, the energy is defined as [25]:

$$E = \int_0^{\tau_p} \frac{U^2 e^{(-\frac{2t}{RC})}}{R} dt \tag{2}$$

From this relationship, the voltage is found to be [25]:

$$U = \sqrt{\frac{ER}{\int_0^{\tau_p} e^{(-\frac{2t}{RC})} dt}} \tag{3}$$

Finally, Equation 1 has been computed by integrating Equation 3 in order to find the needed voltage knowing the resistance, capacitor value and the target energy.

Using Equation 1, it is possible to plot the energy to deliver in function of the voltage that is needed for a certain RC circuit. In Figure 10, the left figure shows the voltage needed using a 80uF capacitor and a pulse duration of 10ms, for values of impedance in the usual range. It is observed that the maximum voltage should be about 3500V for a 180Ω impedance at 350J. In the figure on the right, the same plot is shown but with a pulse duration of 16ms, the maximum voltage is thus reduced to about 3000V. It could be deduced that to optimize the voltage needed, the pulse duration should be adjusted in function of the measured impedance. Knowing that higher impedance patients will need higher energy to defibrillate, it could easily be understood that these patients are the more challenging ones to save.
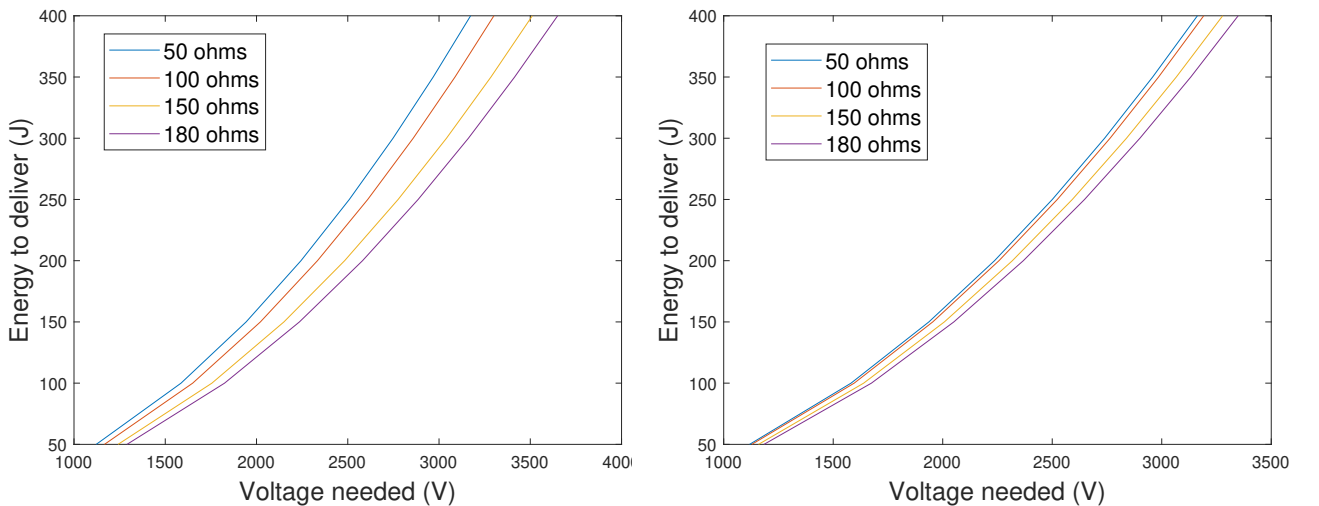

Figure 10: Voltage needed in function of the energy delivered (10/16 ms biphasic pulse)

To resume, the circuit should charge the capacitor using voltages in the range 1000 to 3000V and shock the patient with a biphasic pulse, having a duration adjustable with the impedance measured, by discharging the capacitor through the patient-electrodes path.

The next important point is the charging and discharging time of the circuit. These timing are given by these equations:

$$Tcharge = \frac{CV}{i} \qquad Tdischarge = 5\tau \qquad (4)$$

Where $\tau = RC$.

The charging time is dependent on the current, which adds a new point to consider when designing a defibrillator. Indeed, when converting high voltage, the current is often reduced a lot, which makes it hard to provide enough current to charge the capacitor. A bigger converter provides a larger current, but the device should be as small as possible, which complicates the design. This is one of the reasons why the converter part is a big challenge in this device design. If a 80uF capacitor is used, to keep the charging time in reasonable value (less than 10 seconds to be close to what is on the market), the current should be at least 25mA (as shown in the left Figure 13 and right Figure 11).

Figure 11 shows the influence of the capacitor value on the needed voltage, having an impedance of 100Ω and on the charging time to reach 3000V, having different current values. Lower capacitor values need higher voltage which is harder to provide but allows to reduce the charging and discharging time of the RC circuit. Indeed, as can be seen in the right Figure 11, a lower capacitor value is needed to reduce the charging time. Therefore, a value of 80uF seems to be a good compromise. This value has been chosen arbitrarily by deciding to make a compromise between a maximum voltage of 3000V and a charging time fewer than 10 seconds, with a needed current of at least 25mA. This choice could be adapted in function of the current and voltage that could be delivered by the flyback converter, even if it is at the expense of the charging time.
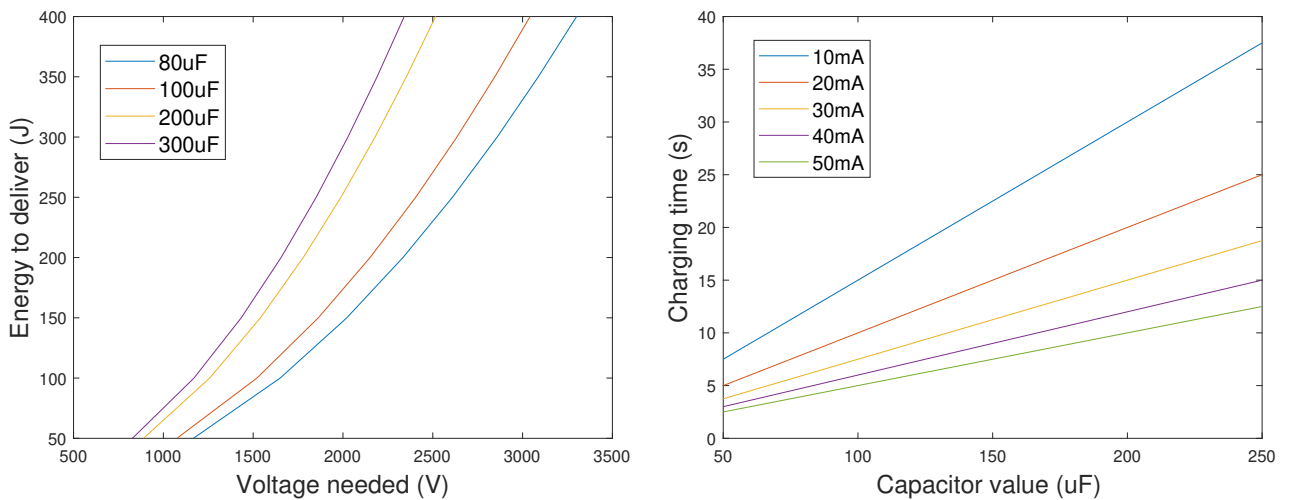
Figure 11: Tuning of the capacitor value

The discharging time is almost equal to 5τ. Indeed, after this amount of time, the voltage is almost reduced to 0V. In Figure 12 is shown the voltage evolution with the time being a multiple of the time constant. After τ seconds, only 37% of the voltage is still present, about 13% after 2τ and 5% after 3τ. Ideally, the discharge time of the circuit should be equal to 5τ to discharge all the energy stored in the capacitor.

However, with the value of capacitor selected to limit the voltage and current, it is impossible to discharge during 5τ as the maximum pulse duration is 20ms. In the right Figure 13, it is clear that it is not possible to discharge more than 87% of the energy in the best cases. One possibility would be to try to keep the impedance under 100Ω to deliver most of the energy by using electrodes with the smaller impedance as possible. However, it is certainly not possible to achieve this in each case, it should be thus kept in mind that only a part of the stored energy is given to the patient. The solution to this problem would be to decrease the capacitor value but it would increase the needed voltage which is not desired as it would increase the size of the device as well as the difficulty to provide enough current.
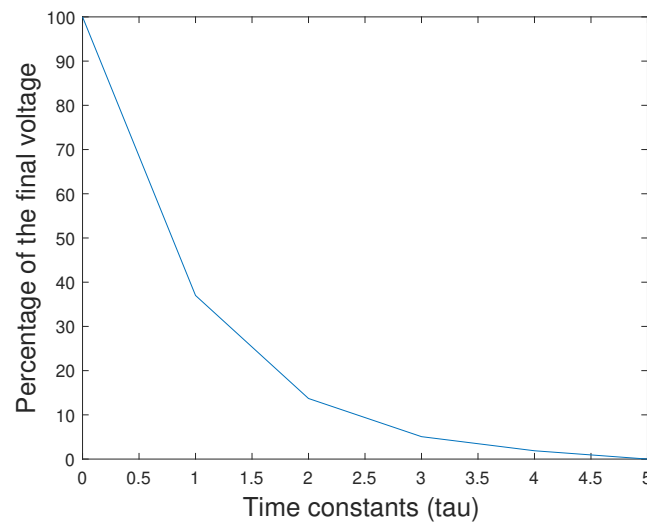
Figure 12: Evolution of the voltage with tau

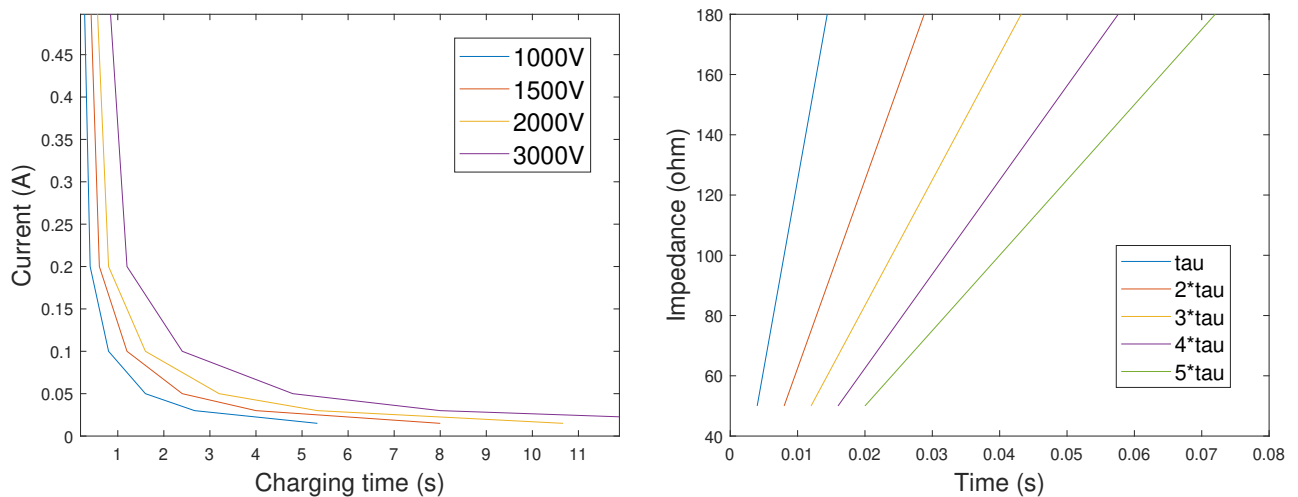**Figure 13:** Charging and discharging time

One last point to analyze is the current delivered to the patient. The current should ideally be between 30A and 37A, as a current higher than 38A could lead to bad effects for the patient [15]. In Figure 14 is shown the delivered current at the beginning of the discharge in function of the voltage at which the capacitor is charged, for different TTI values.
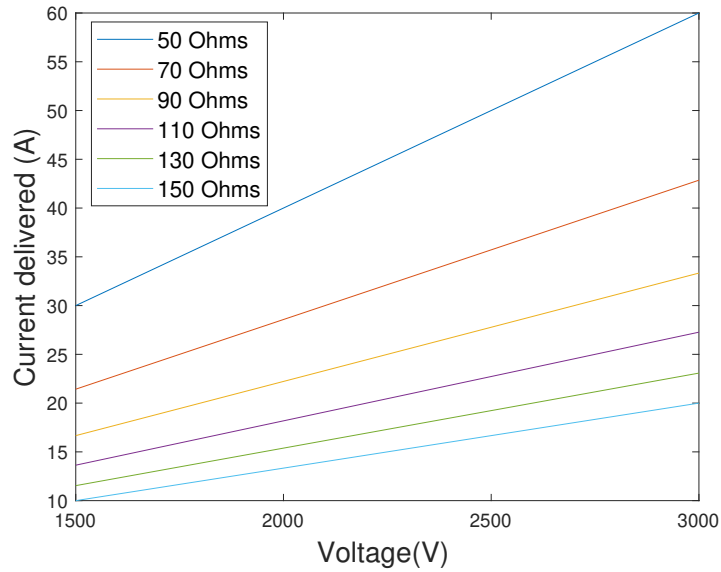
Figure 14: Current delivered to the patient

From Figure 14 can be observed that the current is maximum for lower TTI values, which is logical as V = R*i for a resistor. However, the needed voltage is also lower for lower TTI values. For example, the initial voltage with a 50Ω resistor should be around 2000V, leading to a delivered current of 40A. This is a bit high, as it is better to limit the current to 38A but remains in the adequate range. One should be careful not to use voltage higher than about 2500V with TTI as low as 50Ω to limit the current. On the contrary, high TTI values lead to low delivered current, but as explained in the next Section, TTI larger than 100Ω shouldn't be measured. Moreover, having a lower current leads to a lower harmful impact on tissues and is better if the energy delivered is high enough to defibrillate. Finally, with a TTI of 70 to 80 Ω, which is the median value for common TTI, the current remains in the range 20-40A which is well below 40A. Therefore, for common TTI values, the patient shouldn't be too much harmed.

4.3   Impedance compensation methods

Several methods can be used to compensate for the patient transthoracic impedance. It is important to take this value into account as patients with lower TTI will need a lower amount of energy to be defibrillated. This allows the patient to suffer less damage as a lower current will pass through the electrodes-patient path.

The first step to compensate for TTI is obviously to measure the impedance of the circuit seen by the defibrillator. In this project, this measurement is added to the ECG acquisition in the low voltage part. Once this impedance is known, several adjustments can be done according to the impedance measured. These different methods and what could be adjusted for this compensation are explained below:

- **Current-based compensation:** With this first method, the voltage is increased with the impedance and the biphasic pulse duration as well as the delivered current remain practically constant. For this method, a rectilinear biphasic (RLB or BR) signal is usually used.

- **Energy/Time-based compensation:** The energy remains constant but the voltage and discharge time is adapted to the impedance measured.

- **Voltage-based compensation:** The applied voltage remains constant but the discharge time is modified according to the impedance measured. With this method and the previous one, a biphasic truncated exponential (BTE) waveform is used.

These different waveforms are shown in Figure 15. Several studies have looked at the differences between RLB and BTE waveforms to decide whether one of them was better than the other. It appears that these 2 kinds of waveforms lead to similar success rates, at least for impedance lower than 120Ω. One study from Yongqin Li et al. [24], has demonstrated that for higher impedance, BR waveform could be more efficient. However, this method would use less energy but higher current, cells damage could thus be more important. One other difference between these 2 waveforms is that the BR waveform would need lower energy (120 to 200J) in comparison to the RLB (150 to 360J). But as just explained this leads to the use of higher currents.
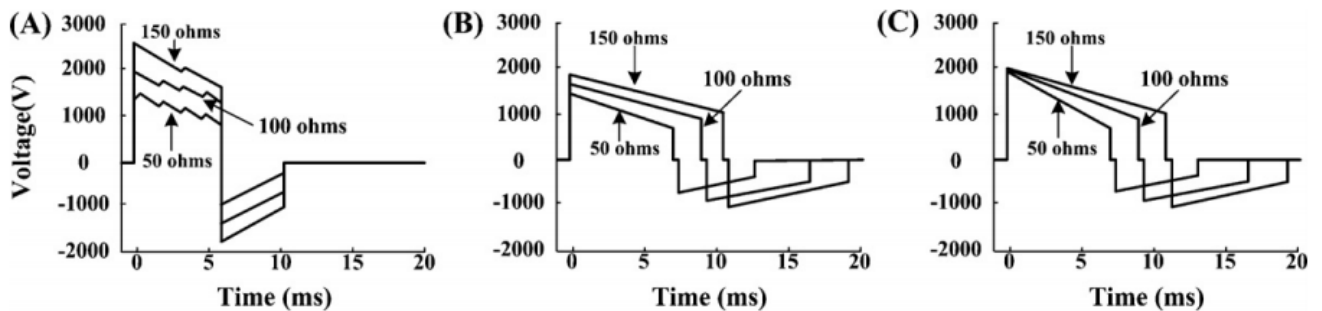

Figure 15: TTI compensation methods: A) Current-based, B) Energy-based c) Voltage-based [27]

According to the compensation method used, some studies seem to conclude that current is more important than energy when talking about the success of defibrillation and so that the current-based method may be better than the energy-based. However, the differences between waveforms don't seem significant; an energy-based compensation method could be used in this project. This choice is motivated by the fact that it may be easier to adapt the voltage used to power the circuit than to regulate the current in the circuit. Moreover, there is more information in the literature about the energy needed to defibrillate according to the measured impedance than about the current needed.

To summarize, an energy-based compensation method is chosen in this project to compensate for the TTI. For a constant energy, the powered voltage will need to be adapted to the measured impedance. Moreover, to limit the needed voltage, the time duration of the biphasic pulse also needs to be adapted to the impedance measured. However, the energy will not be constant through shocks, it will increase after each trial. By looking at what has been done in previous studies, the parameters present in Table 1 could be used. The first shock energy is given at the energy written in the table and the following ones will increase by 50J each shock, with a maximum of 5 shocks. Nevertheless, the maximum energy should remain 360J, no matter the impedance measured.

Impedance (Ω)	30-50	51-70	71-90	91-110	111-130	131-150	151-180	180-200
First shock energy (J)	100	150	150	150	200	200	300	300
Pulse duration	10ms	10ms	15 ms	15ms	15ms	20ms	20ms	20ms
First shock voltage	1600V	1950V	1950V	1950V	2300V	2300V	2800V	2900V
Tau max	4ms	5.6ms	7.2ms	8.8ms	10ms	12ms	14ms	16ms
% of energy not delivered	$\pm9\%$	$\pm15\%$	$\pm13\%$	$\pm15\%$	$\pm25\%$	$\pm20\%$	$\pm28\%$	$\pm30\%$
Adjusted voltage	1650V	2100V	2000V	2400V	2500V	2500V	3000V	3000V

Table 1: Pulse characteristics for different TTI range

It is important to tell that the first shock voltage values were computed without consideration of the circuit time constant but as previously explained, the pulse duration should be equal to at least 3τ to provide enough energy to the patient. Therefore, a modified version of the voltage is provided. This adjusted value is increased in order to provide an excess of energy to compensate for the percentage that is not delivered to the patient. When the impedance is higher than 150Ω, the time constant is too high and it is not possible to provide enough energy to the patient in less than 20ms. The capacitor should thus be charged to the maximum voltage. But again, it is known that impedances higher than 150Ω are considered abnormal and should not be measured [15]. However, as using a maximum voltage of 3000V doesn't allow to give the maximum energy for impedance higher than 100Ω, if possible, the maximum voltage provided should be higher than 3000V or the capacitor value should be increased a bit more.

5 Hardware

As explained in Section 4.1, the hardware part is composed of a low voltage side and a high voltage side that are controlled by a microcontroller. It has been shown that the voltage needs to go up to 3000V in the high voltage side but is in the range 3V to 5V in the low voltage one. This voltage difference increases the complexity of the design as a good protection between these two sides should be present. If the high voltage goes into the first side, the circuit would break. In this Section is explained what is used or could be used in this project for each part.

5.1 Microcontroller

As microcontroller, the ArduinoWiFi MKR1010 is used in this project. Many other possibilities exist but Arduino boards are versatile and the coding environment is user-friendly. This board was chosen mainly because of availability, but other smaller boards or microcontrollers could be chosen to reduce a bit more the size of the device. Indeed, the size of this Arduino board is 61.5 mm by 25 mm which is already quite large as the goal of the project is to reduce to the maximum the size of the device. One good alternative could be to use a MicroPython board that would allow to directly import the classifier model built with the Scikit-learn library in Python.

This circuit board operates at a voltage of 3.3V and is powered by a 5V source through the Vin pin. It can provide a continuous current of 7mA. It is also possible to power the board with a USB cable or a Li-Po battery of 3.7V (see pinout in Figure 16). The board contains different types of pins such as:

- 13 PWM pins;

- 7 Analog pins which can act as digital pins and one analog to digital converter (ADC);

- 8 Digital pins;

- One SCL and one SDA pin for I2C communication.

Thus, digital and analog signals can be read by the board and I2C communication is also possible. The ADC allows reading with a resolution of 8, 10 or 12 bits.
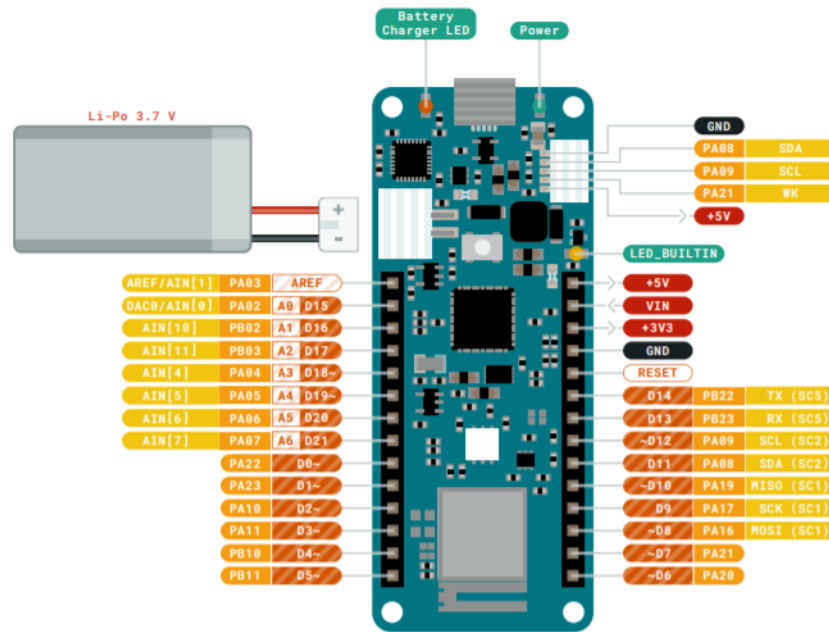
Figure 16: Arduino Board Pinout

5.2   Low voltage signal acquisition

5.2.1   ECG acquisition

To acquire the ECG signal, only two electrodes are available for the acquisition. Therefore, an ECG sensor allowing measurement with only 2 electrodes is needed. By looking at the available sensors on the market, the AD8233 appeared to be the best choice (Figure 17). Indeed, this sensor is miniaturized (2 mm*1.7 mm package) and allows a 2 electrodes configuration. Other sensors are available but many of them are designed to work with at least 3 electrodes. The voltage range of operation of this device is 1.7V to 3.5V, which allows it to be powered by the Arduino board directly (3.3V supply voltage). As can be seen in Figure 17, the device is composed of 5 main parts, 4 amplifiers (IA, A2, A3, A1) and a block that includes different pins to manage how the sensor works (FR, AC/DC, LOD, SDN, RLD SDN).
These parts have different purposes:

- **IA**: the instrumentation amplifier, is used to generate the ECG signal. It allows to integrate the error current determined using two transconductance amplifiers, it integrates deviation from the reference level, increases the common-mode voltage range with a charge pump boosts and gives an overall gain of 100 while rejecting offsets up to 300mV.

- **A1**: the operational amplifier can be used for low-pass filtering and/or to add additional gain to the initial gain of 100.

- **A2**: This one is used to invert the common-mode signal which is present at the IA inputs. It allows to improve the common-mode rejection when a third electrode (the right leg drive) is used. It also allows to make an integrator by connecting a capacitor between RLDFB and RLD to reject some common-mode line noise.

- **A3**: Reference buffer used to create a virtual ground as the device is powered by a single supply. This virtual ground is thus created between +Vs and the system ground.

- **FR and LOD for the fast restore circuit:** Settle time can be quite high due to the low cutoff frequency used in ECG high-pass filters. This part is used to reduce the time needed for the system to settle when a step signal appears. A window comparator is used to detect saturation at the IA output and if electrodes are connected to the subject, high-pass filters are formed and the cutoff frequency is shifted to a higher frequency.

- **AC/DC and LOD pin for the leads off detector:** Two modes are possible, the DC or AC mode. DC detection mode senses when the IA input voltage is within 0.27V and the positive voltage rail. Using 2 electrodes, +IN and -IN are respectively connected to a pull-up and pull-down resistor to make a voltage divider, thus, the common-mode input is set to mid supply. If electrodes are disconnected, LOD is set high. The 2 electrodes AC mode requires a conduction path between both electrodes, this one can be formed by connecting a resistor between each input and the REFOUT pin. A 100kHz current is forced, by the AD8233, into the input terminals to detect if an electrode is disconnected.

- **SDN and RLD SDN:** To enter the low power shutdown mode and to power down the RLD amplifier.
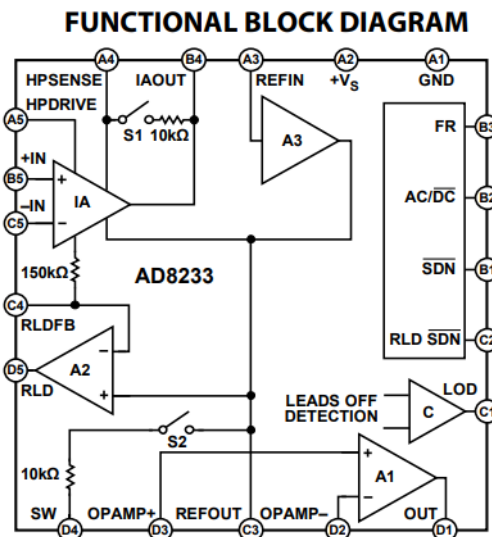

Figure 17: Block diagram of the ECG sensor (AD8233)

This sensor has 20 pins that are described in appendix A. To better understand how this sensor is used in this project, the use of these pins is explained below. The configuration of the ECG sensor in this work has been done using the combination of 2 examples given in the AD8233 Data Sheet. This combination was done using a 2-electrodes configuration for heart rate measurement next to the heart (in the left Figure 18) and the filters used in the 3-electrodes Holter monitor circuit (in the right Figure 18). Indeed, we can't use the RLD pin as a right leg driving electrode would be needed as a third electrode. However, the first configuration is not advised to make an accurate ECG analysis. Filters from the second configuration (Holter monitor) are used as the bandpass is 0.5-40Hz which is adequate to analyze the ECG shape. So the filters of the Holter configuration have been added to the first configuration. The schematic of the final ECG configuration is shown in appendix D.
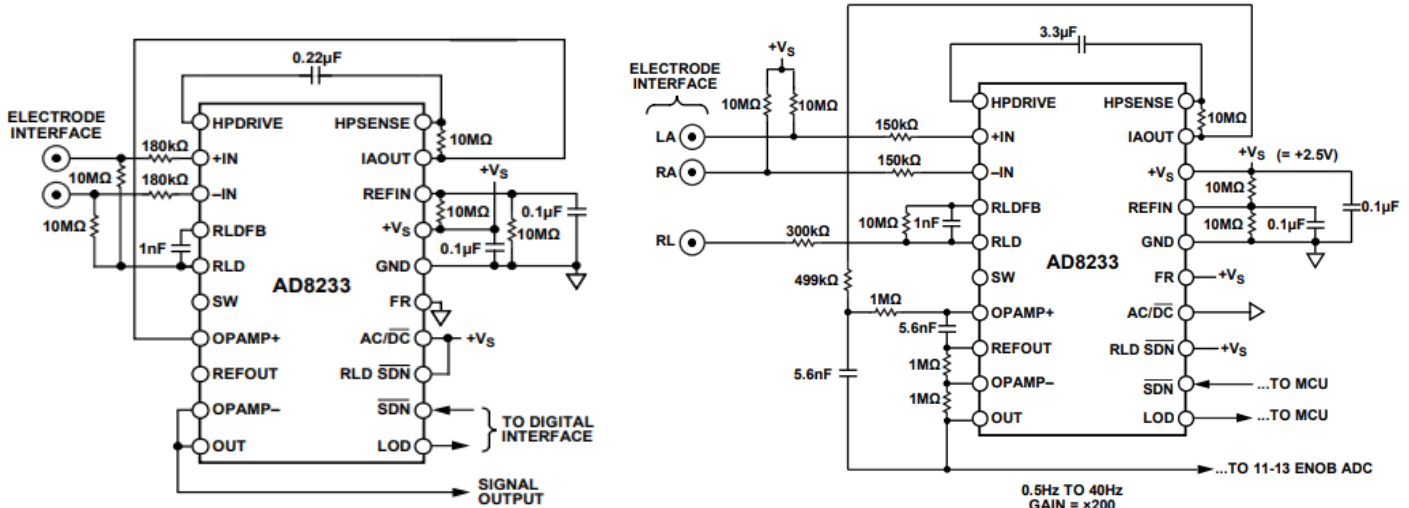
Figure 18: Examples on which ECG configuration is based

Description of the configuration:

- **GND, +VS and REFIN:**

  These pins are used for the device powering. Vs is connected to the 3.3V alimentation of the Arduino board and GND to the ground plane. Moreover, a 0.1uF decoupling capacitor is placed at the power supply. The REFIN pin is then used to set the virtual ground, $10M\Omega$ resistors are used as high values are recommended to limit the power consumption. In addition, a 0.1uF is connected between REFIN and GND for additional filtering. Large capacitors would lead to better noise filtering but would increase the settling time. This settling time is given by $\frac{5*R1*R2*C1}{R1+R2}$ which is equal to 2.5 seconds in this configuration. Maybe using a 0.01uF would have been better to reduce the settling time to 0.25s, but the signal acquired in both configurations should be compared to make this decision.

- **+IN, -IN, RLDFB, RLD:**

  First of all, a resistor is placed at each input pin (+IN, -IN) to ensure that the current never exceeds 10uA ($\frac{+Vs}{10uA} = 330k\Omega$). Then, $10M\Omega$ resistors are connected to RLD as asked for the use of AC leads off detection mode. Finally, a 1nF capacitor is placed between RLDFB and RLD to build an integrator that adds common-mode line rejection.

- **IAOUT, HPDRIVE, HPSENSE, OPAMP+, REFOUT, OPAMP-, OUT:**

  Firstly, a 3.3uF capacitor is placed between HPDRIVE and HPSENSE as well as a $10M\Omega$ between HPSENSE and IAOUT to achieve offset rejection from IA inputs. This configuration also makes a high pass filter with cutoff frequency of:

$$Fc = \frac{100}{2\pi * RC} = 0.48Hz \tag{5}$$

Secondly, a two-pole low pass filter is realized. To this purpose, a 499kΩ resistor is placed between IAOUT and OPAMP+ (R1), a $1M\Omega$ between OPAMP+ and OUT (R2), a $1M\Omega$ between OPAMP- and OUT (R3) and another $1M\Omega$ between OPAMP- and REFOUT (R4) as well as a 5.6nF between OPAMP+ and REFOUT (C2) and between OUT and IAOUT (C1). The cutoff frequency of this whole filter is given by:

$$Fc = \frac{1}{2\pi\sqrt{R1 * C1 * R2 * C2}} = 40.2Hz \tag{6}$$

In addition to this filtering, an extra gain is made from this filter with a value of $1 + \frac{R3}{R4} = 2$. By the way, the whole sensor gain becomes 200.
The output, sensed at the OUT pin, is an analog signal that needs to be converted with the Arduino board ADC.

- **FR:** This pin is connected to +Vs to enable the fast recovery mode.

- **AC/DC:** Connected to +Vs for AC leads off mode. DC leads off mode allows less power consumption, the difference of consumption between these 2 modes should be compared to determine which mode is the best one to use.

- **RLD SDN:** Connected to +Vs to have the RLD amplifier powered.

- **SDN:** The shutdown control input is connected to the ground when the device needs to enter in low power shutdown mode which consumes less than 1uA. Thus, this pin will be driven high when the device is used by the Arduino board.

- **LOD:** Output pin which indicates whether the electrodes are connected (low) or disconnected (high). This pin is read by the Arduino board.

It is important to note that additional protection could be added as the system encounters extreme overload voltages due to the defibrillation part. In the AD8233 Data Sheet, it is advised to use external series resistors and gas discharge tubes (or neon lamps which are cheaper) as protection as well as clamping resistors and low leakage diode to keep the voltage below the AD8233 maximum ratings.

5.2.2   Impedance measurement

To acquire the impedance, the circuit used in the Pmod IA (`https://reference.digilentinc.com/_media/reference/pmod/pmodia/pmodia_sch.pdf`) board has been recreated. Indeed, the schematic of this board is available at this link and only few modifications were made to use it in this project. The Pmod IA can be powered by 3.3V to 5.5V, as the 3.3V, of the Arduino board will be used to supply the impedance measurement system, the ADP150 has not been used in the project. This component was used as a linear regulator to provide a 3V voltage source. Moreover, it is possible to use an external clock but this component was not used either, as the 16.776 MHz clock of the AD5933 will be used. This board is said to be able to measure impedance as low as 100 Ω and up to 100MΩ. However, prior experiments have been done with this board and lower impedances were measured with good accuracy too.

Thus, the different components needed to make this impedance measurement system are:

- AD5933:

  This is the main component, a high precision impedance converter that contains a frequency generator with a 12-bit resolution ADC. It allows to excite an external impedance at a given frequency. The component samples itself the response signal using its ADC and a discrete Fourier transform. The output is given as a real and imaginary impedance part. This component is powered with a 2.7 to 5.5V power supply and is recommended for analysis of bioelectrical impedance. The pin description can be found in appendix B.

- AD8606:

  The AD8606 is a dual low noise operational amplifier. It combines low offsets, low noise, low input bias currents and high speed. These features allow the AD8606 to be used in a lot of different applications.

- ADG849:

  This component is a single-pole dual through switch having ultralow on-resistance. This switch allows using two different gain setting resistors. Either by connecting a 20Ω or a 100 KΩ resistor. This resistor is involved in the gain factor calculation.

The initial Pmod IA board has 5 pins which are kept in this project. These pins are connected to the Arduino board.

- VCC: Supply voltage. Connected to the 3.3V supply of the Arduino.

- GND: Ground. Connected to the board ground.

- SCL: I2C serial clock connected to the Arduino SCL.

- SDA: I2C serial data connected to the Arduino SDA.

- SEL: This pin is connected to VCC to use the 20Ω gain setting resistor by switching the ADG849 switch.

As can be understood from the presence of the SCL and SDA pins, the communication with the Arduino Board is made via I2C interface. I2C is a bus communication that consists of a pair of lines, SDA and SCL. Each device connected to the bus can read these lines. The configuration of a I2C bus with 2 devices can be seen in Figure 19. Communication is done between a master and a slave that can be specified when running the code. In this case, the master is the Arduino board. The master is the one generating a clock signal on SCL line. The component that needs to be included in the transaction with the Arduino is selected by specifying its address when initiating the communication. A transaction can occur only when SCL is low. The value read by the Arduino will be the value of SDA during a low to high transition of SCL. At each transaction, the data is exchanged in groups of 8bits. The transfer direction is determined as follows: 0 if the master is the sender; 1 if the master is the receiver.[32]
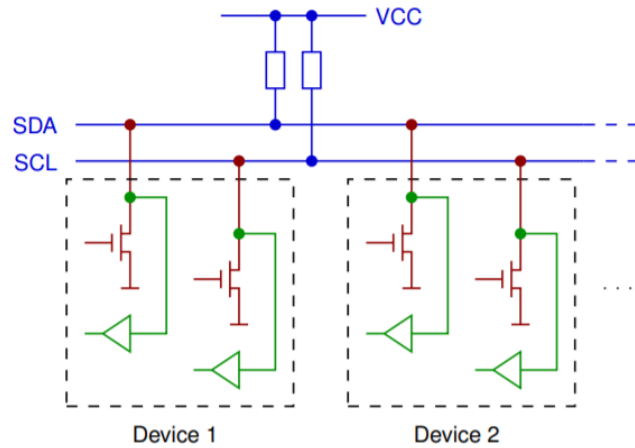
Figure 19: Configuration of an I2C bus

5.2.3   Switch

As the ECG and TTI acquisitions are made separately, a switch is needed to connect electrodes to both systems, one at the time. Indeed, these acquisitions take turn one after the other, electrodes can't be connected to both systems simultaneously. By the way, a single-pole dual through switch is needed.

The ADG1636 component has been selected in this project. This switch is powered by a +5V, -5V dual supply. The small size of this component, being 4mm*4mm, allows it to be used in small portable devices. Moreover, the typical on-resistance is about 1Ω ensuring that the TTI measured is not significantly affected by this component. Conduction is possible in both directions, allowing the excitation frequency signal from the impedance acquisition system to pass through the switch in the reverse direction. In addition to these characteristics, the maximum transition time of the switch is about 209ns allowing quick switching between the two acquisition systems.

The structure of this switch is shown in Figure 20. Pin description of this component can be found in appendix C.
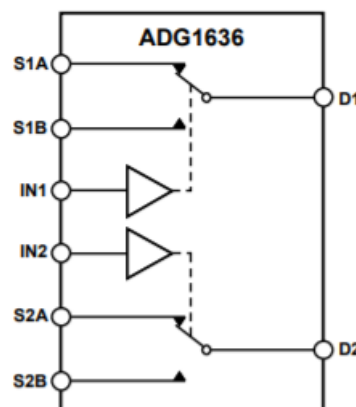

Figure 20: Switch structure (ADG1636)

In this project, these pins are connected to the followings:

- **D1:** Connected to the first electrode;

- **D2:** Connected to the second electrode;

- **VSS:** -5V power supply;

- **VDD:** 5V power supply;

- **GND:** Board ground;

- **EN:** To the 5V power supply in order to always enable the switch;

- **IN1:** Connected to an analog pin of the Arduino to control S1A and S1B switching position. If is set to 0, S1A is off and S1B on. If set to 1, S1A is on and S1B off.

- **IN2:** Connected to an analog pin of the Arduino to control S2A and S2B switching position. If is set to 0, S2A is off and S2B on. If set to 1, S2A is on and S2B off.

- **S1A/S2A:** Connected to the impedance system acquisition. They conduct when IN1 and IN2 are set to 1.

- **S1B/S2B:** Connected to the ECG system acquisition. They conduct when IN1 and IN2 are set to 0.

5.2.4   DC-DC converter

Finally, the low voltage board uses a DC-DC converter to convert power from a 9V battery into a -5V, 5V dual supply. This kind of battery is chosen as it can provide a good amount of power while having a size relatively small.

The TRN 1-0521SM from Traco Powers has been selected in this project. This component allows converting 9V in a +/- 5V dual supply. Moreover, it is of compact size, 11.9 x 11.3 x 8.0 mm and has a 1600 VDC isolation as well as a short current protection. These features are particularly useful for application in which space is limited. Finally, the output current of this component can go up to 100mA and an efficiency of about 79% is guaranteed.

By using a 9V battery having 600mAh capacity to power the low voltage board, acquisitions could be done for about a maximum of 8 hours. Indeed, the typical input current without load needed by the converter is 35mA. The total duration is given by $\frac{600}{35} = 17 hours$. However, usually only fifty percent of the battery capacity is useable, meaning that the maximum use time could be reduced to 8 hours. Moreover, consumption considering the total circuit load should be calculated to exactly know how much time the battery could last. The battery should be selected with care as some have a discharging curve more pronounced than others. Some batteries can only provide 9V for one hour, meaning that the device powering would not last long.

5.3 High voltage part

5.3.1 High voltage Converter

One of the main challenges of this project is to realize a small converter able to convert up to 3000V from a small battery. This challenge is even more tricky as the current needed to charge the capacitor needs to be at least 25mA to remain in a relatively small amount of charging time (see Section 4.2).

In the context of defibrillator devices where there exists a huge voltage difference, an isolated converter is advisable. This is why the flyback converter topology appears to be the adequate solution. This converter isolates the primary circuit from the secondary using a coupled inductor. A diode is present in the secondary circuit to prevent current to flow during the first phase. Indeed, during the first phase, energy is stored in the coil as the current can't flow through the secondary circuit. In the second phase, the primary circuit is opened, the current flows in the opposite direction in the secondary part and the flow can pass through the diode. The energy accumulated in the coil during the first phase can be released in the secondary by this way. To control the switch in the primary, a PWM signal is used and allows to control the amount of energy stored.
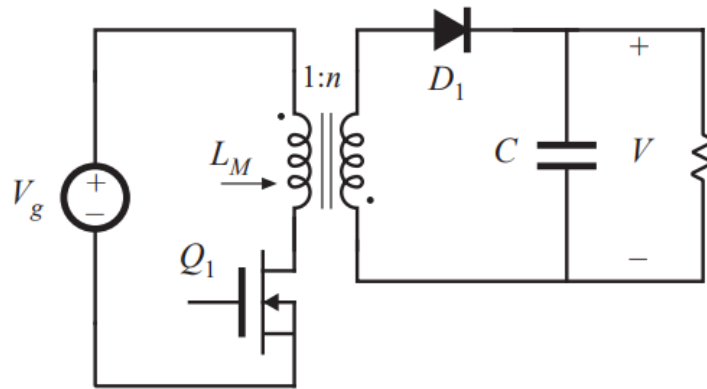

Figure 21: Flyback converter topology [35]

From this configuration, the following relationship can be deduced:

$$\frac{Vo}{Vin} = n\frac{Don}{Doff} \tag{7}$$

With Vo the voltage in the secondary and Vin the voltage in the primary; n is the ratio of turns in the second coil over the number of turns in the first coil ($\frac{N2}{N1}$); Don and Doff are the switching times duration.

Moreover, flyback converter can work in two possible modes, the continuous or the discontinuous conduction mode:[36]

- **CCM**
  With this mode, not all the energy stored in the primary is transferred to the secondary. The MOSFET is turned on when energy is still present in the primary. Like is shown in Figure 22, the current never reaches zero. This configuration allows using a lower current peak to obtain the desired average current. This feature makes the CCM a good choice for the project as a smaller battery is usually able to provide a smaller peak current.

- **DCM**

  With this mode, all the energy stored in the primary part of the transformer is transferred to the secondary at each cycle. The MOSFET is turned on just after the current has reached zero. This type of converter is usually smaller, which is a feature wanted with the device. However, the peak current needed is higher and so the battery to provide this current would certainly be bigger too, which is not desired.
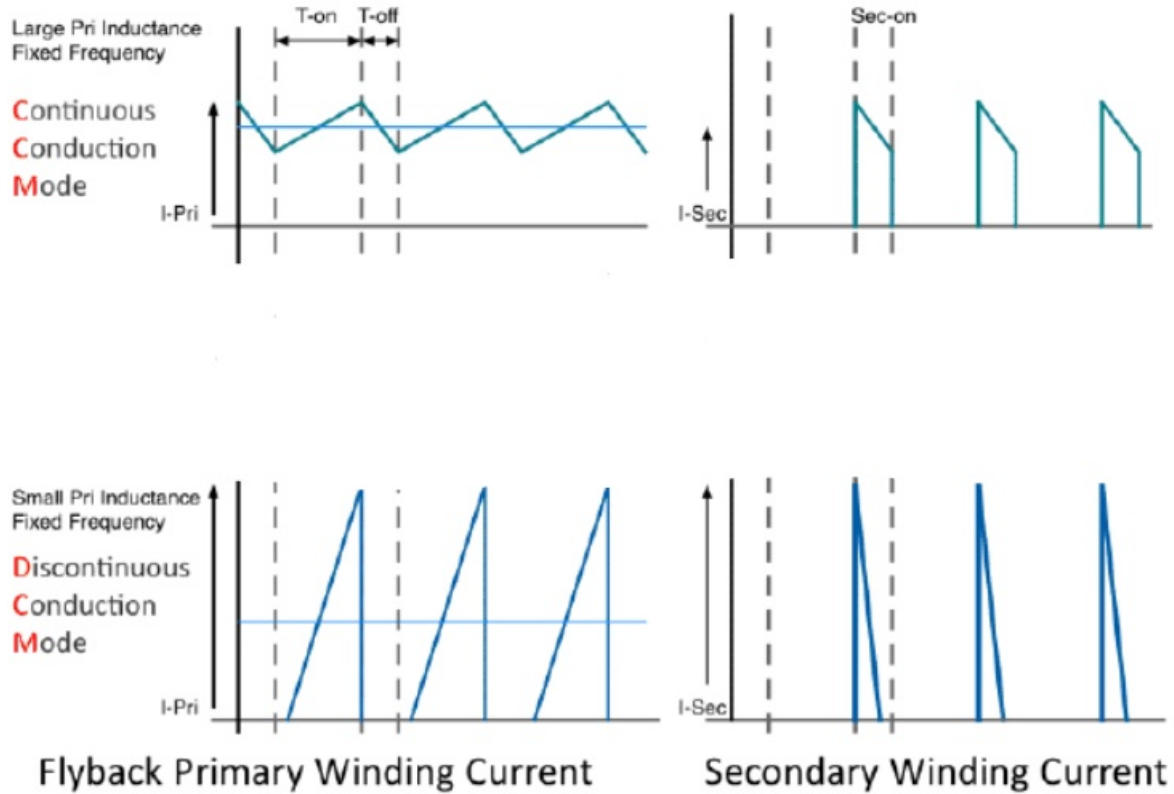

Figure 22: CCM and DCM currents waveforms [36]

Let's illustrate how the circuit behaves in CCM using a small ripple approximation [35]. First of all, in addition to the transformer, a small magnetizing inductance in parallel with it can be added when modeling the flyback. The 2 following phases encounter by the flyback are thus represented in Figure 23.

First phase: The primary switch, Q1, is on and the diode in the secondary, D1, is off. The following relations described the circuit:

$$V_L = V_g \qquad i_C = -\frac{V}{R} \qquad i_g = I \tag{8}$$

Second phase: The primary switch, Q1, is off and the diode in the secondary, D1, is on. The following relations described the circuit:

$$V_L = -\frac{V}{n} \qquad i_C = \frac{I}{n} - \frac{V}{R} \qquad i_g = 0 \tag{9}$$
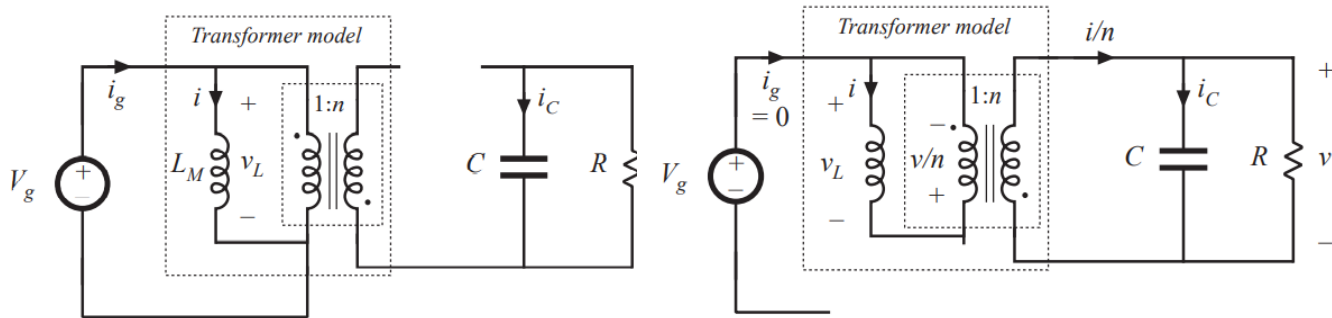
Figure 23: Two phases of the flyback converter model [35]

Flyback seems to be an adequate solution for this kind of application. Nevertheless, it won't be so easy to design the perfect converter. Indeed, there are some compromises between the size of the device and the power needed. Simulations should be done to better understand which of the 2 modes would be adequate in this project and what would be the design needs.

A good solution when doing a converter for defibrillator devices could be to work at the limit between continuous and discontinuous mode. This would allow not to lose energy in between cycles and to take advantages of features from both modes. This kind of converter is also called self-oscillating converter as it monitors itself when the current reaches zero to switch to the next phase. Nevertheless, as the peak current would need to be higher than in continuous mode it should be verified if this is possible. In-depth investigations, as well as simulations, should be done to determine what would be the adequate mode of operation.

An explanation is presented here below about the continuous current mode topology that could be used in this project. First of all, as the goal of the flyback is to charge a capacitor, a topology of circuit as shown in Figure 24 should be used. Ideally, no resistor is present in the secondary as the electrodes should be disconnected from the flyback when charging the capacitor. This is necessary in order to avoid discharges into the patient between pulses. However, some parasitic resistors would be present, but they are not considered at the moment.
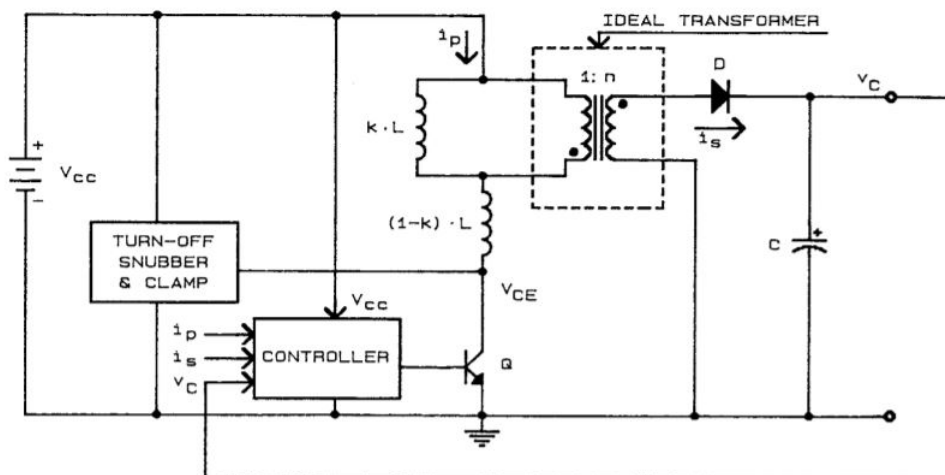

Figure 24: Flyback circuit topology [37]

One point to consider is the number of pulse in function of the target energy. The maximum energy is 360J, considering a switching frequency of 50kHz and a charging time of 10 seconds, the energy per pulse needs to be: [38]

$$E_{pulse} = \frac{360J}{50kHz * 10s} = 720uJ \tag{10}$$

The efficiency of the converter will need to be taken into account as the energy per pulse is actually the energy divided by the efficiency. Using the equation describing the inductance value, the peak current and the needed inductance are found to be: [38]

$$I_p = \frac{2 * E_{pulse}}{V * T_{pulse}} = 12A \qquad L = \frac{V_1 * T_{pulse}}{I_p} = \frac{2 * E_{pulse}}{I_p^2} = 10uH \tag{11}$$

V is the primary voltage (12V) and T_{pulse} the maximum on time per pulse (10 seconds/2*500000 pulses) considering the on and off times equal.

As the maximum current peak is 12A, if it is considered that the mean current will be about 10A, a battery able to provide 1.67Ah is needed. Indeed, 10A during 10 seconds is the minimum to deliver one shock. However, several shocks could be delivered, if a maximum of 3 shocks is assumed, the whole battery capacity should be 5Ah. Large batteries can provide this amount of current, this is why finding an adequate powering system is challenging.

5.3.2 Biphasic pulse generation

Once the capacitor is charged, the energy still needs to be delivered to the subject. As it has been explained in Section 4.1, a biphasic pulse needs to be released through the subject-electrodes path. In order to do that, the capacitor will need first to discharge in one direction, from electrode one to electrode two, then in the other direction. To achieve this, a bridge using four switches is an adequate solution, this configuration is shown in Figure 25.
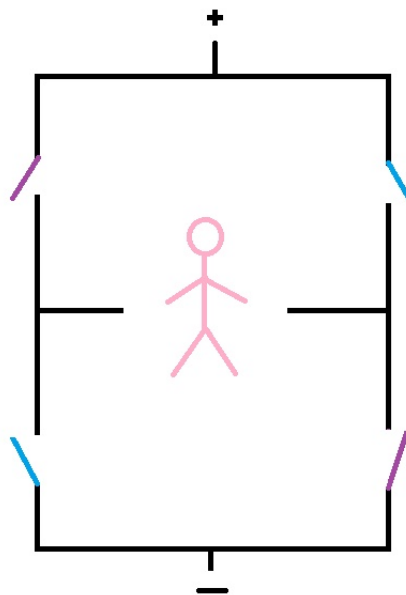

Figure 25: Bridge configuration

This release of energy would occur in 3 steps:

1. Purple switches are closed and blue switches opened. The discharge pulse follows the purple switches' path (from the left to the right).

2. Transition time, when the purple switches are opening and the blue switches are closing. This step should be as fast as possible and lower than a few milliseconds.

3. Blue switches are closed and the purple ones opened. The discharge is continued through the blue switches path (from the right to the left).

To generate this pulse, switches need to be fast and to be able to withstand huge voltage. There exist two kinds of switches that can meet these features: the IGBTs and the Sic MOSFETs.

SiC MOSFETs

Silicon carbide MOSFET is a quite recent type of MOSFET that is being more and more investigated for high voltage applications. Before their discovery in the 1970s, bipolar transistors (BJTs) were widely used [44]. These are characterized by a high base current needed and slow turn off features. However, MOSFETs outperformed BJTs with their voltage-controlled ability and lower losses. Now, MOSFETs are by far the most common components used in microelectronics.

Metal oxide semiconductor transistor, MOSFET (Figure 26), is a component used as a switch or to amplify signals. They have an almost infinite input impedance, allowing them to capture entire signals when amplifying. They can be controlled with almost no current, as the voltage is the important physical quantity to control them. Indeed, MOSFET is on when the gate to source voltage is higher than a certain threshold. In this mode, the current can flow between the drain and the source.
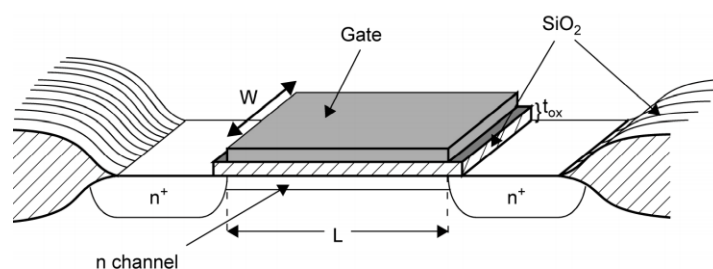

Figure 26: MOSFET configuration [47]

The SiC MOSFET, is a new generation of MOSFET that has emerged several years ago. They have a high electric breakdown field, about 10 times the one of Silicon. One other characteristic is their strong atomic bond, providing them good thermal conduction. The on-resistance is usually low (mΩ) and can be decreased by increasing the dopant concentration. However, by doing that the withstand voltage is decreased. Common Si MOSFETs can withstand voltage up to 1000V against 3300V for SiC MOSFETs [43]. The first MOSFET of this kind was built in 1992 [46]. Nevertheless, SiC MOSFETs are only at the early stage for high voltage applications.

Indeed, even if new technologies have emerged, the substrate price limited the research during the past few years. However, in 2016 the cost was already reduced to 8% of its 2012 price [46]. Therefore, these devices should be more and more commercialized with time. Nowadays, SiC MOSFETs are mainly able to withstand voltages up to 1.7kV but some going up to 3.3kV start to appear on the market.

IGBTs

Insulated gate bipolar transistors (IGBTs) appeared in the 1980's as a compromise between MOSFETs and bipolar transistors [44]. Indeed, they were intended to encounter the high current applications' limitation of BJTs and MOSFETs. They possess the output switching and conduction of bipolar transistors with the voltage-controlled feature of the MOSFETs. They have the configuration shown in Figure 27 and works similarly to the MOSFETs. One of the main issues with these transistors is the turn-off losses. A significant tail current during turn-off is generated due to the accumulation of minority carriers [43]. They are usually made of Si but some studies have analyzed the benefit of using SiC instead [42]. Obviously, as for the MOSFETs, switching characteristics are better but their use is certainly limited by the higher substrate price.
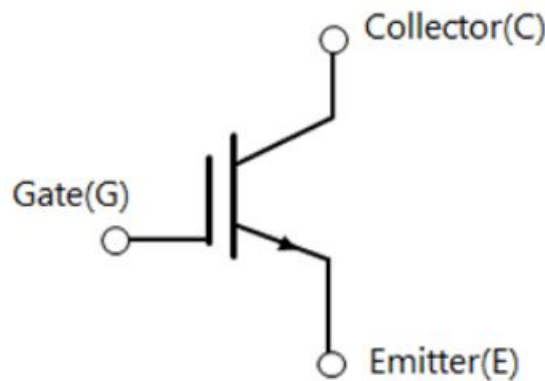

Figure 27: IGBTs configuration [39]

Comparison between IGBTs and SiC MOSFETs

First of all, SiC MOSFETs are expected to replace IGBTs, at least up to a certain voltage range. Nowadays, SiC MOSFETs can go up to 3.3kV but are more commonly limited to 1.7kV. It is usually told that IGBTs should be used for higher than 1000V applications. However, it is less and less true as MOSFETs technologies are improving. These MOSFETs have a higher switching frequency and are advised for frequency higher than 200kHz. However, IGBTs should be used for power higher than 5kW. Indeed, MOSFETs can't usually be used in high power circuit and should be limited to less than 500W applications [44]. SiC MOSFETs have faster switching capability and can be easily miniaturized as they can be used at high frequency. They also have lower switching and conduction losses but they are also more sensitive to parasitic [41]. A study [46] comparing a MOSFET and an IGBT used in the same application has shown that SiC MOSFETs lost 124 and 243 mJ when switching against 695 and 1370 mJ for IGBTs. For low power application, SiC MOSFETs are thus more adequate. For high power applications, losses with IGBTs could be small enough to be non-significant.

In this project, as a high power high voltage circuit is made, IGBTs could be the better choice. Indeed, they need to handle a voltage going up to 3kV and only few MOSFETs have been commercialized withstanding this voltage. It is certainly too soon yet to use SiC MOSFETs in high current applications. It is still a promising solution on which an eye should be kept. Moreover, the switching frequency of IGBTs is lower than MOSFETs but as the transition time could go up to one or two milliseconds, it shouldn't be an issue as IGBTs have usually a switching time in the microseconds range. The main drawback in this application may be the size that could be smaller if using MOSFETs.

Driver system

In order to drive these switches, a specific circuit would be necessary. Several drivers exist on the market and could be selected to drive the switches gate. However, protection should be present between the drivers and the board. The best solution could be to use an isolated DC/DC converter that would be tied between the drivers and the board. This solution is adequate as the switching speed can be up to 1 or 2ms which is not especially fast.

5.4   Circuit relay

To be able to switch electrodes between the low voltage acquisition board and the high voltage one, a reliable switch needs to be used. As the voltage difference between these two boards is huge, the use of a reliable relay would be the best choice.

Relays are switches that operate with an electrical signal to connect or disconnect a circuit. There exist two main types of relay, electromechanical and solid-state.

- **Electromechanical** relays are composed of 4 main parts: an electromagnet, mechanically movable contacts, switching points and a spring. When a current pass through the electromagnet, a magnetic field is generated around it. The moving parts are attracted to it, the relay is energized. If the current stops, the relay is de-energized and the contacts come back to their initial position. The general configuration of these relays is shown in the left Figure 28. [33]

- **Solid-state** relay (SSR) are composed of 3 main parts: the input circuit, the isolation part and the output circuit (as shown in the right Figure 28). The input and output circuit are usually isolated through an optical link. Indeed, when the input circuit LED emits light, the light operating switch in the output circuit closes allowing current to flow in the output circuit. [34]

SSR relays are usually faster than electromechanical relays, they provide physical isolation, have a higher life expectancy and are less subject to wear. However, the resistance is higher in the output circuit than the one of an electromechanical relay and they are less resistant to overload conditions, SSR can easily be destroyed if a spike goes above the relay limits. This is why an electromechanical relay should be used in this project. [34]
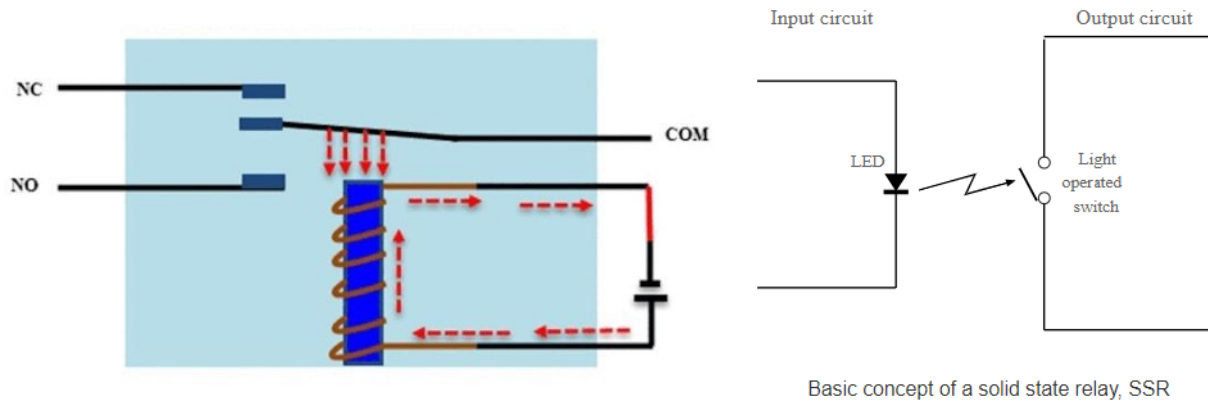
Figure 28: Relays structure [33], [34]

The G6K surface mounting DC electromechanical DPDT relay has been chosen in this project. This relay is the smallest mounting area relay that could be found, its area is given by 5.2 (H) * 6.5 (W) * 10 (L) mm. It can be powered by a 5V supply. The operating set time and release reset time are maximum 3ms each which is clearly sufficient for the application. Some experiments should be done to verify the reliability of this component in the project conditions. If the component can't withstand the maximum defibrillation pulse, another relay could be found but having a size a little higher.

This relay is used in combination with the diode MBRA210LT3G and the MOSFET FDV303N as can be seen in Figure 68 of appendix D. Indeed, the relay is connected between a 5V supply voltage and a MOSFET having its source at the ground and its gate connected to an Arduino pin. When the MOSFET gate voltage is lower than threshold voltage (0.8V), meaning that the pin is set low, the electrodes are connected to the high voltage board. When the gate voltage exceeds the threshold, the relay is connected between the 5V supply source and the ground. This leads to a current flowing through the coil. This current creates a magnetic field that attracts the moving parts and thus connects the electrodes to the low voltage board. When the gate voltage becomes again lower than the threshold voltage, the power stored in the coil is released in a path created between the diode and the coil.

5.5   Printed Circuit Board

A PCB has been made for the low voltage part. This one comprises the Arduino board, the ECG and impedance systems acquisition, a DC-DC converter, the ECG/Impedance switch and the relay needed to separate the high voltage from the low voltage side. This board is shown in Figure 29. Its size is 7*8.3 cm, it is relatively small but could be reduced even more. Indeed, almost half the PCB size is taken by the Arduino board but as previously explained, a smaller board could be used.
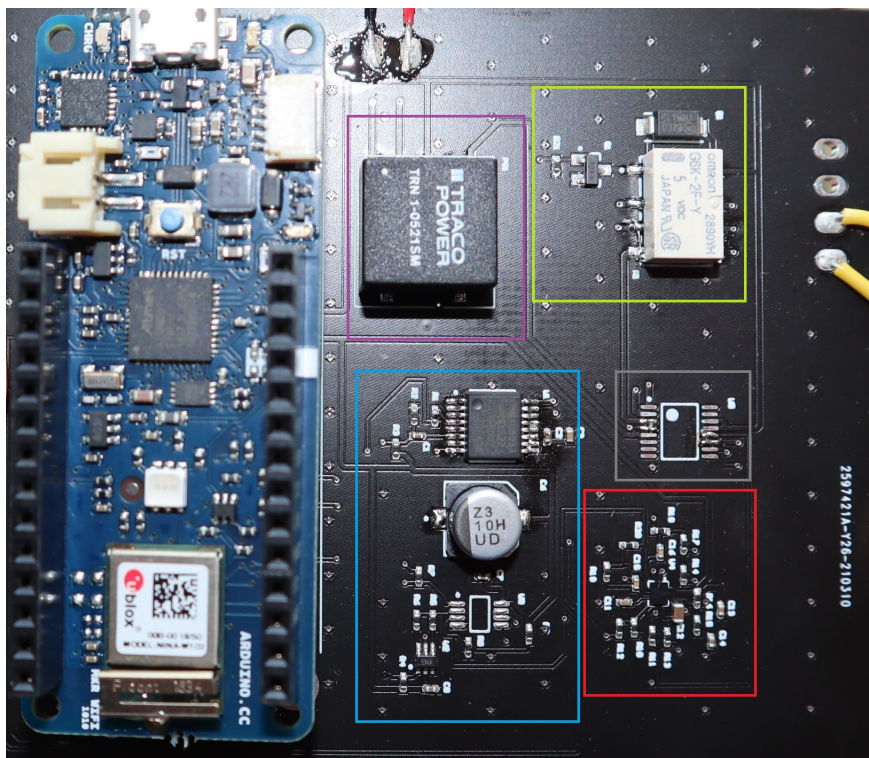

Figure 29: Low voltage PCB

The different parts of the board are surrounded by a box:

- **DC-DC converter**

- **Relay**

- **Impedance measurement**

- **ECG acquisition**

- **Switch**

As it can be seen from the picture of the PCB, two components are missing. Due to stock shortage, the OPAMP AD8606 needed to acquire low impedances as well as the ADG1636 switch, have not been acquired in time. Therefore, only the ECG acquisition was possible using this board. However, the PMOD IA has been used to make impedance measurements.

6 Software

6.1 ECG signal classification

The ECG signal needs to be analyzed in order to detect ventricular tachycardia and fibrillation. Indeed, a shock will be delivered only if the ECG rhythm is detected as shockable. To meet standards, the detection algorithm should have sensitivity higher than 95% and specificity higher than 98%. Already good algorithms exist with accuracy up to 98%. As it is shown in the paper from Y.Xu et al. [49], the specificity is usually better than the sensitivity. Indeed, it is not desired to shock people that shouldn't be, as it would be very harmful to them.

In this section, is searched a model that could reach or even outperform existing models by using common features of ECG. As it is a growing field that is more and more used with time, machine learning models will be made and compared. In order to train and test models, ECG recordings from 2 databases are used. These 2 databases can be found in the Physionet Bank [48]. The first database used is the MIT-BIH Malignant Ventricular Ectopy Database (VFDB) that comes from the publication Greenwald SD. Development and analysis of a ventricular fibrillation detector. M.S. thesis, MIT Dept. of Electrical Engineering and Computer Science, 1986. The second one is CU Ventricular Tachyarrhythmia Database (CUVT) from "Nolle FM, Badura FK, Catlett JM, Bowser RW, Sketch MH. CREI-GARD, a new concept in computerized arrhythmia monitoring systems. Computers in Cardiology 13:515-518 (1986)". In appendix G are shown some examples of recordings that can be found in these databases.

6.1.1 Training/Test set

CUVT database: This database includes 35 recordings of 8 minutes with subjects experiencing ventricular tachycardia, flutter (rapid VT) and fibrillation.

VFDB database: In this one, some episodes of VT, as well as VF, are present but other annotations can be found too. As the goal of the model is to detect shockable rhythms (VF and VT), each rhythm, different from these two, is classified as normal.

An annotation file is provided with each ECG recording. These files include the annotation of each recording by signaling when the rhythm change and what is the rhythm. Verification of these annotations would have been great to do, to be sure to work with well-labeled recordings, but this step was not feasible in this project. In order to build the training/test set, windows of 10 seconds have been extracted from each recording, with their corresponding label. Either a window is classified as normal rhythm or as shockable rhythm. In order to do this, one MATLAB code for each database has been created.

These codes take as input ECG recordings as well as annotation files and follow several steps to extract these windows:

- The current recording is imported in MATLAB with its signal information (sampling frequency and gain). The signal is scaled using the gain and the time matrix made knowing the sampling frequency.

- Once the recording is correctly imported in MATLAB it needs to be pre-processed as advised in some papers [50], [51]:

  1. Mean subtraction;

  2. Application of a 5 order moving average filter;

  3. High pass filter with a 1Hz cutoff frequency (0.5Hz may have been a better choice as it is more often advised but this does not result in big differences);

  4. Low pass Butterworth filter with a 30Hz cutoff frequency.

- The annotation file is read through and each window of 10 seconds staying at a constant rhythm is kept and classified either to the normal or shockable set.

- Finally, each window is verified. The ones having artefacts, that could be due to a defibrillation shock, are removed.

Each window has a size of 10 seconds, this allows to test different window sizes. Indeed, using windows of 10 seconds is already quite large, smaller windows are often used.

6.1.2   ECG Features

In order to train models, useful features need to be extracted from ECG windows. Most of the features have been found in the paper [51] and [50]. The ones looking the most relevant have been computed using information from original papers in which they were explained. A total of 28 features have finally been computed. These include temporal, spectral and complex types of feature. Before doing this step, windows have been normalized by putting the mean to 0 and dividing each sample, by the maximum value of the window, to keep values in the range -1 to 1. This allows using both databases simultaneously. In the following features' description item, examples of features are shown for one normal and one shockable rhythm from the VFDB database. These two signals are shown in Figure 30. Nevertheless, it is important to keep in mind that normal rhythm recordings are not always as clear as in this example. Indeed, in appendix G is shown an example of a normal rhythm recording that looks closer to a shockable rhythm. This explains why for some recordings, the values of the features computed on normal rhythms may be closer to the one of VT/VF (shockable) rhythms.

- **TCI [52]:** Threshold crossing interval is the average interval between the crossings of the binarized signal. Each second of the window, the peak is computed and a threshold is set to 20% of this peak. The signal is binarized by putting to one, values above the threshold and to zero, values below. This gives a signal having its values to 1 when a peak is detected (see Figure 32). Once the binary signal is acquired, t1, t2, t3 and t4, as shown in Figure 31, need to be computed. To simplify this step, a subwindow of the signal is kept by putting t1 and t4 to 0 seconds.

  TCI can be found using this relationship:

  $$TCI = \frac{WindowSize(s)}{(Npeaks - 1) + \frac{t_2}{t_1 + t_2} + \frac{t_3}{t_3 + t_4}} \qquad (12)$$
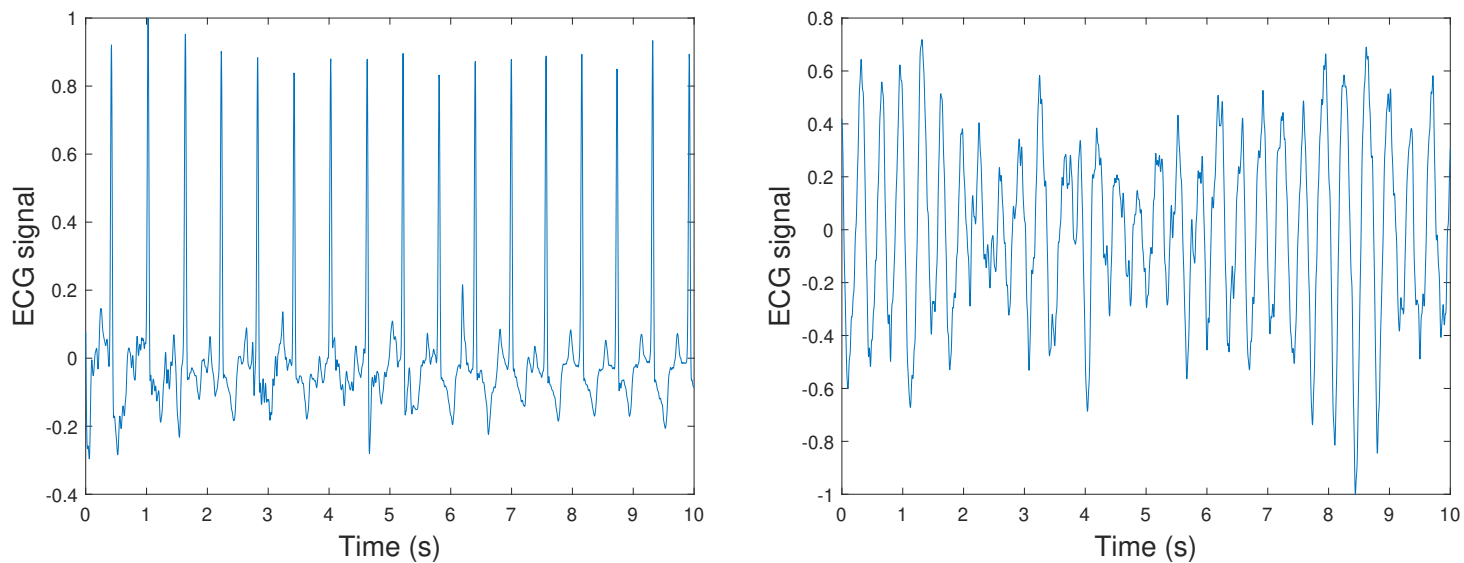
  This feature should be lower for shockable rhythms.

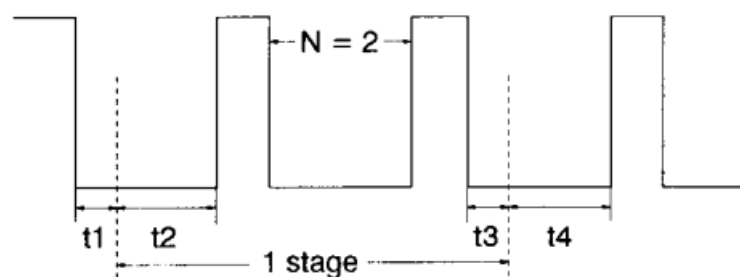**Figure 30:** 10 seconds signals used to illustrate features

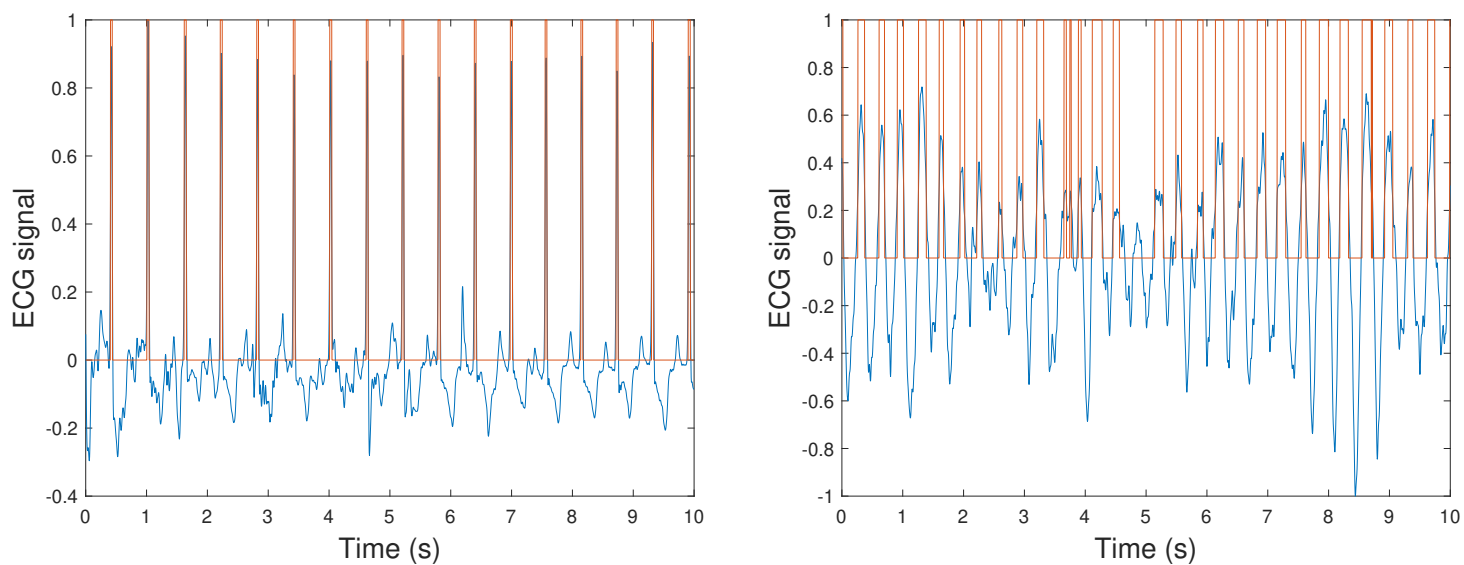**Figure 31:** TCI convention of the binarized signal [52]

Figure 32: Binarized signal used for the TCI computation

- **MAV[53]:** Mean absolute value is computed by taking the mean of the absolute value of the signal:

$$MAV = \frac{1}{N} \sum_{n=0}^{N-1} |x(n)| \tag{13}$$

With n being the number of samples in the window. This feature should be larger for shockable rhythms.

- **Count [54]:** This feature is in fact divided in 3 subfeatures:

    1. Count1: The number of samples in the interval 0.5*max(AbsFS) to max(AbsFS);
    2. Count2: The number of samples in the interval mean(AbsFS) to max(AbsFS);
    3. Count3: The number of samples in the interval mean(AbsFs)-MD to mean(AbsFS)+MD. MD being the mean deviation.

The first step is thus to compute the signal AbsFS. This is the absolute value of the digital integer-coefficient filter output. This filter is computing using:

$$FS_i = \frac{14FS_{i-1} - 7FS_{i-2} + \frac{S_i - S_{i-2}}{2}}{8} \tag{14}$$

Applying this filtration results in a signal having its frequencies in the range 13 to 16.5 Hz. The resulting signals are shown in Figure 33.
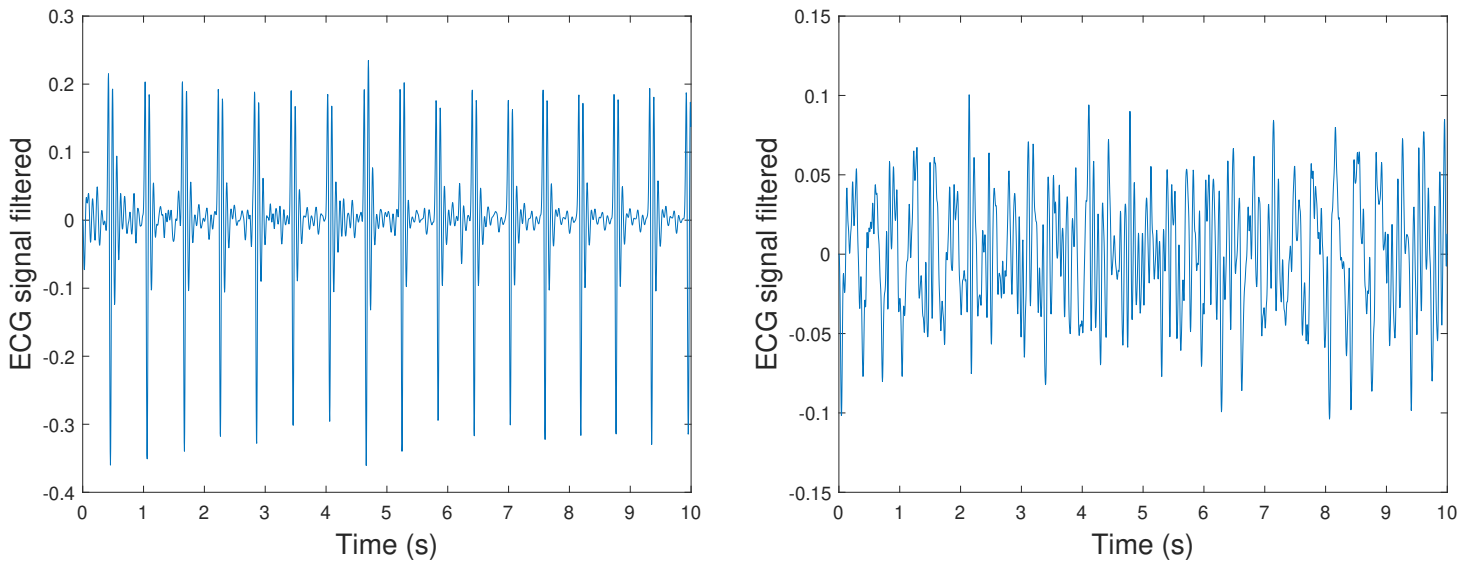

Figure 33: Signals filtered with the digital integer-coefficient filter

- **Bwt [55]:** This feature is the interval around the 0mV line that contains a certain percentage of the total number of samples. It should be larger for VT and VF rhythms. However, this feature hasn't been used exactly as how it is defined. Indeed, the feature seemed more useful when using an alternative version of it. Instead of taking the interval in which a certain percentage of the data is, the percentage of data contained in the interval [-0.15,0.15] has been taken. The interval was chosen by looking visually at different signals and by testing which interval gave the bigger difference between normal and shockable rhythms.

- **BCP** [55]**:** This feature represents the percentage of time the signal first difference squared (illustration in Figure 34) is below a certain threshold. The threshold has been decided to be 0.002 by comparing results on shockable and normal rhythms using different thresholds.
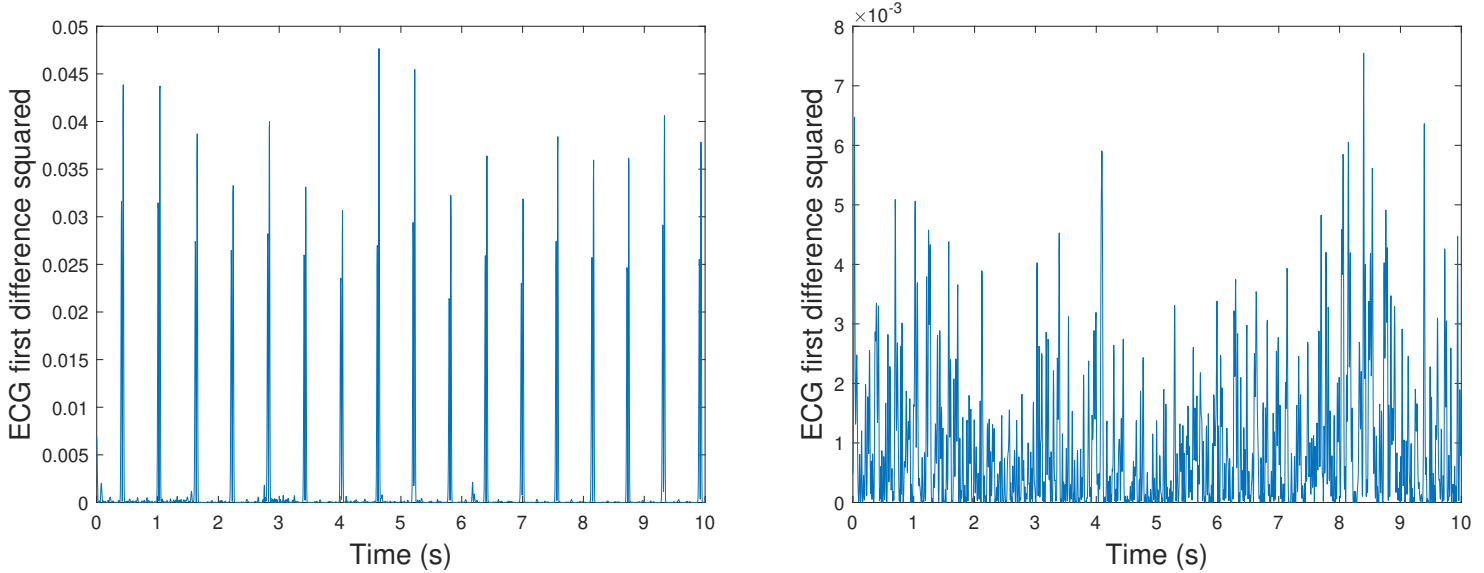

Figure 34: Square of the first difference of the ECG signal

- **Frequency domain features** [50]**:** Four features are computed using the Fast Fourier Transform of the ECG signal (examples in Figure 35):

  1. **FSMN:** This is the first spectral moment normalized over the 20 first harmonics. This has a lower value for VF (should be closer to 1).

$$FSMN = \frac{1}{F}\frac{\sum x_i f_i}{\sum x_i} \qquad (15)$$

  F is the reference frequency, the frequency of the component having the greatest amplitude; x_i is the amplitude of the frequency i.

  2. **A1:** The sum of amplitudes between 0.5Hz and $\frac{F}{2}$ over the sum of amplitudes between 0.5Hz and 20F.

  3. **A2:** The sum of amplitudes between 0.7F and 1.4F over the sum of amplitudes between 0.5Hz and 20F.

  4. **A3:** The sum of amplitudes in a band of 1.2Hz around second to eighth harmonics (2F to 8F) over the sum of amplitudes between 0.5Hz and 20F.

- **Complexity measure** [50][56]**:** Another binarized signal is computed by a proposed procedure. Then several features can be calculated using this signal. The process follows the following steps.

  – Nc, the number of samples between 10% Vn (negative peak) and 0 as well as Pc, the number of samples between 0 and 10% Vp (positive peak) are computed;

  – If Pc + Nc is lower than 40% of the number of samples, the threshold is put to 0; if Pc is lower than Nc, the threshold is 20% of Vp; else the threshold is 20% of Vn;
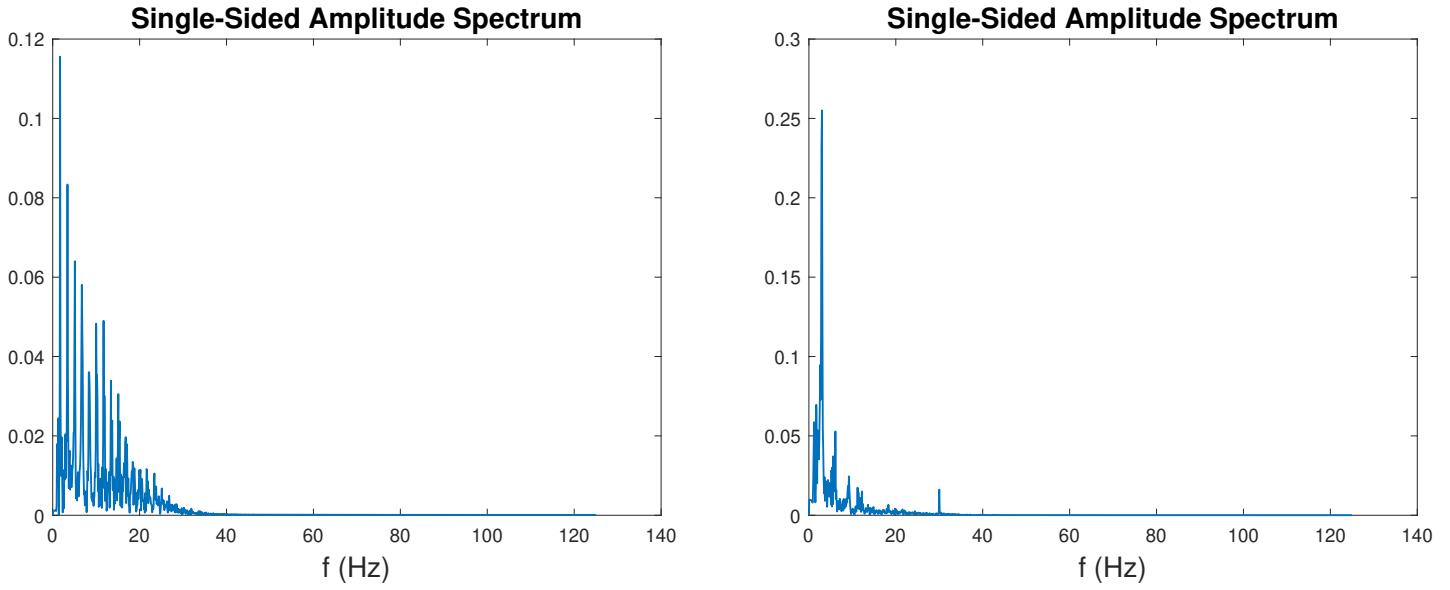
Figure 35: Fast Fourier Transform

– Once the threshold is found, each sample lower than this threshold is set to 0 and each one bigger than the threshold is set to 1.

This results in the binary signal shown in Figure 36.

Once this binarized signal obtained, the complexity measure, c, is calculated by following a small algorithm. S and Q are two strings, SQ is their concatenation and SQp is SQ without the last element. The initial conditions are given by $c = 1, S = s_1, Q = s_2$ and $SQp = s_1$. After some steps $S = s_i, ..., s_r$ and $Q = s_{r+1}$. If Q is a substring of SQp, S remains the same and Q becomes Q with one element added until Q is not a substring anymore. When Q is not a substring of SQp, S becomes Q $(s_1, ..., s_{r+1}, ..., s_{r+i})$, $Q = s_{r+i+1}$ and $c = c + 1$.
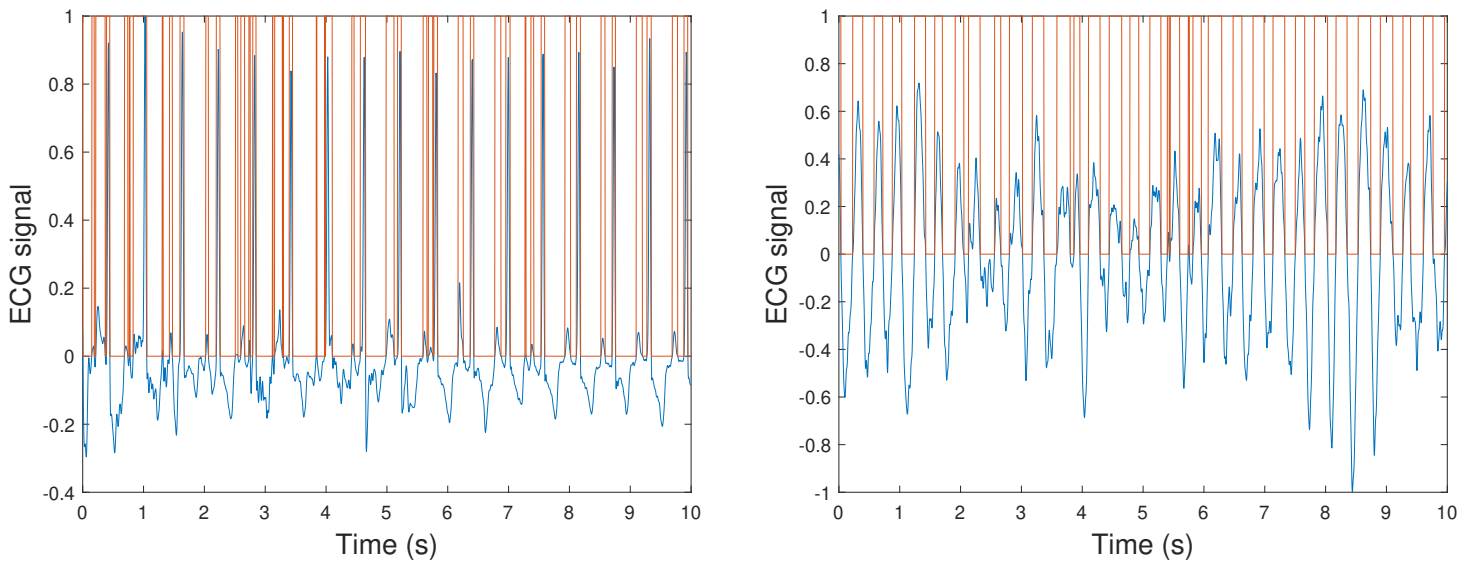

Figure 36: Binarized signal

- **Covariance** The signal variance can be computed on the original ECG signal and on the binary signal computed previously. It should be higher for shockable rhythms.

- **Leakage VF filter** [50]: A narrowband pass filter having as central frequency, the mean frequency, is applied to the signal. In other word, the ECG signal is combined with its image shifted by half a period.

$$Leakage = \frac{\sum_{i=1}^{m} |V_i + V_{i-\frac{T}{2}}|}{\sum_{i=1}^{m} |V_i| + |V_{i-\frac{T}{2}}|} \tag{16}$$

- **Area:** This feature can be computed for the binary and original signal. In the first case, it is defined as the maximum between the sum of all bins and the sum of all inverted bins. In the second case, it is defined as the area under the curve.

- **Bin frequency:** Count the number of transitions from 0 to 1 and 1 to 0, divided by the window size.

- **Kurtosis:** This feature is a descriptor of the probability distribution sharpness of the signal. It can be directly computed using the *kurtosis* function in **MATLAB**.

- **Phase Space**[58]: This last feature uses a phase space representation of the signal to highlight the differences between normal and shockable rhythms. This phase space takes the original ECG signal as abscissa and the signal shifted of tau as ordinate. Tau is chosen to be 0.5 as advised in the reference paper. The phase space is divided into 400 0.1*0.1 boxes in the space -1 to 1. The feature is computed to be the number of visited boxes over the total number of boxes. It should be higher for VF/VT rhythms as they are represented by more points in the phase space (as shown in Figure 37). Indeed, a clear normal ECG activity recording shows a perpendicular distribution of its samples.
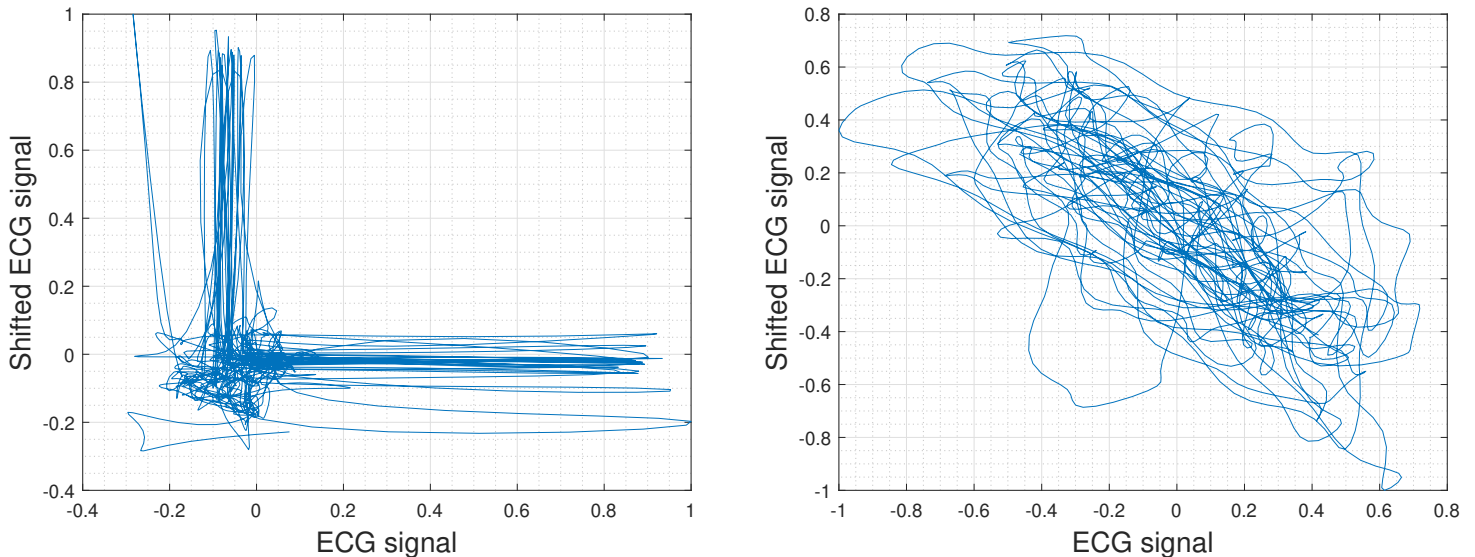

Figure 37: Phase Space

6.1.3   Features selection

First of all, the entire set was divided into a training set and a test set (containing 25% of all data). Shockable rhythms have been labeled to 1 and normal rhythms to 0. Moreover, six matrices of features have been computed to make different analysis:

1. Features computed with 10 seconds window from the VFDB database;

2. Features computed with 10 seconds window from the CUVT database;

3. Features computed with 5 seconds window from the VFDB database;

4. Features computed with 5 seconds window from the CUVT database;

5. Features computed with 10 seconds window using both databases;

6. Features computed with 5 seconds window using both databases;

In order to determine which of the features are the most useful, the random forest classifier from the Scikit-learn library of Python is used. This classifier is one of the best that can be found and allow displaying features importance.

As each window of ECG recordings has been binarized, using two different methods during the features' computation step, features that are based on a binary signal will be computed on both binary signals, for each window. This is done to see if one signal appears to be better than the other.

By working with the random forest classifier, taking 150 estimators, only the 17th most important features have been kept for the next steps. The classification has been done several times to ensure that the importance ranking didn't change significantly by using different training sets. The importance ranking has also been analyzed with each matrix of features. A typical features importance ranking, using these 17th most important features, is shown in Figure 38. These values have been found using all windows of 10 seconds. By reducing to this subset of features, the score on the test set, to classify normal rhythm hasn't changed (about 98%). However, the score on the test set for the classification of shockable rhythm has been a bit reduced (from about 95.2% to 94.1%).

6.1.4   Models

In this part are compared and investigated different models made using the Python Scikit-learn library. These models are tuned and trained using both databases with 10 seconds windows recording. Only classifiers are used as the goal is to classify either if the signal is normal or shockable. A validation subset is kept to score each classifier and 5-fold cross-validation is used to tune model parameters. In order to better analyze the accuracy of each method, sensitivity and specificity are used. Sensitivity is defined as the proportion of correctly classified positives (shockable rhythms), specificity is the proportion of correctly classified negatives (normal rhythms).
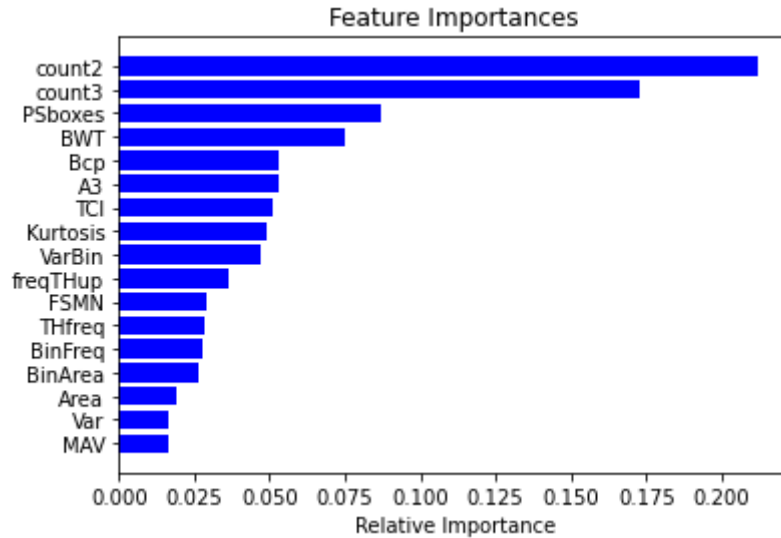
Figure 38: 17 most important features

Neural Network Classifier   The first classifier is the neural network classifier, MLPClassifier from scikit-learn. This classifier is quite strong and often gives accurate results with low bias but higher variance. It is possible to play on the number of hidden layers and the number of neurons inside each of them, but also on alpha, the penalty parameter. To properly use this classifier, features are normalized between -1 and 1. Moreover, the maximum number of iterations has been increased from 200 to 2000 to ensure convergence.

The three parameters will be tuned one at a time. First of all, the number of hidden layers is tuned by keeping the number of neurons to a constant value and the penalty parameter to 0.0001. In order to see if different combinations give different results, five different number of neurons were tested to tune this first parameter. In Figure 39 is shown the influence of the number of hidden layers using 10 neurons in each layer. Tuning using others number of neurons have also be done but it gave same results. The adequate number of layers appears to be around 20, when the accuracy seems to stabilize. To ensure a certain margin, 30 hidden layers will be kept.
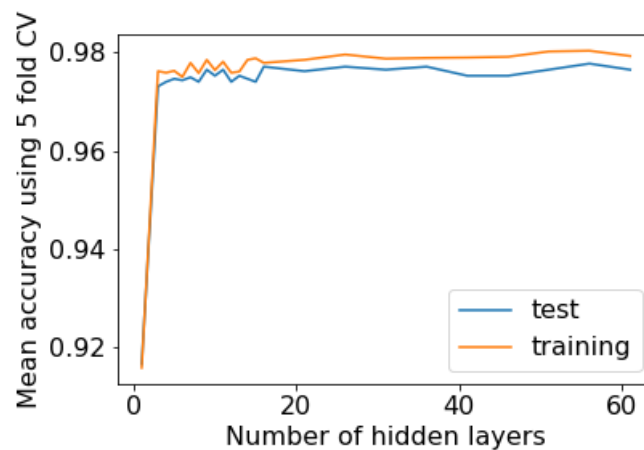

Figure 39: Tuning of the number of hidden layers

The second parameter to be tuned is the number of neurons in each layer. This is one by keeping the number of hidden layers to 30, as previously found. As seen in Figure 40, the adequate number of neurons per layer appears to be around 25 to ensure a maximal accuracy.
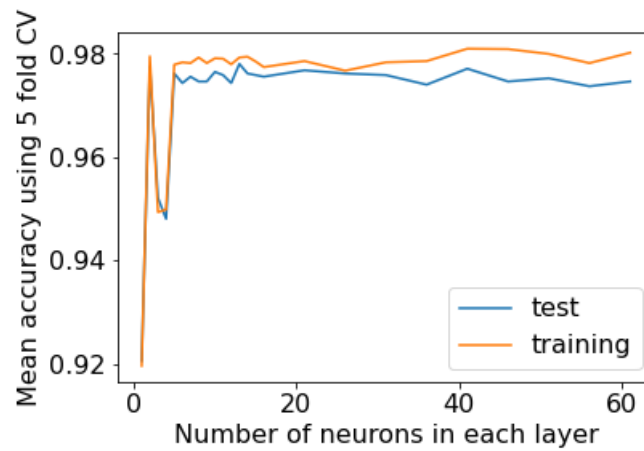

Figure 40: Tuning of the number of neurons

Finally, the penalty parameter has been tuned and found to give better results with a value of 0.00001 (as shown in Figure 41).
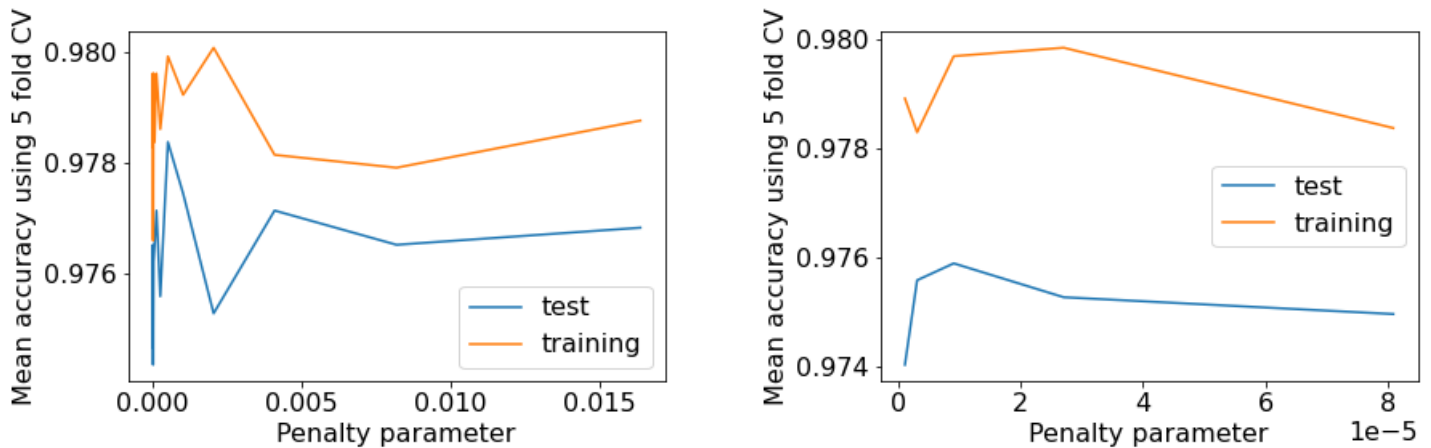

Figure 41: Tuning of the penalty parameter

Using these tuned parameters, a sensitivity of 0.976 of and a specificity of 0.983 are found on the test set. Indeed, 15 out of 910 are classified as shockable whether they are not and 4 out of 168 are classified as normal rhythm when they were shockable. As shocking people who don't need it would have bad effects, it is possible to tune the threshold on the probability of predictions. Indeed, the threshold is 0.5 but by putting it to 0.6, only 11 out of 910 normal rhythms are classified as shockable (0.988%). However, the sensitivity is decreased to 95% as 9 out of 168 shockable rhythms are wrongly classified.

Decision tree classifier   The Decision tree classifier makes a simple tree to classify the data. It takes as input the maximum depth of the tree, which needs to be limited in order to avoid overfitting on the training set. At each node, the best feature is used to make a split. This is why this method is useful to determine feature importance. The feature selected at each node depends on the impurity measure of each feature. This measure is often obtained using the Gini index.

Using this simple model, it is seen that the model only uses one significant feature to classify the data. Indeed, as shown in left Figure 42, accuracy doesn't significantly increase with the depth. Moreover, when using a depth of 7, features importance are shown in right Figure 42. Only count2 is a significant feature when using this model. However, even if the specificity is 98.3%, the sensitivity is only about 87.5%.
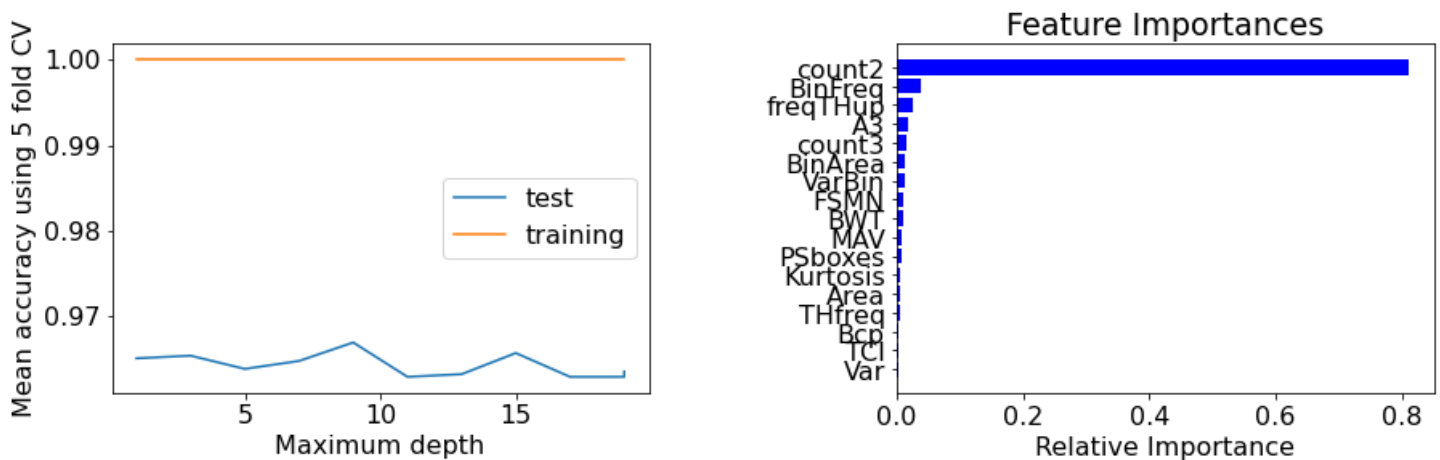

Figure 42: Decision tree classifier

Bagging   The bagging classifier is an ensemble method using bootstrap samples constructed from the original training set. It combines the predictions of several models by averaging them. Bagging methods reduce the variance but increase a bit the bias of the model. With this classifier, mainly the number of base estimators in the ensemble can be tuned.

The first classifier used is the decision tree. By tuning the number of estimators as well as the maximum depth, results shown in Figure 43 can be found. The adequate number of estimators is 60 with a maximum depth of 5. The specificity on the test set is 98.6% and the sensitivity 94.6%.

The second classifier bagged is the neural network. Parameters found by tuning the MLP classifier have been kept and only the number of estimators has been tuned in this part. This resulted in an adequate number of estimators of about 30 (see Figure 44). However, specificity and sensitivity have not been improved using this method. Indeed, they are respectively of 98.5% and 95.8%.
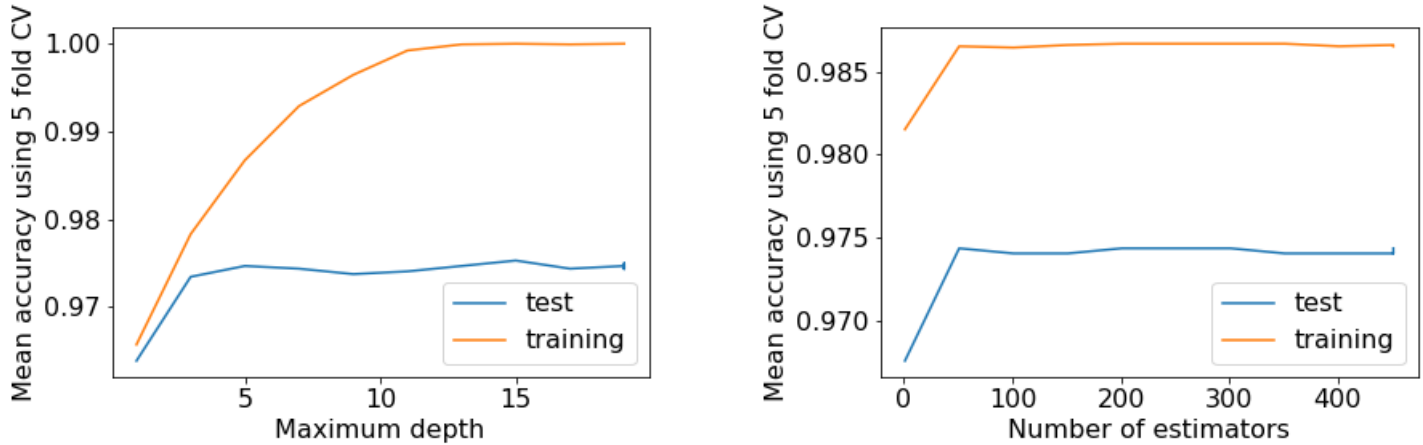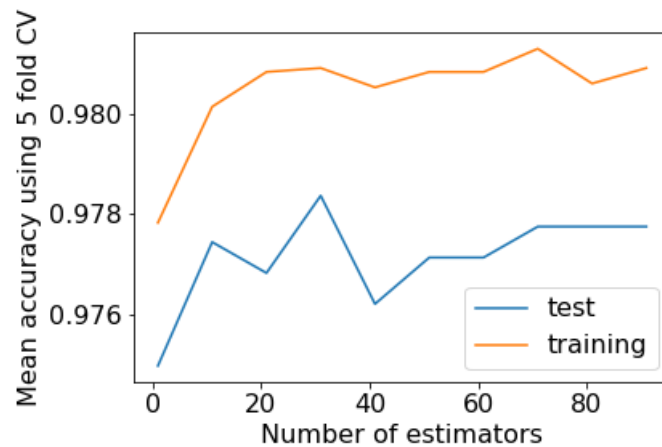
Figure 43: bagging trees

Figure 44: Number of estimators tuned using bagging MLP

Random Forest   This other bagging classifier is quite similar to bagging trees. A given number of estimators can be told as parameter to the classifier and it averages all these models, which are trees. It is possible to play on the number of estimators and the number of samples used for each estimation, to acquire better results as possible. But it is also possible to tell the maximum number of features. Indeed, this one is different from the bagging classifier as it can consider only a subset of features at random for the split at each node.

The trees maximum depth, as well as the number of estimators, can be tuned. Using again 5-fold cross validation, a maximum depth of 5 using 10 estimators appeared to be the adequate parameters (Figure 45). Sensitivity and specificity are respectively 94% and 98.5%.

Gradient boosting tree   This ensemble method is based on boosting, it allows reducing bias by combining several weak models. It is possible to play on the number of estimators and the maximum depth of trees to find the adequate model for the problem. Obviously, increasing the depth will lead to overfitting and the upper bound will be limited by this. On the other hand, increasing the number of estimators should increase the accuracy but it will also be limited by the overfitting.
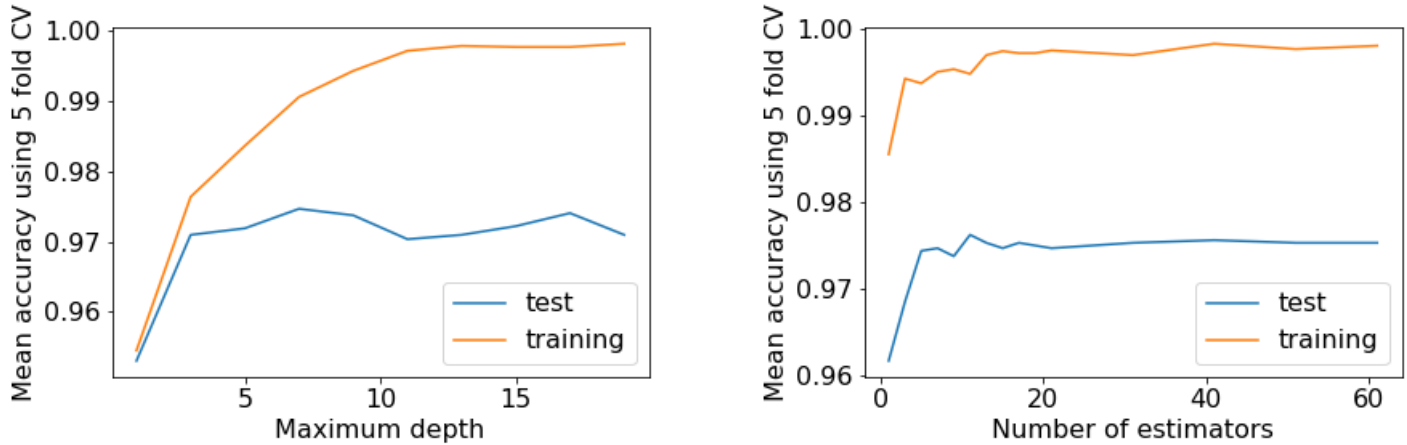
Figure 45: Random forests

The number of estimators and maximum depth have been tuned still using 5-fold cross-validation. As can be seen from Figure 46, the optimal number of estimators is about 40 and the maximum depth around 7. Using these parameters, the specificity and sensitivity appear to be 0.99 and 0.92 %.
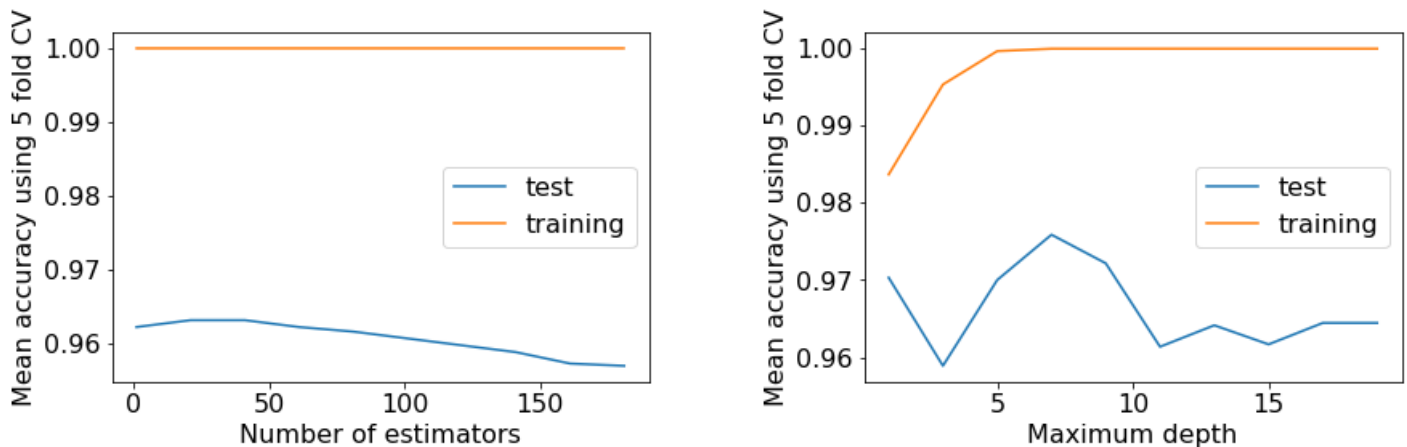

Figure 46: Boosting trees

Adaboost Another boosting method is the Adaboost.
Models are built one at a time on a modified version of the data. The final prediction being a weighted sum of the predictions of each model. If some cases are more difficult to classify, the algorithm will focus on these ones to adjust weights. The number of estimators can be tuned to obtain better results.

Using the Decision tree classifier as base estimator gave results shown in Figure 47. Scoring on the test set is not excellent (a specificity of 98% and a sensitivity of 88%) and the number of estimators doesn't seem to impact these ones.
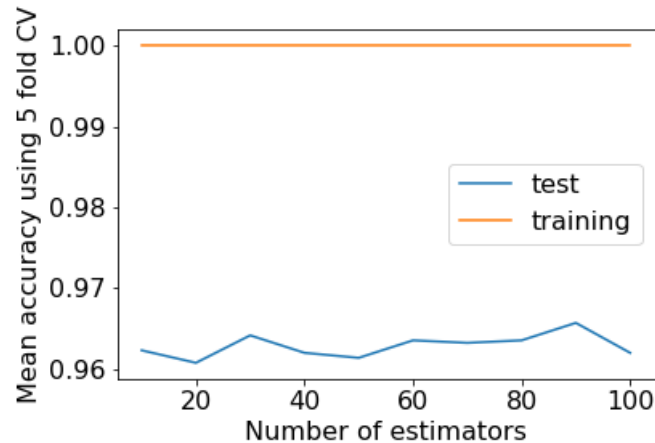
Figure 47: Adaboost

6.1.5   Final model results

By comparing these different models, it appears that the MLP classifier is the best one. This classifier is chosen as the final model. To recall, the optimal parameters using this one are 30 hidden layers having each one 25 neurons using a penalty parameter of 0.00001. It is interesting to note that stacking this model with others like the random forest classifier didn't give better results.

To try to take maximum advantage of this model, several things have been investigated. First of all, the probability threshold can be tuned to increase the specificity of the algorithm. Indeed, it is important not to give a shock when it is not needed as it could kill the patient. A second trick used is to give predictions on 2 following 5 seconds windows and change prediction until 2 following ones agree. This allows keeping prediction only if the algorithm is quite sure about its prediction. It could also prevent wrong predictions due to movement.

To better analyze the efficiency of this model and to determine what could give better predictions, scoring using different sets are shown in Table 2. In each case, the test set is 25% of the training set. In the case in which 2 predictions over 5 seconds subwindows are used, the specificity and sensitivity are given without consideration of the non-classified windows. Indeed, 25 windows out of 1078 were not classified as the predictions of both subwindows didn't agree. This number of non-classified windows increased up to 28 windows using a threshold of 0.8. Recall that, the sensitivity is defined as the percentage of correctly classified shockable rhythms and the specificity as the percentage of correctly classified normal rhythms.

Set	Sensitivity	Specificity
10 seconds windows from both databases	0.964	0.985
10 seconds windows database VFDB	0.971	0.987
10 seconds windows database CU_VT	0.903	0.981
5 seconds windows from both databases	0.954	0.979
5 seconds windows database VFDB	0.925	0.99
5 seconds windows database CU_VT	0.924	0.982
10 seconds windows from both databases using threshold=0.6	0.95	0.99
10 seconds windows from both databases using threshold=0.7	0.945	0.99
5 seconds * 2 windows from both databases	0.98	0.99
5 seconds * 2 windows from both databases using threshold=0.7	0.979	0.992
5 seconds * 2 windows from both databases using threshold=0.8	0.973	0.992

Table 2: Accuracy of the model using different set

From these results, it appears that using predictions from 2 consecutive windows of 5 seconds could be the best solution. The time needed to predict may increase a bit in certain cases more difficult to predict but it ensures an excellent accuracy of classification. Another observation is that recordings from the CU_VT database are more misclassified than the ones from the VFDB database. This is certainly due to the difference in the number of recordings in each database (1178 windows of 10 seconds for CU_VT against 3136 for VFDB). Another possibility could be that the CU_VT recordings labels contain more mistakes. Finally, the accuracy to predict shockable rhythms is also lower than the one of normal rhythms, but this could be explained by the same reason. Indeed, only 16.5% of the dataset are shockable rhythms. With more data, the proportion between normal and shockable rhythms could be equalized and the sensitivity would certainly be a bit better.

6.2 Arduino board control

6.2.1 ECG signal acquisition

To record ECG activity, the PCB made in this project has been used (see Figure 48). As 2 long wires are used to connect electrodes to the skin, they have been twisted in order to avoid picking up noise. Indeed, before doing this step the signal acquired was mainly 50Hz and the ECG activity was barely not detectable. A 9V battery is used to power the circuit and as previously explained, this voltage is DC-DC converted in a 5V output that is used to feed the Arduino board. It is also possible to power the Arduino and AD8233 using only the USB connector but when using this powering while recording ECG, a lot of noise is picked up.
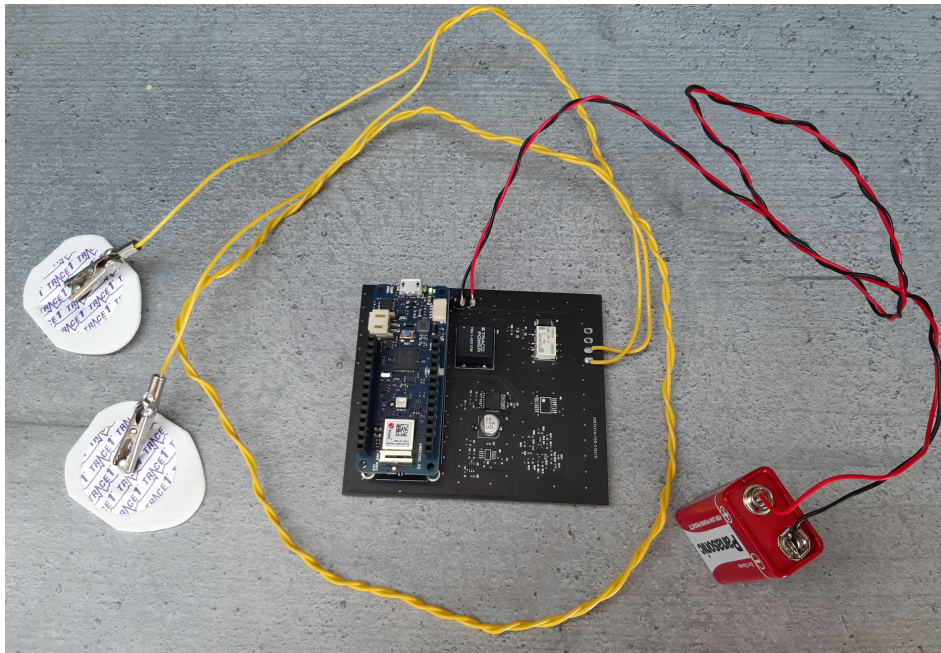

Figure 48: Circuit used to acquire ECG activity

To acquire an ECG signal several pins need to be set and read:

- The pin A6 needs to be high to connect the relay to the low voltage side of the circuit;

- Pin A3 and A4 are set low to connect the switch to the ECG system acquisition of the PCB.

- Pin 0, SDN, is set high to power on the AD8233.

- Pin A5, LOD, is read and needs to be low, meaning that the electrodes are connected, to start the acquisition.

- The recording is acquired at the output pin A1 after being converted through the ADC of the Arduino board.

First of all, the ECG signal has been observed using the oscilloscope. An example of what is recorded is shown in Figure 49. On the left figure is the initial signal acquired. After putting the PCB in a Faraday cage and connecting the subject to the ground, the signal shown on the right figure has been obtained. It is clear that a lot of noise is present in the recording but there is a lot of noise in the lab. These could be filtered digitally afterwards.
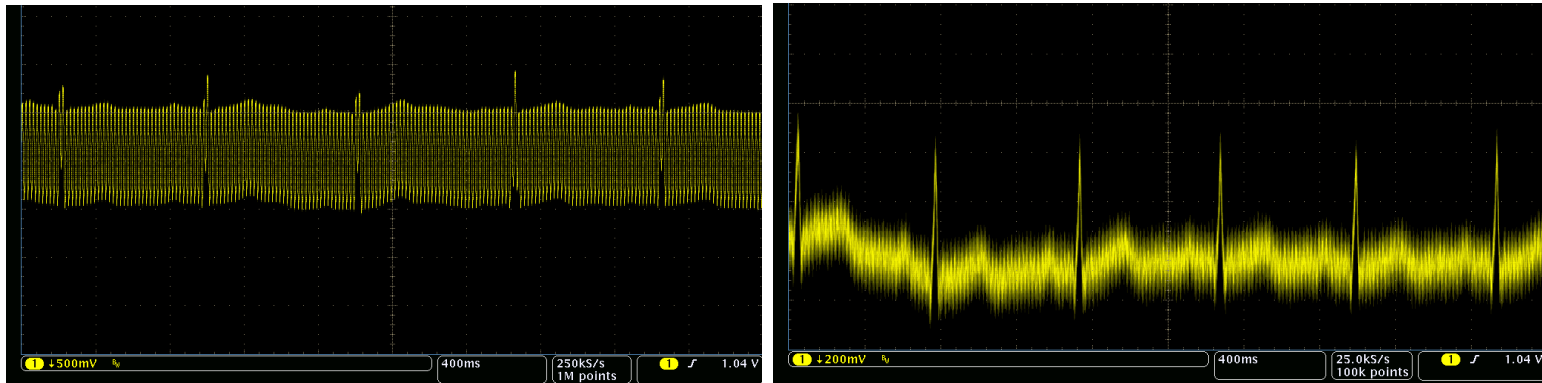

Figure 49: ECG recording on the oscilloscope

Then, the signal has been acquired using directly the USB connection to power the PCB as it was easier to first look at recordings using the Serial port in direct (Figure 50). An example of recording obtained using this configuration is shown in Figure 51. Even if the voltage is 5VDC, quite a lot of noise is picked up using the USB cable connected to the computer. However, it is possible to filter the signal and to already obtain good quality recordings. In real condition, the circuit would only be powered by the 9VDC battery. Therefore, ECG activity has been recorded while disconnecting the circuit from the computer (circuit in Figure 48). Doing this gave a really high-quality signal even before applying digital filters (see Figure 52). Finally, recordings by asking the subject to move have also been done to look at the influence of movement on the signal quality (Figure 53). It is also important to note that in function of which electrode is on which position, ECG peaks could be in positive or negative values (an example of recording having negative peaks is the one using USB powering).

It is possible to apply several filtration steps on noisy ECG recordings in order to remove artifacts and noise. These steps are the following:

1. Mean subtraction in order to have a 0 mean signal;

2. Moving mean 5th order filter to smooth the signal. It acts as a low pass filter by taking the mean over 5 consecutive data points;

3. High pass filter with a cutoff frequency of 1Hz or 0.5Hz;

4. Low pass filter with a cutoff frequency equals to 30Hz;

5. Notch filter with a 50Hz cutoff frequency to get rid of the 50Hz noise. This kind of filter allows to get rid of a certain frequency (see more information in Appendix H). The bandwidth of this filter has been put to 40 as frequencies above 30Hz are not desired.

In Figures 51 to 53 are shown different recordings along with their filtered versions. To better understand the filtration steps, in Appendix I are illustrated the impact of the filtration on the recordings Fast Fourier Transform.
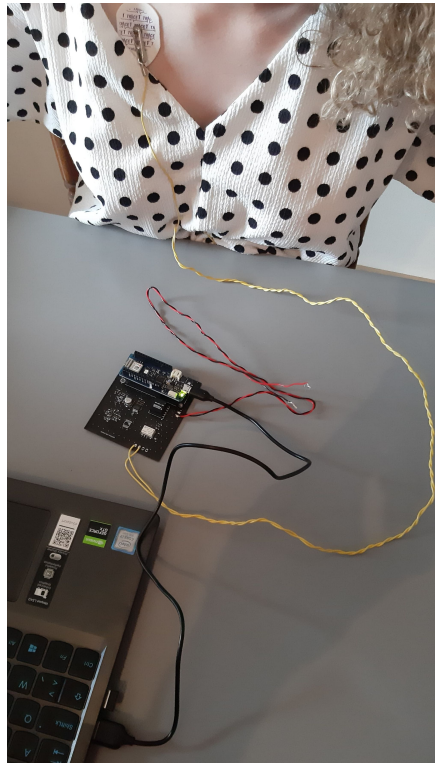
Figure 50: ECG recording using USB powering

The signal shown in Figure 51 is an example of signal acquired by using the computer USB as power supply, it is observed that the final signal is still a bit noisy but the ECG activity is easily recognizable. Little oscillations are induced in the signal and shouldn't be present. This phenomenon is due to the high pass filter. The sampling frequency is only an estimation as data points are acquired in real-time in MATLAB after being processed in Arduino. This makes it difficult to accurately determine the sampling frequency. This estimation leads to some inaccuracy during filtration steps that results in these oscillations.

In Figure 52 is shown a signal acquired using the 9VDC battery to power the PCB. Almost no noise is picked up with this configuration. To filter the signal, only steps 1 to 4 have been applied. Indeed, the 50Hz noise is low, thus the 30Hz low pass filtering is enough. The sampling frequency has been reduced by putting some delay in Arduino allowing to measure it more accurately, directly by looking at the timing in Arduino IDE.

Finally, an analysis of the effect of body movements on the signal has been done. In Figure 53 is shown one recording containing a lot of artifacts due to movement along with two different filtrations. On the left, a high pass having a cutoff frequency of 1Hz has been applied against a cutoff frequency of 4Hz on the right. Taking 1Hz as cutoff frequency doesn't remove a lot of noise but even if using 4Hz remove the majority of the artifacts, it is not a good option as it also removed information about ECG activity. Indeed, it is advised not to filter frequency above 1Hz.
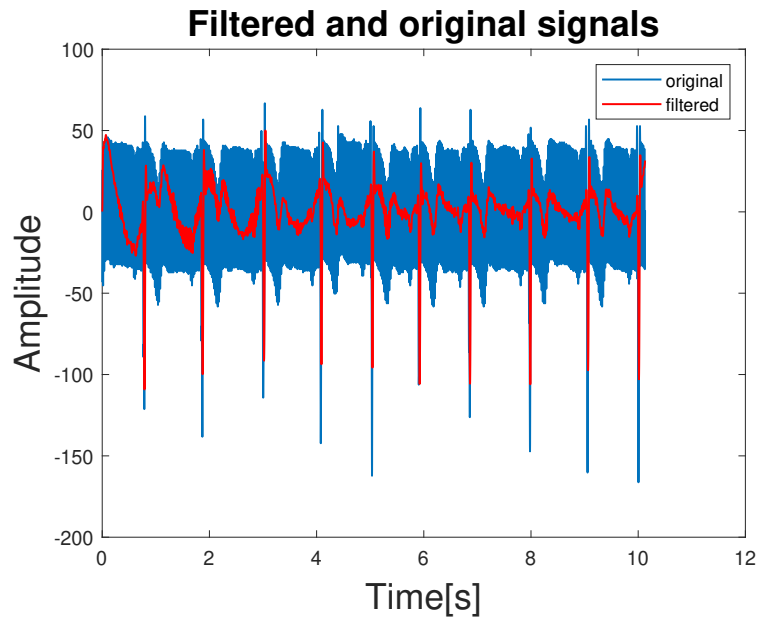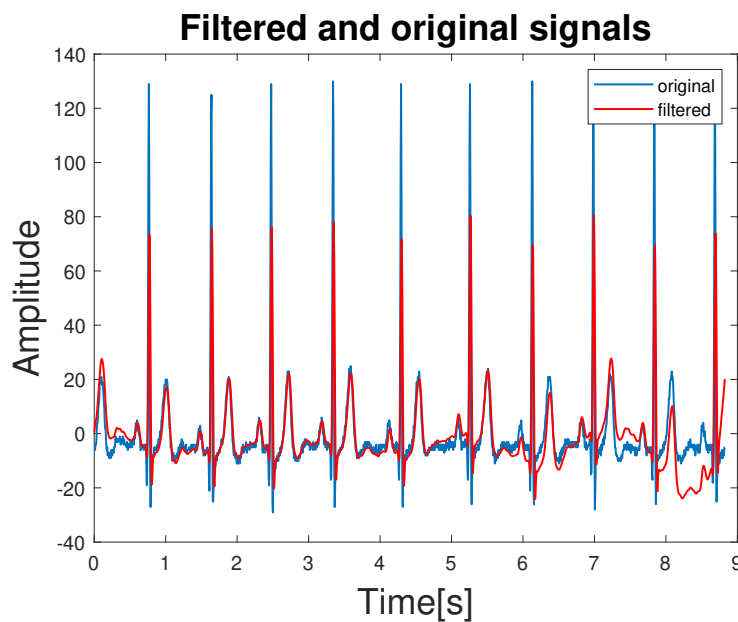
Figure 51: Recording using USB powering

Figure 52: Recording using 9VDC battery

Other solutions should be found to deal with movements. One solution could be to add an accelerometer to the board, as the board should be put on the patient when using the final defibrillator device. This would allow to sense movement and stop the current recording if too much movement is detected. One other solution could be to add an algorithm able to detect if the signal contains artifacts of movement. This could be implemented using threshold conditions on the signal variability, minimum and maximum. As can be seen from the different figures, when movements occur, data points are more spread around the mean and this could be used to detect bad quality signal. It could be considered that if the signal goes above 45 in the direction opposite the peaks' direction, the recording needs to restart. However, this may not work when recording ventricular tachycardia or fibrillation.
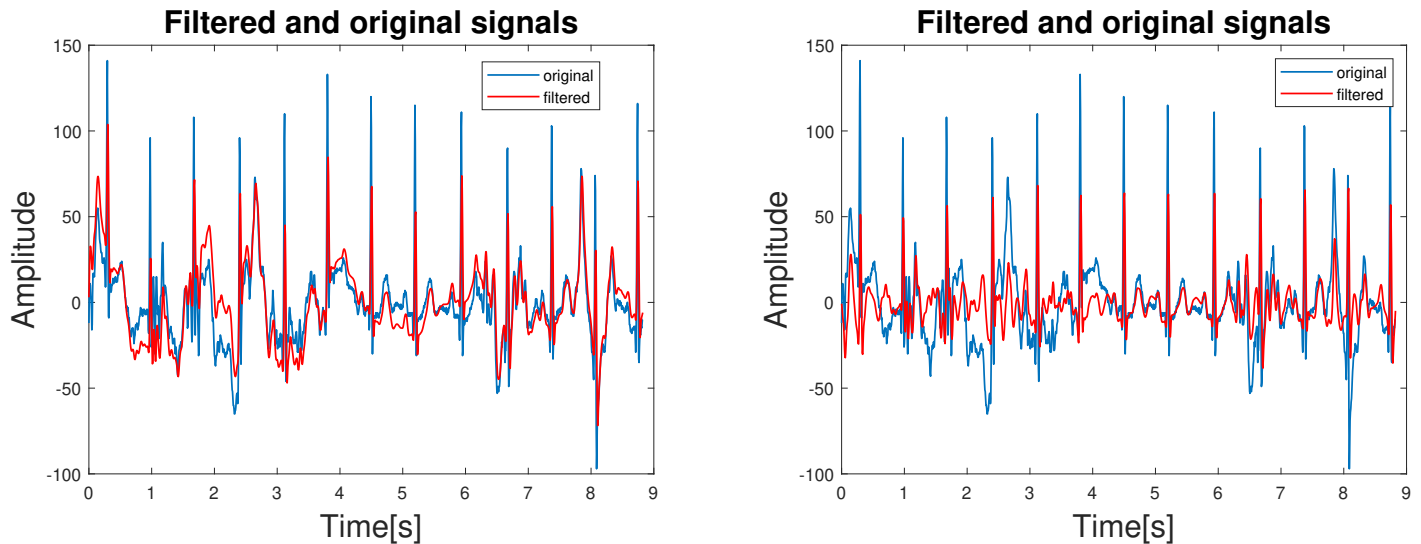
Figure 53: Recording using 9VDC with movements

Accuracy of the classifier model   To verify the efficiency of the model found in Section 6.1.5, features were computed using normal ECG recorded with the PCB. Several windows of 10 seconds have been recorded to see if normal rhythms are well classified. These include some recordings containing artifacts due to movements, some recordings with negative peaks by interchanging electrodes position as well as recordings with a lot of 50Hz (that have been filtered as previously explained). The model appears to be robust as all 5 seconds subwindows were classified as expected with a probability of 1 to be a normal rhythm. It could be concluded that with the quality of the ECG activity acquired using this board, 5 seconds should be more than enough to classify rhythms. As no experiments can be conducted on shockable rhythms, using a second window to support the first prediction is still advised.

Circuit consumption   To analyze the consumption of the board when recording ECG activity, an ammeter was used while doing a recording. As can be seen in Figure 54, the average current consumed is 35mA. This consumption corresponds to the typical input current needed by the converter as explained in Section 5.2.4. It is interesting to note that just when connecting the circuit, the consumption goes up to 50mA. This peak is certainly due to the time needed to charge all capacitors.
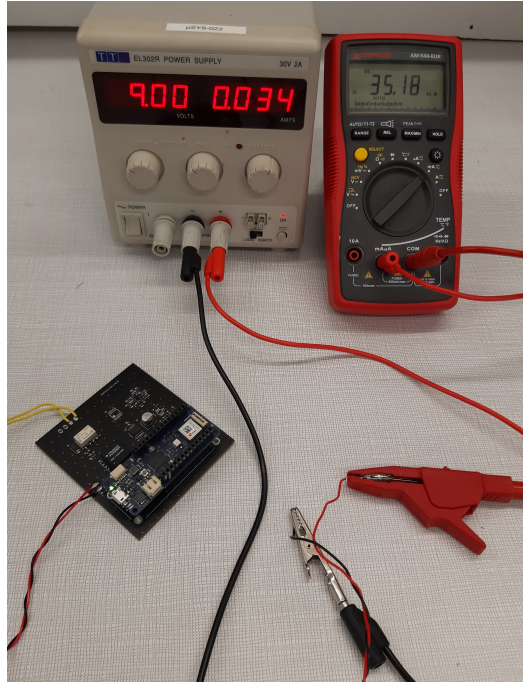
Figure 54: Circuit consumption

6.2.2   Impedance measurement

As the schematic of the Pmod IA has been copied in this project for the impedance measurement, its reference manual is used to make the code to control the impedance acquisition system. Moreover, an open-source Arduino code already existed for the Pmod IA control. Thus, this code has been used as a basis for this implementation part.

Initiation   The AD5933 uses I2C protocol to communicate with the Arduino board. Its address, the slave address, needs to be defined at the beginning of the code, this one is 0x0D. Then, each register addresses of the AD5933 are defined by giving a name to each of them.
The clock frequency is set to 16.776 MHz, the AD5933 internal clock speed.
A frequency sweep can easily be set. The start frequency is set to 70kHz, the increment frequency to 10kHz and the number of increments to 5. This is also done by setting registers to adequate values (see Table 3). This frequency sweep is not necessarily useful in this project as it is mainly used to characterize an impedance profile. In this case, the impedance is considered to be purely resistive and shouldn't be affected too much by the frequency. However, the frequency sweep has been implemented to verify if the impedance stays constant during the sweep and to check if electrodes stay well-connected during the whole measurement. Indeed, if one of the measurement is abnormal, the sweep will need to restart.

Calibration   Before doing any measurement, the gain factor needs to be calculated. AD5933 needs to be put in standby mode and PGA gain set to 1. This is done by setting bytes D15 to D12 of the control register to 1011 and D8 to 1. The excitation voltage and calibration frequency are chosen as well by setting the adequate values in their corresponding registers (see Table 3). Finally, a 99.2Ω resistor is placed between the two connectors to simulate electrodes-TTI impedance and calibrate in the good range of values.

Knowing the measured impedance, the gain factor can be calculated using these relations:

$$Magnitude = \sqrt{(RealData)^2 + (ImaginaryData)^2} \tag{17}$$

$$GainFactor = \frac{1}{KnownImpedance * Magnitude} \tag{18}$$

This gain can be used for further impedance measurement as long as PGA gain, output excitation voltage and current-to-voltage gain setting resistor remain constant.

Register values   The following Table 3 resumes register values that need to be defined. Using this configuration measurement are given in a really fast timing and to increase the accuracy, the final impedance can be taken as the mean over several measurements (e.g.: 10 in 2.7s).

Control	0x80 0x81	D15-D8 D7-D0	D10-D9: 11, D8: 1, D3 = 0	1Vp-p, PGA=1, internal clock
Start frequency	0x82 0x83 0x84	D23-D16 D15-D8 D7-D0	00100010 00101110 10100010	Initial frequency at 70kHz
Increment frequency	0x85 0x86 0x87	D23-D16 D15-D8 D7-D0	0100 11100010 00010111	10kHz per step
Nb of increments	0x88 0x89	D15-D8 D7-D0	0 0101	5 increments
Nb settling time cycles	0x8A 0x8B	D15-D8 D7-D0	D9-D10= 11, D8-D0 = 111111111	gain 4, 2044 cycles

Table 3: Register values

Results   First of all, the gain factor has been computed using a 99.2Ω pure resistor. Knowing the resistor value, only the gain was missing. The mean gain at 100kHz over 100 measurements was found to be 50787. As the gain was set at 100kHz, all measurements will be taken at this frequency. This 100kHz signal passing through the resistor is shown in Figure 56. The accuracy of measurement has been analyzed first, by looking at the measured impedance when connecting pure resistors (see Figure 55).
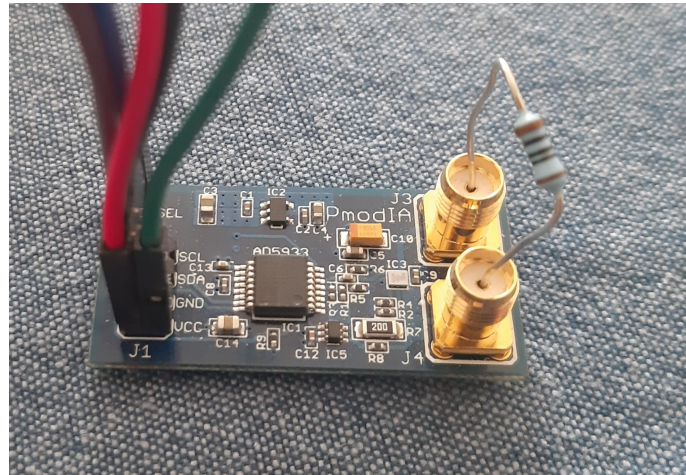
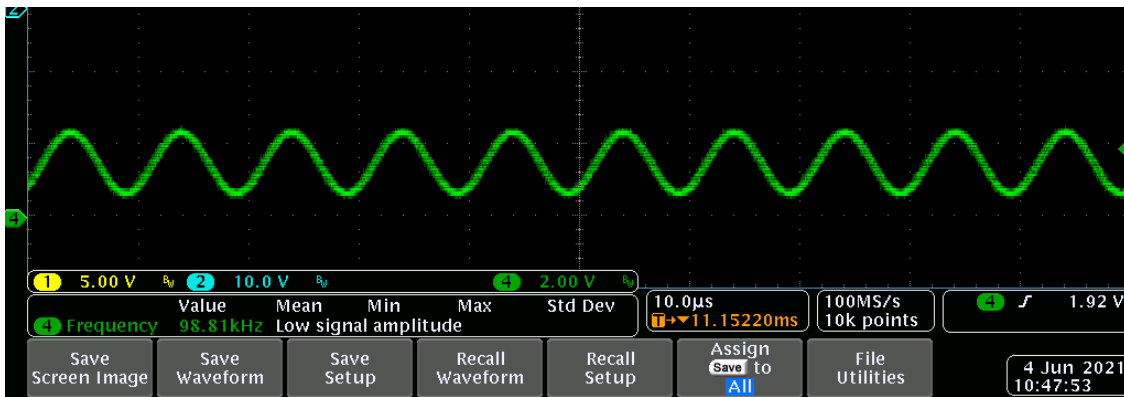**Figure 55:** Measurement with the PMOD IA

Figure 56: 100kHz signal

Then, electrodes pads have been connected to different subjects to see if the measured values are situated in the expected range. Small electrodes and big defibrillator pads have been compared (see Figure 57). In Table 4 are shown all measurements along with their expected impedance.

Figure 57: Electrode pads

What is connected	Expected impedance	Measured impedance
Resistor	99.2Ω (calibration one)	99.2Ω
Resistor	90.3Ω	90.7Ω
Resistor	47Ω	47.2Ω
Resistor	68Ω	67.5Ω
Resistor	150Ω	148.8Ω
Resistor	94Ω	94.6Ω
Resistor	218Ω	216.5Ω
Resistor	386Ω	385.5Ω
Resistor	675Ω	671.7Ω
Small electrodes to subject 1	> 200Ω	2500Ω
Small electrodes to subject 2	> 200Ω	2270Ω
Big electrodes to subject 1	50Ω-150Ω	73Ω
Big electrodes to subject 2	50Ω-150Ω	79Ω

Table 4: Analysis of the impedance measurement

The first observation looking at these values is that measurements are quite accurate. The more the impedance value is far from the 99.2Ω calibration, the more its value is far from the real one. As TTI measured should be located between 50 and 100 Ω, the accuracy should be quite good given the results obtained by measuring resistors in this range of values.

Using small electrodes gave huge impedance measurement which is what was expected as the impedance increases when the electrodes' area decreases. Using big electrodes on 2 different subjects gave similar results, the common range of impedance would be the 71-90Ω. This should be verified on other subjects but it agrees with the fact that the common TTI is situated between 50 and 100Ω. Moreover, being in this range means having initial energy at 150J and a pulse duration of 15ms which are easily achievable. It has been shown that having a TTI higher than 150Ω could lead to difficulty to defibrillate as the energy is limited to 360J and the voltage to 3000V but these measurements agree that 150Ω TTI is an abnormal value that shouldn't be measured. (see Section 4.2)

The I2C bus communication has also been observed with the oscilloscope. In figure 58, is shown a part of the data transferred during the impedance measurement. Only a part of the data transferred for one measurement is shown, as the frequency is really high, it is complicated to picture the entire information. In this example, is observed the value written in registers 0x85 and 0x86, which are part of the increment frequency value. It can be verified that the values 0100 (04) and 11100010 (E2) are respectively put in registers 0x85 and 0x86. Finally, 1A corresponds to 00011010 in the binary system. The first 8 bits are always sent by the master (Arduino) and it corresponds to the slave address (the 7 first bits) followed by the direction of the communication (last bit). In this case, the slave address is 0x0D (0001101) and the master is the sender (bit set to 0), which is correct.

Figure 58: I2C communication

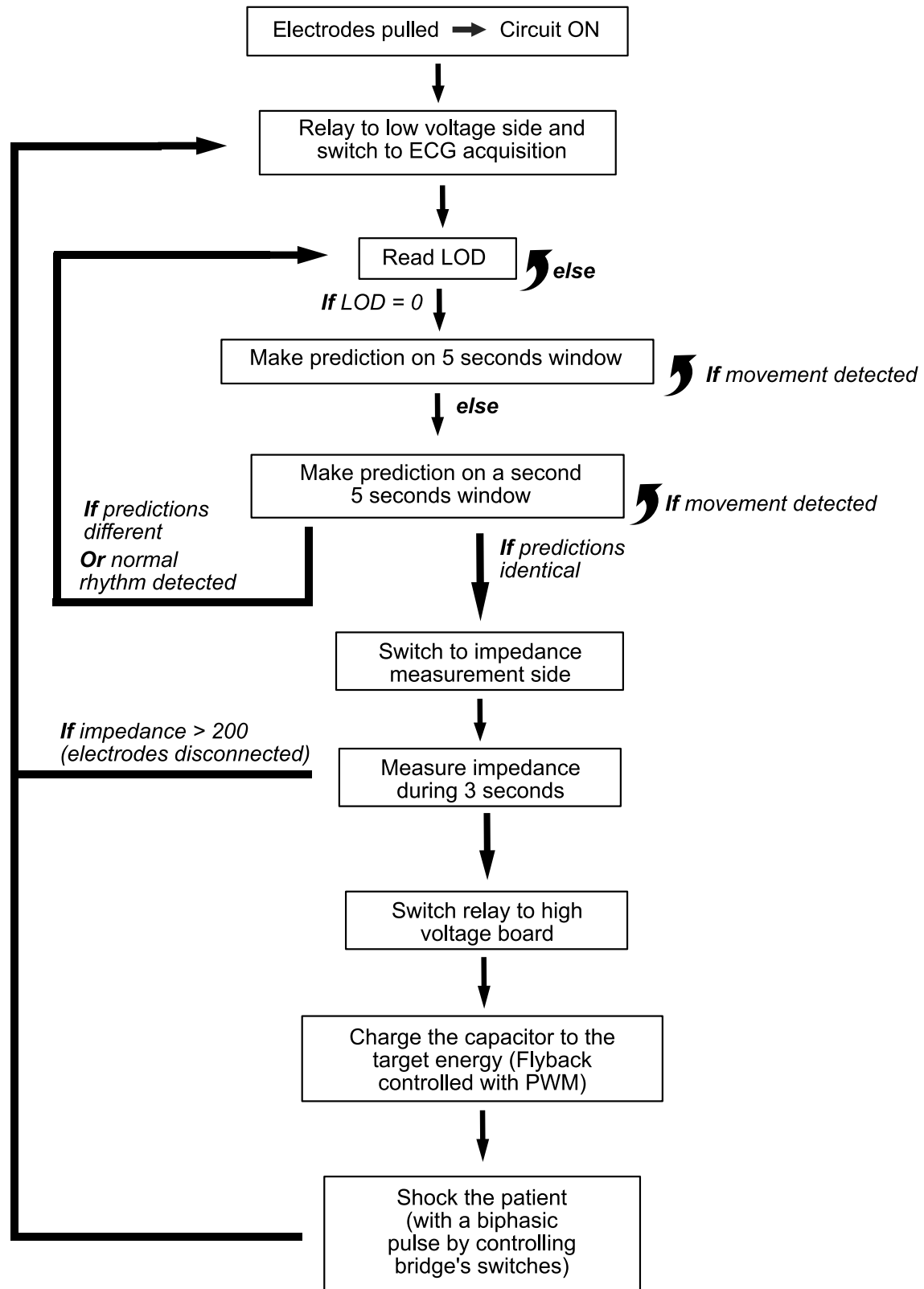## 6.3 Structure of the entire algorithm

Figure 59: Structure of the algorithm

7   Perspectives and conclusion

The goal of this project was to design an automatic external defibrillator that is fully automatic and of small size. The project has been divided into three main parts (1) the realization of a PCB able to measure the transthoracic impedance as well as to record the ECG activity, (2) some solutions that could be implemented to produce and deliver the defibrillation pulse, (3) the software algorithm to control the PCB board using an Arduino board and a model implemented in Python to detect ventricular tachycardia and fibrillation.

In the first part, a small PCB has been made and is able to record ECG activity with almost no noise. It can also measure the transthoracic impedance with high accuracy. The size of the board could be reduced further for a final implementation, for instance, using a smaller board and a denser layout.

In the second part, a global solution has been proposed to deliver the defibrillation biphasic pulse. A lot of investigations and the realization of a prototype (using smaller voltage in a first time) would be needed to better understand the needs and possibilities to implement this part. The main challenge remains the design of the flyback, a lot of simulations should be done and compared to understand what is possible. Nevertheless, the harder point would be to power the flyback with a small battery that would deliver enough current. This part would need to be investigated in an entire project in order to find a possible solution.

Finally, algorithms to deal with the PCB board acquisition have been implemented mainly to filter the ECG activity and to classify the recorded rhythms. The final model chosen is a neural network classifier able to classify the activity with a sensitivity of 97.3% and a specificity of 99.2%, using the result over two subwindows of 5 seconds. The model could be even more accurate by verifying the label provided in both databases used in this project and having more windows labeled as shockable rhythms (VT/VF). The model is not yet able to be converted in Arduino IDE, therefore, the best solution would be to use a MicroPython board having the same characteristics as the Arduino Board to directly import the model in it.

To conclude, this project covers all parts needed in the realization of an automatic external defibrillator and put forward solutions to reduce the size of this device. In order to provide a complete solution to design a small portable AED, an entire project should focus on the high voltage part. This project would need to make simulations and design a prototype able to manage the defibrillation pulse. The project should focus on the powering system and flyback converter that remain the main issue. Indeed, the size of the device is still limited by the size of the battery able to provide enough current to defibrillate.

References

[1] Srivathsan et al. *Ventricular tachycardia and ventricular fibrillation*, Expert reviews, 2009.

[2] Roy M. John et al. *Ventricular arrhythmias and sudden cardiac death*, Lancet Vol.380, October 27, 2012.

[3] Gavin D. Perkins et al. *European Resuscitation Council Guidelines for Resuscitation 2015 Section 2. Adult basic life support and automated external defibrillation*, European Resuscitation Council, 2015.

[4] BRUCE A. KOPLAN et al. *Ventricular Tachycardia and Sudden Cardiac Death*, Mayo Clinic Proceedings, March 2009.

[5] The Brussels Time. *Belgians 'less likely' to survive cardiac arrest*, https://www.brusselstimes.com/news/belgium-all-news/health/56765/belgians-less-likely-survive-cardiac-arrest-rates/, 2019.

[6] Philippe Kolh, *ANATOMIE ET PHYSIOLOGIE DU SYSTEME CARDIOVASCULAIRE*.

[7] Benoit Plourde et al. *Sudden cardiac death and obesity*, 2014.

[8] Abdennasser Bardai et al. *Epilepsy Is a Risk Factor for Sudden Cardiac Arrest in the General Population*, PLOS ONE, 2012.

[9] Ann-Sofie Forslund et al. *Risk factors among people surviving out-of-hospital cardiac arrest and their thoughts about what lifestyle means to them: a mixed methods study*, BMC Cardiovascular disorders, 2013.

[10] Boston Scientific. *Causes and Risk Factors for Sudden Cardiac Arrest*, https://www.sicdsystem.com/en-US/sudden-cardiac-arrest/causes-risk-factors.html, 2021.

[11] Eloi Marijon et al. *Warning Symptoms Are Associated With Survival From Sudden Cardiac Arrest*, Annals of Internal Medicine, 2016.

[12] Janice L.et al. *Electrophysiology of ventricular fibrillation and defibrillation*, Crit Care Med 2000, vol. 28, No. 11.

[13] Charles D. Deakin, Jonathan J.S. Ambler, Steven Shaw, *Changes in transthoracic impedance during sequential biphasic defibrillation*, Resuscitation, 2008.

[14] RICHARD E. KERBER et al. *Transthoracic Resistance in Human Defibrillation Influence of Body Weight, Chest Size, Serial Shocks, Paddle Size and Paddle Contact Pressure*, 1981.

[15] RICHARD E. KERBER et al. *Energy, current, and success in defibrillation and cardioversion: clinical studies using an automated impedance-based method of energy adjustment*, THERAPY AND PREVENTION-ARRHYTHMIA, Vol. 77, No. 5, May 1988.

[16] V. Krasteva, A. Cansell I. Daskalov. *Automatic adjustment of chopping-modulated defibrillation pulses to patient transthoracic resistance*, Journal of Medical Engineering Technology, 27:1, 11-18, DOI: 10.1080/0309190021000025882, 2003.

[17] V. Krasteva et al. *Automatic adjustment of biphasic pulse duration in transthoracic defibrillation*, Journal of Medical Engineering Technology, Volume 24, Number 5, (September/October 2000), pages 210 – 214.

[18] V. Krasteva et al. *Possibilities for predictive measurement of the transthoracic impedance in defibrillation*, Journal of Medical Engineering Technology, Volume 25, Number 5, (September/October 2001), pages 195 – 200.

[19] V. Krasteva et al. *Transthoracic impedance study with large self-adhesive electrodes in two conventional positions for defibrillation*, Physiol. Meas. 27 (2006) 1009–1022.

[20] Suneet Mittal et al. *Comparison of a Novel Rectilinear Biphasic Waveform With a Damped Sine Wave Monophasic Waveform for Transthoracic Ventricular Defibrillation*, Journal of the American College of Cardiology, Vol. 34, No. 5, 1999.

[21] Faisal Alatawi et al. *Prospective, randomized comparison of two biphasic waveforms for the efficacy and safety of transthoracic biphasic cardioversion of atrial fibrillation*, Heart Rhythm Society, 2005.

[22] Roger D. White et al. *Transthoracic impedance does not affect defibrillation, resuscitation or survival in patients with out-of-hospital cardiac arrest treated with a non-escalating biphasic waveform defibrillator*, Resuscitation 64 (2005) 63–69.

[23] A. E. Portela, J. Folgueras, 0. Colorado. *Energy Adjustment Method Based on Transthoracic Impedance for a Biphasic Defibrillator*, IEEE 2003.

[24] Yongqin Li et al. *A comparison of defibrillation efficacy between different impedance compensation techniques in high impedance porcine model*, Resuscitation 80 (2009) 1312–1317.

[25] Yang Shengjun Ge Xin Wang Xu Wu Xiaomei Fang Zuxiang. *Study on energy compensation in automated external defibrillator* , 2011 IEEE.

[26] Fulvio Kette et al. *Electrical features of eighteen automated external defibrillators: A systematic evaluation*, Resuscitation 84 (2013) 1596–1603.

[27] Giuseppe Ristagno et al. *Current is better than energy as predictor of success for biphasic defibrillatory shocks in a porcine model of ventricular fibrillation*, Resuscitation 84 (2013) 678–683.

[28] Charles D. Deakin et al. *A comparison of rectilinear and truncated exponential biphasic waveforms in elective cardioversion of atrial fibrillation: A prospective randomized controlled trial*, Resuscitation 84 (2013) 286–291.

[29] Yi Shan et al. *The effects of phase duration on defibrillation success of dual time constant biphasic waveforms*, Resuscitation 81 (2010) 236–241.

[30] Jacopo Ferretti, Licia Di Pietro, Carmelo De Maria. *Open-source automated external defibrillator*, HardwareX 2 (2017) 61–70.

[31] David Williams *Physical principles of defibrillators*, Anaesthesia and intensive care medicine, 2012.

[32] Bernard Boigelot *Embedded systems*, https://people.montefiore.uliege.be/boigelot/cours/embedded/slides/embedded-2020.pdf, April 2020.

[33] Electronics Hub. *What is Relay and How it Works?*, https://www.electronicshub.org/what-is-relay-and-how-it-works/, April 25, 2016.

[34] Electronics notes. *Solid State Relay, SSR*, https://www.electronics-notes.com/articles/electronic_components/electrical-electronic-relay/solid-state-relay-switch.php, 11 April 2021.

[35] Fabrice Frébel *Elements of Power Electronics PART II: Topologies and applications*, September 17th, 2020.

[36] Homemade Circuit Projects. *How to Design a Flyback Converter – Comprehensive Tutorial*, https://www.homemade-circuits.com/how-to-design-a-flyback-converter-comprehensive-tutorial/, January 29, 2020.

[37] Nathan O. Sokal, Life Fellow, IEEE, and Richard Redl, Senior Member, IEEE; *Control Algorithms and Circuit Designs for Optimal Flyback-Charging of an Energy-Storage Capacitor (e.g., for Flash Lamp or Defibrillator)*, IEEE TRANSACTIONS ON POWER ELECTRONICS, VOL. 12, NO. 5, SEPTEMBER 1997.

[38] Kirby Creel Senior Design Engineer Datatronics; *TRANSFORMER DESIGN FOR CHARGING DEFIBRILLATOR CAPACITORS*, http://www.datatronics.com/pdf/transformer_design_for_charging_defibrillator_capacitors.pdf, 14 May 2021.

[39] Components 101. *A Brief Overview of IGBT - Insulated Gate Bipolar Transistor*, https://components101.com/articles/what-is-igbt-working-operation-symbol-and-types, 06 April, 2020.

[40] Alexander Bolotnikov et al. *Overview of 1.2kV – 2.2kV SiC MOSFETs targeted for industrial power conversion applications*, IEEE 2015.

[41] Helong Li, Stig Munk-Nielsen. *Detail Study of SiC MOSFET Switching Characteristics*, IEEE 2014.

[42] S. Ryu et al. *Ultra High Voltage IGBTs in 4H-SiC*, IEEE 2013.

[43] Toshiba Electronic Devices Storage Corporation. *Comparison of SiC MOSFET and Si IGBT*, SiC MOSFET Application Note, 2020-08-17.

[44] Carl Blake and Chris Bull. *IGBT or MOSFET: Choose Wisely*, International Rectifier.

[45] Gangyao Wang et al. *Performance Comparison of 1200V 100A SiC MOSFET and 1200V 100A Silicon IGBT*, 2013.

[46] Alinaghi Marzoughi et al. *Characterization and Evaluation of the State-of-the-Art 3.3 kV 400 A SiC MOSFETs*, EEE TRANSACTIONS ON INDUSTRIAL ELECTRONICS 2016.

[47] Jean-Michel Redouté. *Integrated circuit devices and modelling*, Microelectronics and IC design, 2020.

[48] Goldberger, A., Amaral, L., Glass, L., Hausdorff, J., Ivanov, P. C., Mark, R., ... Stanley. *PhysioBank, PhysioToolkit, and PhysioNet: Components of a new research resource for complex physiologic signals.*, https://www.physionet.org/, Circulation [Online]. 101 (23), pp. e215–e220, 2000.

[49] Yang Xu, Dong Wang, Weigong Zhang, Peng Ping, Lihang Feng *Detection of ventricular tachycardia and fibrillation using adaptive variational mode decomposition and boosted-CART classifier*, Biomedical Signal Processing and Control 39 (2018) 219-229.

[50] Qiao Li, Cadathur Rajagopalan, Senior Member, IEEE, and Gari D. Clifford, Senior Member, IEEE. *Ventricular Fibrillation and Tachycardia Classification Using a Machine Learning Approach*, IEEE TRANSACTIONS ON BIOMEDICAL ENGINEERING, VOL. 61, NO. 6, JUNE 2014.

[51] Carlos Figuera et al. *Machine Learning Techniques for the Detection of Shockable Rhythms in Automated External Defibrillators*, PLOS ONE | DOI:10.1371/journal.pone.0159654 July 21, 2016.

[52] Nitish V. Thakor, senior member IEEE, Yi-Sheng Zhu and Kong-Yan Pan. *Ventricular Tachycardia and Fibrillation Detection by a Sequential Hypothesis Testing Algorithm* , IEEE TRANSACTIONS ON BIOMEDICAL ENGINEERING. VOL. 37, NO. 9. SEPTEMBER 1990.

[53] Emran M Abu Anas, Soo Y Lee, Md K Hasan. *Sequential algorithm for life threatening cardiac pathologies detection based on mean signal strength and EMD functions*, BioMedical Engineering OnLine 2010.

[54] Irena Jekova and Vessela Krasteva. *Real time detection of ventricular fibrillation and tachycardia*, Physiol. Meas. 25 (2004) 1167–1178.

[55] Unai Irusta et al. *A high-temporal resolution algorithm to discriminate shockable from nonshockable rhythms in adults and children*, Resuscitation 83 (2012) 1090–1097.

[56] Xu-Sheng Zhang et al. *Detecting Ventricular Tachycardia and Fibrillation by Complexity Measure*, EEE TRANSACTIONS ON BIOMEDICAL ENGINEERING, VOL. 46, NO. 5, MAY 1999.

[57] Irena Jekova. *Shock advisory tool: Detection of life-threatening cardiac arrhythmias and shock success prediction by means of a common parameter set*, Biomedical Signal Processing and Control 2 (2007) 25–33.

[58] Anton Amann, Robert Tratnig, and Karl Unterkofler. *Detecting Ventricular Fibrillation by Time-Delay Methods*, IEEE TRANSACTIONS ON BIOMEDICAL ENGINEERING, VOL. 54, NO. 1, JANUARY 2007.

Appendix:

A   ECG sensor pins description

Ball No.	Mnemonic	Description
A1	GND	Power Supply Ground.
A2	+Vs	Power Supply Terminal.
A3	REFIN	Reference Buffer Input. Use REFIN, a high impedance input terminal, to set the level of the reference buffer.
A4	HPSENSE	High-Pass Sense Input for Instrumentation Amplifier. Connect HPSENSE to the junction of R and C that sets the corner frequency of the dc blocking circuit.
A5	HPDRIVE	High-Pass Driver Output. Connect HPDRIVE to the capacitor in the first high-pass filter. The AD8233 drives this pin to keep HPSENSE at the same level as the reference voltage.
B1	$\overline{\text{SDN}}$	Shutdown Control Input. Drive $\overline{\text{SDN}}$ low to enter the low power shutdown mode.
B2	AC/$\overline{\text{DC}}$	Leads Off Mode Control Input. Drive the AC/$\overline{\text{DC}}$ pin low for dc leads off mode. Drive the AC/$\overline{\text{DC}}$ pin high for ac leads off mode.
B3	FR	Fast Restore Control Input. Drive FR high to enable fast recovery mode. Otherwise, drive it low.
B4	IAOUT	Instrumentation Amplifier Output Terminal.
B5	+IN	Instrumentation Amplifier, Positive Input. +IN is typically connected to the left arm (LA) electrode.
C1	LOD	Leads Off Detection Comparator Output.
C2	RLD $\overline{\text{SDN}}$	Right Leg Drive Shutdown Control Input. Drive RLD $\overline{\text{SDN}}$ low to power down the RLD amplifier.
C3	REFOUT	Reference Buffer Output. The instrumentation amplifier output is referenced to this potential. Use REFOUT as a virtual ground for any point in the circuit that requires a signal reference.
C4	RLDFB	Right Leg Drive Feedback Input. RLDFB is the feedback terminal for the right leg drive circuit.
C5	−IN	Instrumentation Amplifier, Negative Input. −IN is typically connected to the right arm (RA) electrode.
D1	OUT	Operational Amplifier Output. The fully conditioned heart rate signal is present at this output. OUT can be connected to the input of an ADC.
D2	OPAMP−	Operational Amplifier Inverting Input.
D3	OPAMP+	Operational Amplifier Noninverting Input.
D4	SW	Fast Restore Switch Terminal. Connect this terminal to the output of the second high-pass filter.
D5	RLD	Right Leg Drive Output. Connect the driven electrode (typically right leg) to the RLD pin.

Figure 60: Pins description AD8233

B   AD5933 pins description

Pin No.	Mnemonic	Description
1, 2, 3, 7	NC	No Connect. Do not connect to this pin.
4	RFB	External Feedback Resistor. Connected from Pin 4 to Pin 5 and used to set the gain of the current-to-voltage amplifier on the receive side.
5	VIN	Input to Receive Transimpedance Amplifier. Presents a virtual earth voltage of VDD/2.
6	VOUT	Excitation Voltage Signal Output.
8	MCLK	The master clock for the system is supplied by the user.
9	DVDD	Digital Supply Voltage.
10	AVDD1	Analog Supply Voltage 1.
11	AVDD2	Analog Supply Voltage 2.
12	DGND	Digital Ground.
13	AGND1	Analog Ground 1.
14	AGND2	Analog Ground 2.
15	SDA	I²C Data Input. Open-drain pins requiring 10 kΩ pull-up resistors to VDD.
16	SCL	I²C Clock Input. Open-drain pins requiring 10 kΩ pull-up resistors to VDD.

Figure 61: Pins description AD5933

C AD1636 pins description

Pin No.		Mnemonic	Description
TSSOP	**LFCSP**		
1	15	IN1	Logic Control Input.
2	16	S1A	Source Terminal. This pin can be an input or output.
3	1	D1	Drain Terminal. This pin can be an input or output.
4	2	S1B	Source Terminal. This pin can be an input or output.
5	3	V_{SS}	Most Negative Power Supply Potential.
6	4	GND	Ground (0 V) Reference.
7, 8, 15, 16	5, 7, 13, 14	NIC	No Internal Connection.
9	6	IN2	Logic Control Input.
10	8	S2A	Source Terminal. This pin can be an input or output.
11	9	D2	Drain Terminal. This pin can be an input or output.
12	10	S2B	Source Terminal. This pin can be an input or output.
13	11	V_{DD}	Most Positive Power Supply Potential.
14	12	EN	Active High Digital Input. When this pin is low, the device is disabled and all switches are off. When this pin is high, the Ax logic inputs determine the on switches.
N/A[1]	0	EPAD	Exposed Pad. Tie the exposed pad to the substrate, V_{SS}.

[1] N/A means not applicable.

Figure 62: Pins description ADG1636

D Circuit schematic

The schematic of the low voltage board can be found in Figures 63 to 68.
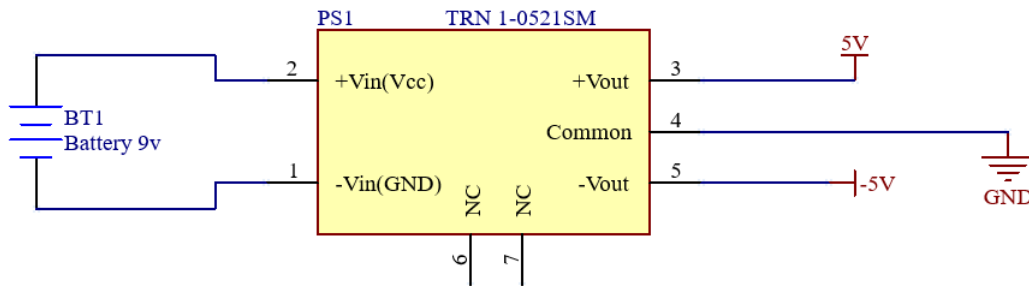
Figure 63: DC-DC schematic
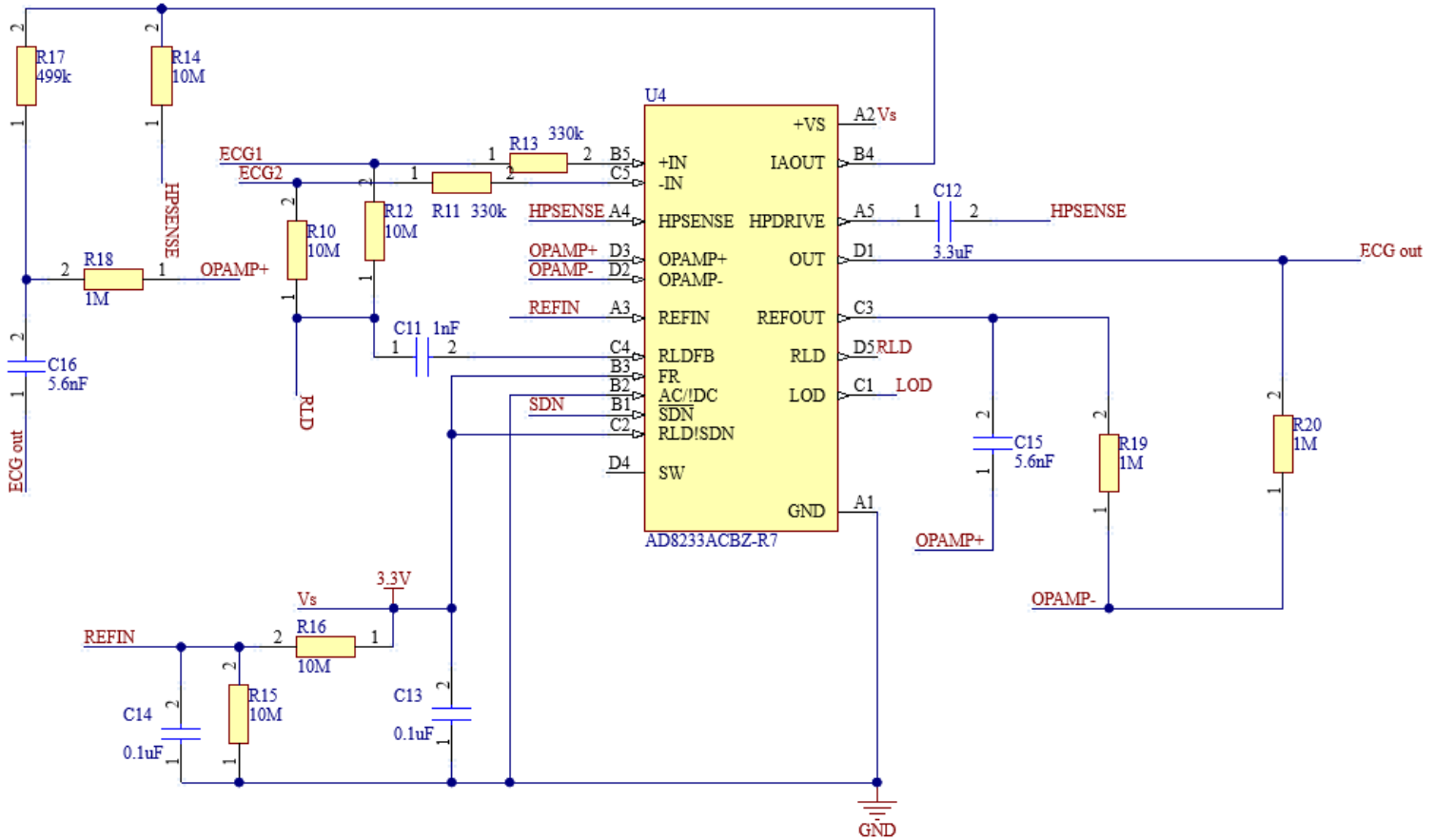
Figure 64: ECG acquisition part schematic
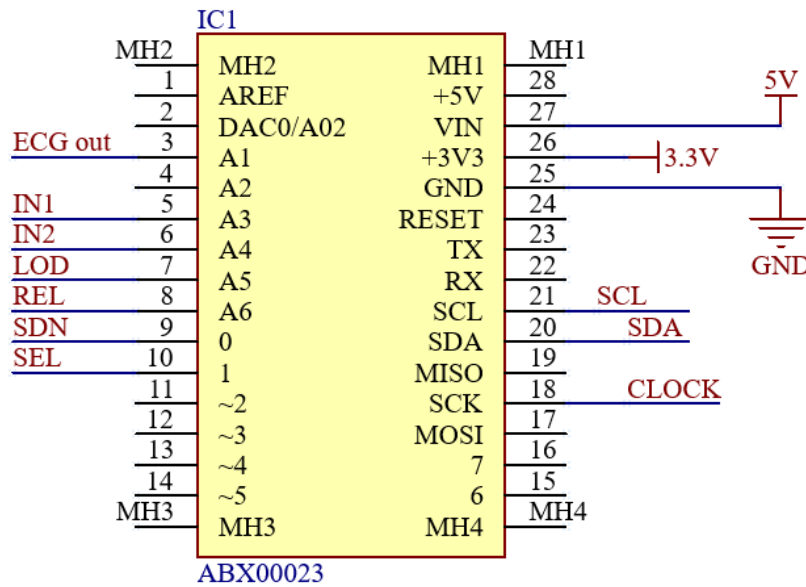
Figure 65: Arduino schematic

Figure 66: Impedance acquisition part schematic
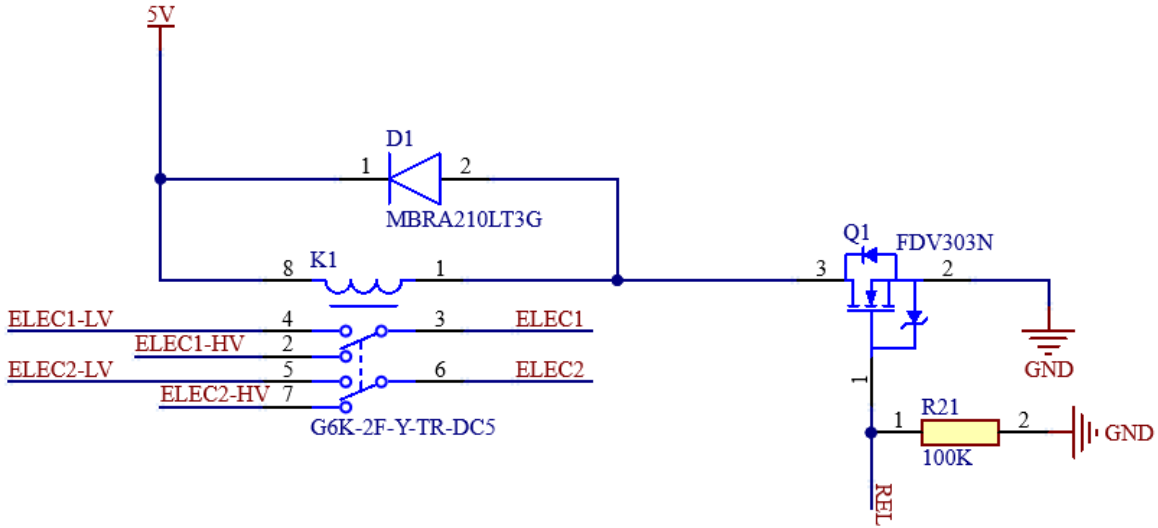

Figure 67: Switch schematic

Figure 68: Relay schematic

E   PCB

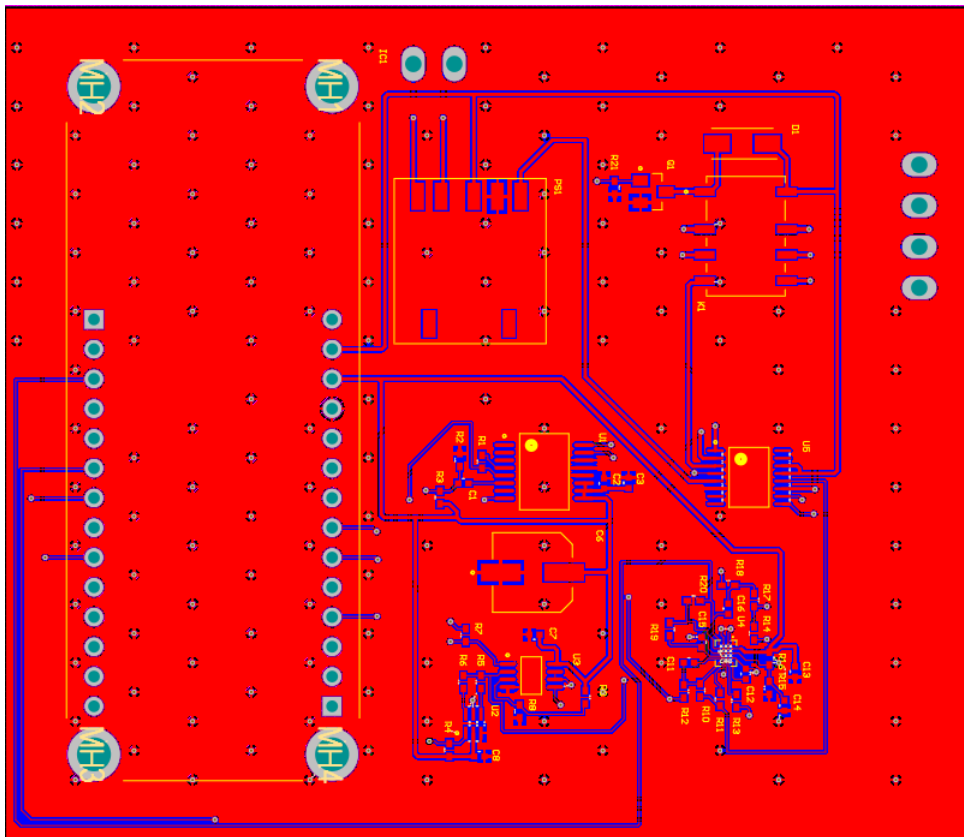The low voltage PCB's top and bottom layers can be found respectively in Figure 69 and 70.
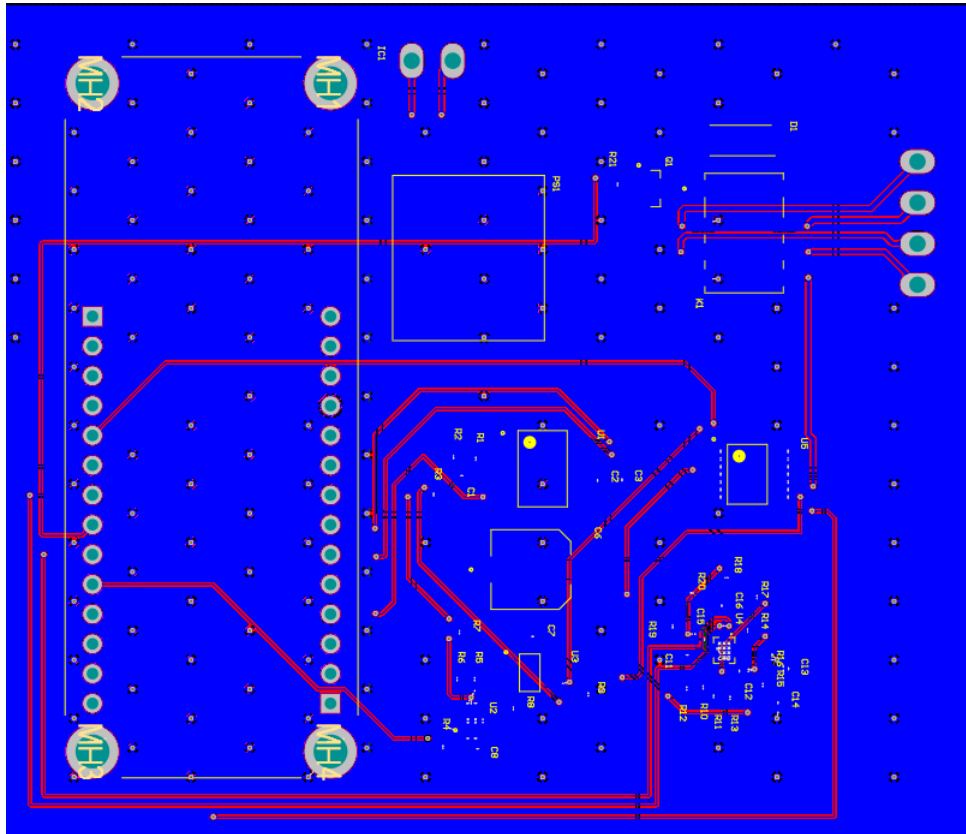

Figure 69: PCB top layer

Figure 70: PCB bottom layer

F   PCB components price

- **Microcontroller:** Between 20€ and 30€ (price of the Arduino or other possible solutions) ;

- **AD8233:** 3.63€;

- **AD5933:** 15.5€;

- **AD8606:** 3€;

- **ADG1636:** 4.22€;

- **AD8233:** 3.63€;

- **Relay:** 3.41€;

- **DC-DC:** 12.5€;

- **Battery:** 1.5€;

The PCB price is about 60€ including all components HTVA (the price could be reduced by ordering in quantity).

G   Examples of recordings from both databases

In Figures 71 to 74 are shown some recordings from both databases used to train the machine learning model built in this project. In this Section, signals have not yet been normalized between -1 and 1 but have 0 mean.

These illustrate that various quality and shape of signals can be found. This is why all recordings may not be included in the training set to give better scoring. Indeed, all recordings should be reviewed by a doctor in order to determine which one should be used in this project.

For example, the ones in Figure 71 are not clear ECG recordings and one should consider if there is a benefit in adding these to the training set. Two other bad quality signals are shown in Figure 72, the one on the left seems to have a lot of artifacts and shouldn't be used. The one on the right looks like a shockable rhythm and one should verify if this shouldn't be classified differently or removed because this is due to artifacts.
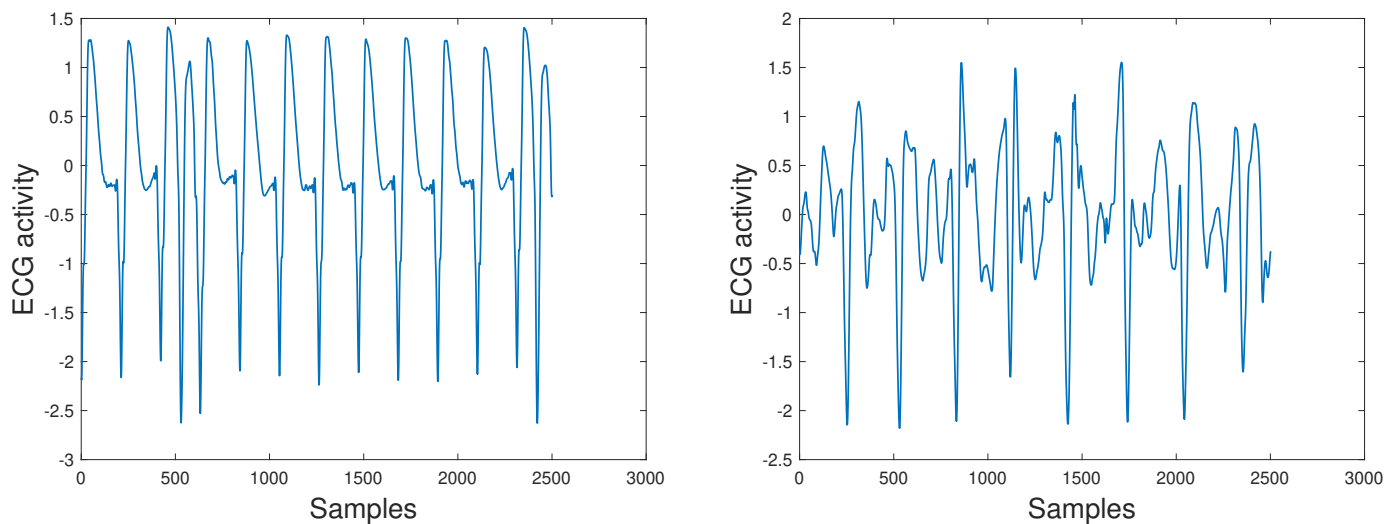
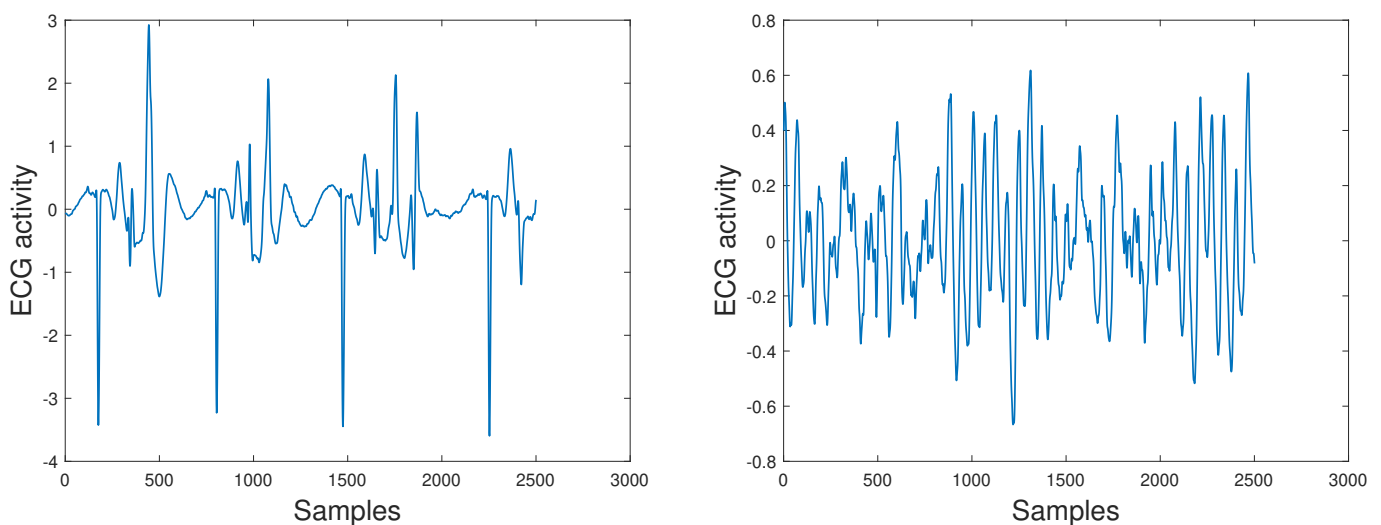**Figure 71:** Recordings of normal rhythms from CUVT database

Figure 72: Recordings of normal rhythms from VFDB database

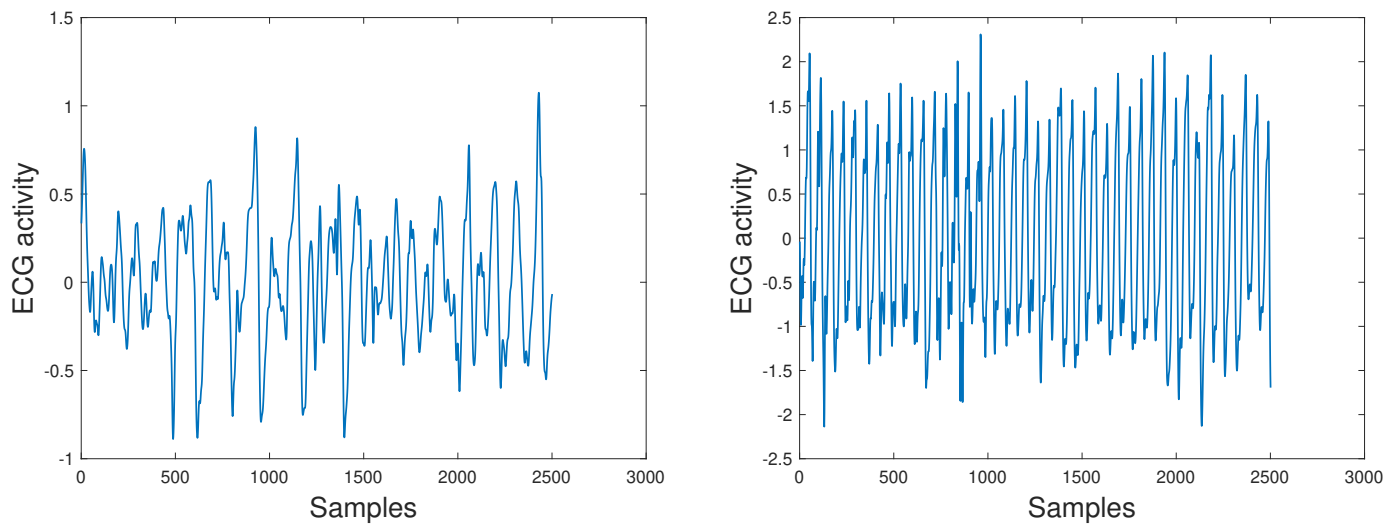In Figure 73 and 74 are shown examples of shockable rhythms that can be found in both databases.

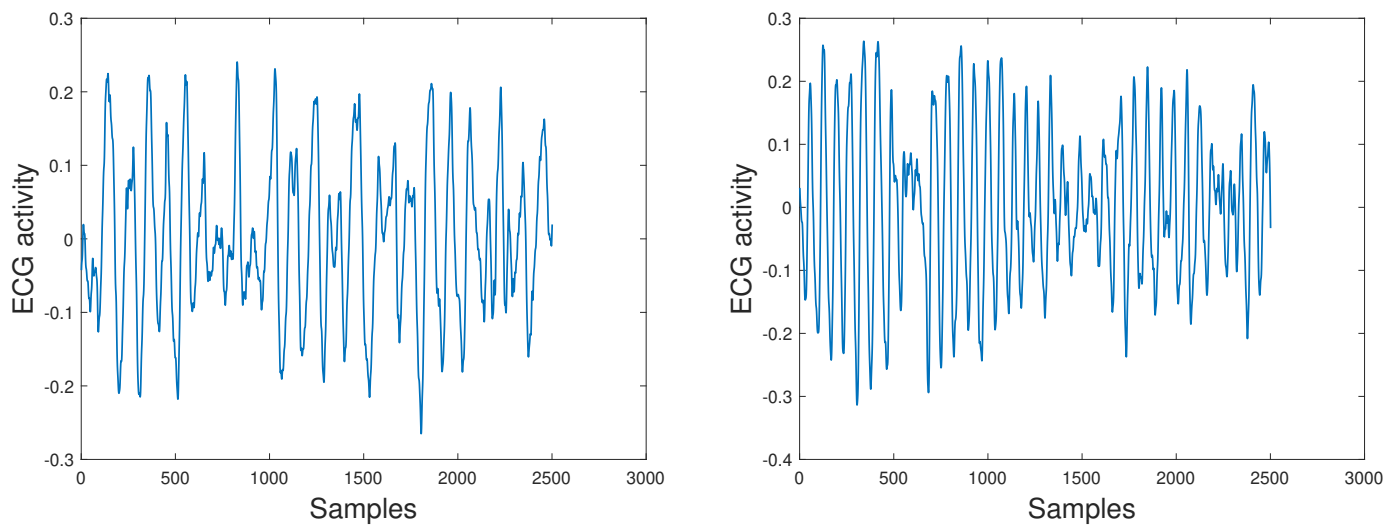**Figure 73:** Recordings of shockable rhythms from CUVT database

Figure 74: Recordings of shockable rhythms from VFDB database

H   Notch filter

50Hz noise is the most common noise that can be found in Europe. Indeed, most AC power supplies have a frequency of 50Hz. Therefore, a notch filter could be really useful. Indeed, this kind of filter allows to get rid of a certain frequency. The magnitude of this filter is illustrated in Figure 75. A certain bandwidth can be selected to manage the narrowness of the filter.
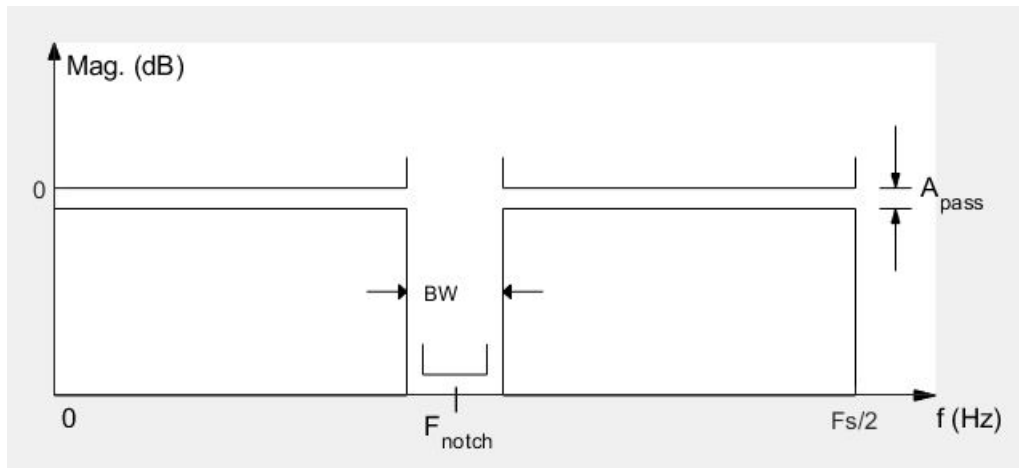
Figure 75: Caption

In this project, a 50Hz notch filter is applied on recordings made using a USB wire connected to the computer to power the PCB. One example is the one applied on recordings having a sampling frequency of 770Hz using a bandwidth of 40Hz. The magnitude and pole of this filter are shown in Figure 76 and 77.
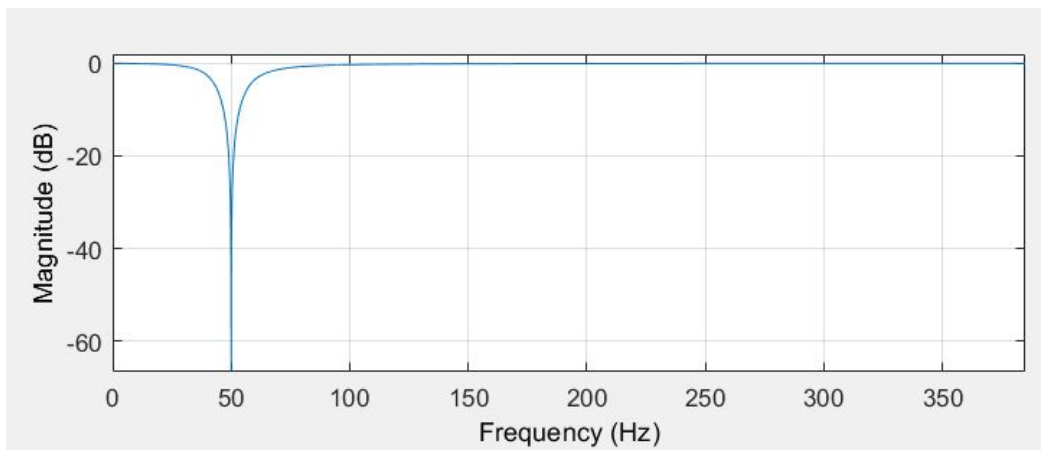

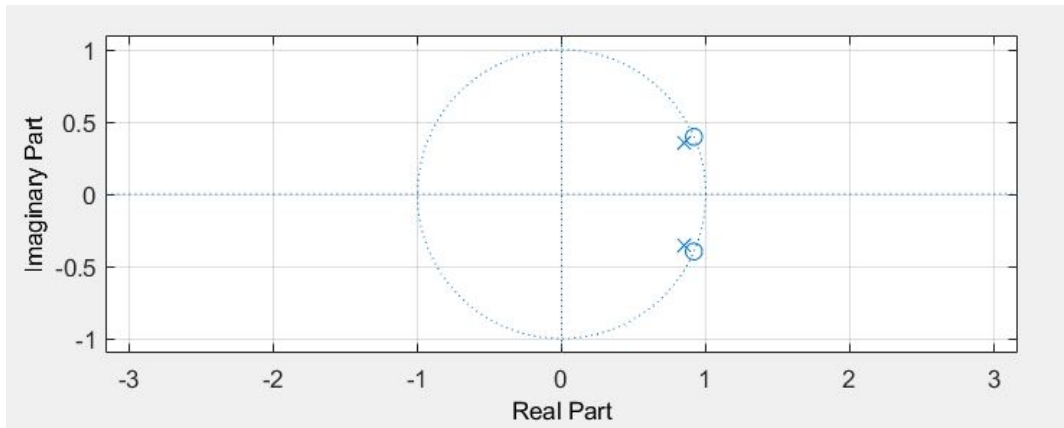**Figure 76:** Magnitude of a Notch filter

Figure 77: Pole of a Notch filter

I   FFT analysis

When applying filters to a signal, it is easier to represent the signal using its Fast Fourier Transform. This transformation allows to see how the signal is distributed in the frequency domain. In Figures 78 to 80 are shown FFT of different recordings along with their filtered version.

In Figure 78, is shown the FFT of a recording when the PCB is powered by the 9VDC. There is some low-frequency noise that should be removed but the 50Hz noise is tiny. After filtration, it is observed that all the 50Hz noise is removed even without applying a 50Hz notch filter. Indeed, the noise is so small that the low pass filter removes all of it. There is still a bit of DC noise but the amplitude of it went from 500 to 8. After filtration, most of the data points are in the range 0.5-30 Hz, meaning that the ECG activity is well recorded and barely any noise remains in the final signal.
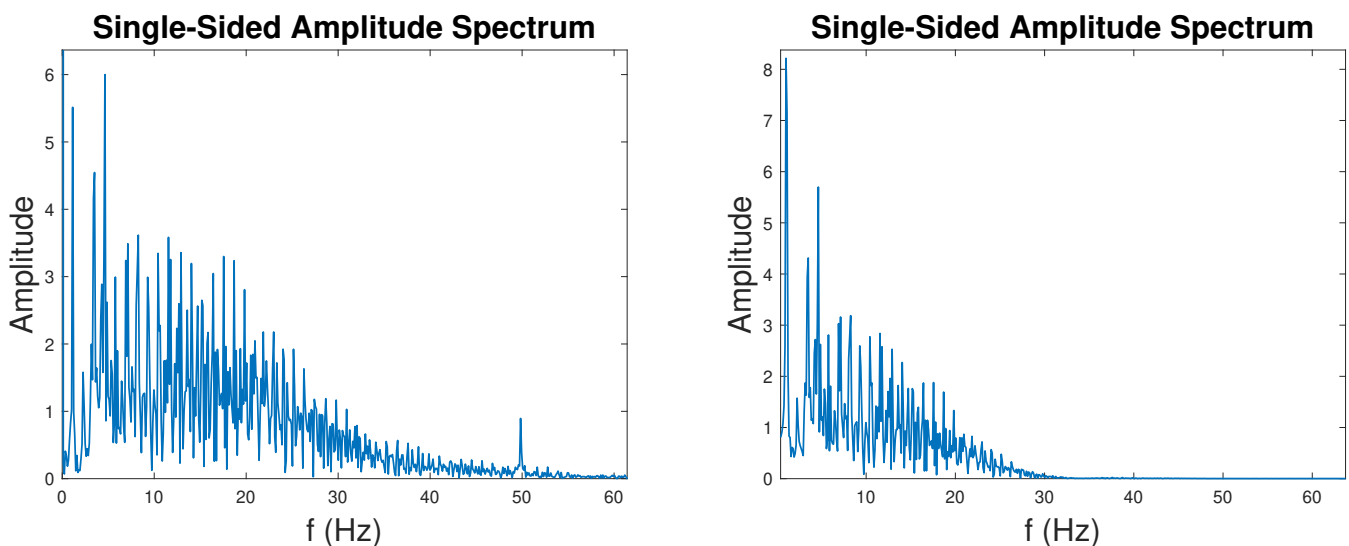

Figure 78: FFT of ECG activity recorded using the 9VDC

In Figure 79, is shown the FFT of a recording when the power supply used to power the Arduino is a USB output of a computer. It is directly noticed that 50Hz noise is predominant. After applying all filtration steps, including the 50Hz notch filter, the FFT of the signal is almost rid of all noise but it remains a bit more than when the board was powered with the 9VDC battery.
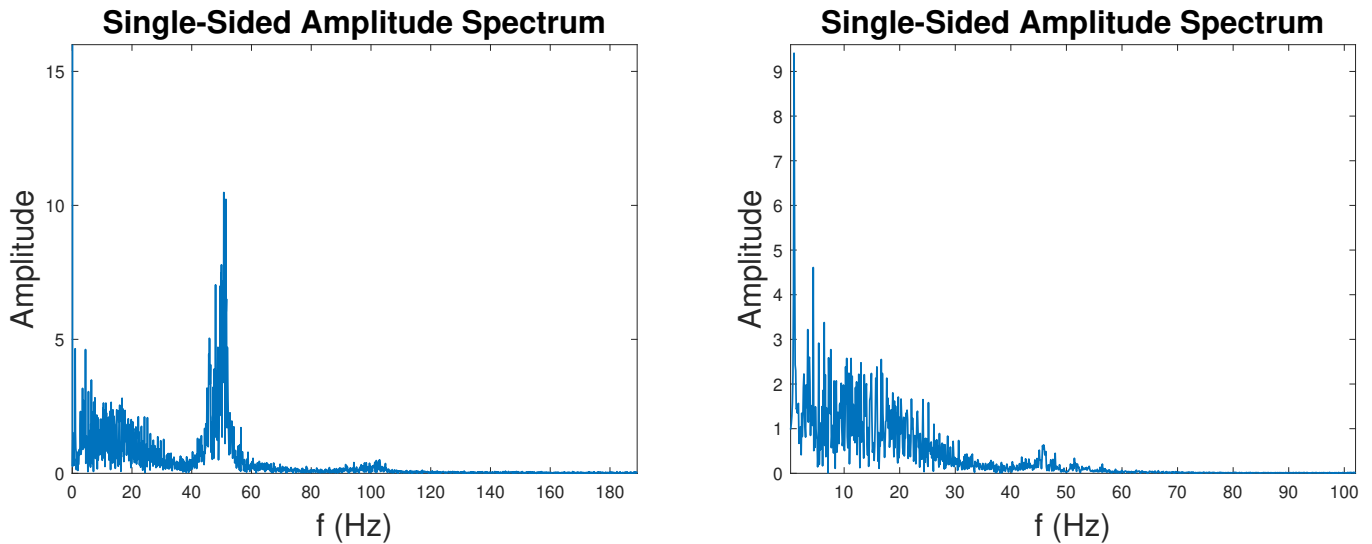

Figure 79: FFT of ECG activity recorded using USB connection to power

Finally, in the left Figure 80 is illustrated an example of FFT when using the 9VDC power supply and containing body movement artifacts. The main difference with the case in which the subject is still, is the presence of more low-frequency noise. After applying the 1Hz high pass filter (right Figure 80), this noise is a bit reduced but is still present. To get rid of this noise, it would be necessary to apply a high pass filter having a higher cutoff frequency. However, it is not possible as it is desired to keep frequency above 1Hz to record all ECG activity.
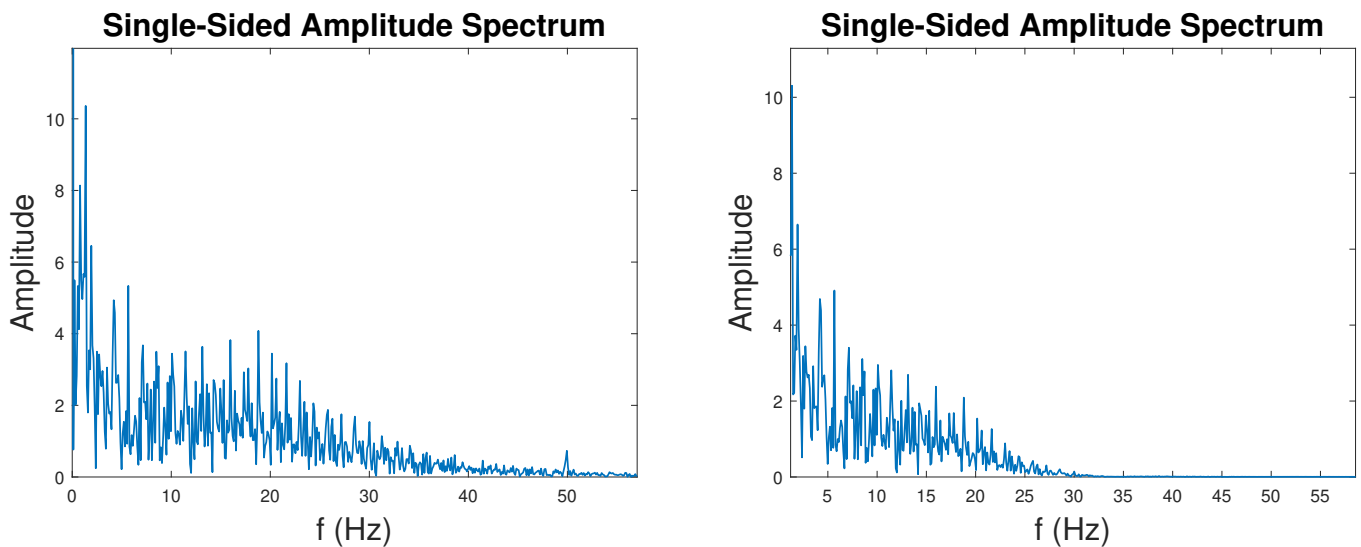

Figure 80: FFT of ECG activity recorded using the 9VDC with body movements